博士論文

Study of phosphorus biogeochemistry at atmosphere and ocean interface: Sea-surface microlayer

（大気と海洋境界面でのリンの生物地球化学的研究）

Sujaree Bureekul

スジャリ　ブリクル

Abstract

Sea-surface microlayer (SML) is a boundary layer between atmosphere and ocean. The operational depth layer between 1 – 1,000 μm differentiates by its unique physiochemical characteristic from the underneath subsurface water (SSW). It is a micro-environment serving as a modulating media for materials synthesis, transformation and cycling in biogeochemical process including phosphorus, one of essential nutrients for marine productivity. The relatively uniform distribution of phosphorus in marine aerosols over the remote North Pacific Ocean (0.07-0.09 nmol m^{-3}, Furutani et al., 2010) without a major supply from riverine input. This may suggest the alternate contribution from seawater, as a source of phosphorus. The interface layer; SML is expected to involve in this contribution.

The composition of phosphorus in SML exhibited differently from SSW as a result of the interfacial physical and biogeochemical process. Phase distribution of phosphorus in SML is influenced by its chemical transformation in subsurface water and is governed by adsorption/desorption on particle surfaces, biological uptake and remineralization. In this study, seawater including SML were collected on 3 cruises; SWNP-2010 in the Subtropical Western North Pacific, CRI-2010 in the Coastal Sea around the Ryukyu Islands and EEP-2012 in the Equatorial Eastern Pacific region.

Total dissolved phosphorus (TDP) was a major phosphorus pool in the SML and accounted for 90-98% of total. Level of total dissolved phosphorus (TDP) was higher in High Nitrate, Low Chlorophyll-a (HNLC) seawater (TDP= 0.9 - 2 μM; EEP-2012) than the oligotrophic seawater (0.1-0.4 μM; SWNP-2010 and CRI-2010). Concentration of particulate phosphorus in SWNP-2010 and CRI-2010 were reported at 21-38 nM and 1-26 nM, for SML and SSW. In EEP-2012, particulate

phosphorus concentration in SML was similar to the aforementioned but lower in the SSW (4 – 18 nM).

Enrichment factor (EF) determined as the concentration ratio of substances between SML and SSW. For TDP, soluble reactive phosphorus (SRP) and dissolved organic phosphorus (DOP), enrichment factor were ranged from 0.7-2.5, 0.1-4.1 and 0.3-2.7, respectively. For particulate phosphorus, except the SWNP-2010, particulate organic phosphorus was more dominant in the SML. The low background concentration of particulate phosphorus (<20 nM in the SSW) contributed to higher enrichment factor and varied from 0.5 to 72.

High enrichment of particulate phosphorus (TPP) at a factor of 72 was observed in the SML sample from station 1 (0°N, 95.5°W) in EEP-2012. In this sample, concentration of particulate phosphorus rose to the same concentration level with dissolved phosphorus (SML_{TPP}=0.59 – 1.3 µM, SML_{SRP} = 0.84µM). This change was concurrently observed with high concentration of particulate iron (81 nM, EF=11). Single particle analysis by a scanning electron microscopy with energy dispersive X-ray spectroscopy (SEM/EDX) showed a greater in number of biogenic particles especially diatom and microorganism particles in the SML. Percentages of phosphorus content in single particles measured by SEM/EDX was generally higher in the SML particles than those in SSW. There were more particles ware contained with phosphorus in the SML (77%) than the SSW (11%) and the enrichment factor estimated by the SEM/EDX analysis was 75.

Thus, there was an increase of particle surface active area for the adsorption of phosphorus as a result of the increase in number of larger particles including bio-particles (diatom and other microorganism) in the SML. The vertical profiles of TPP and pFe showed also the peaks in the SML along with other particulate element namely pSi, pAl and pCa, indicating that the enhancement was occurred in the SML interior. The most probable explanation of this occurrence was that it was the resultant of the external atmospheric deposition of scarce micronutrients to the SML. Although SML

is quite a small material reservoir, its biogeochemical dynamics and properties are unique. The observed *biogeochemical enrichment* emphasizes its rapid response to external perturbation and its significant role in microbe-mediated materials synthesis and transformation of chemical compositions and their cycling.

Not only receiving substances from the atmosphere, SML is also served is the intereaction media for the bubble bursting process, supplying seawater materails and providing space for the formation of marine aerosols. Bubble bursting experiments offered the study of ocean-derived substances without such background concentration. An experiment of bubble bursting using SML, SSW and SUR (Bucket water sampling) as the bubble bursting media demonstrated that phosphurus is vastly enriched in aerosols both inorganic and organic content. Sea to air fractionation factor (F_{Na}) detemined as the factor of the concentration ratio of phosphorus to soduim between the ejected aerosols from the bubble bursting and sea water. In this study, the fractionation of phosphorus by all forms was displayed at a factor of 10^2 - 10^3. F_{Na} greater than 1 indicating the enrichment of ejected aerosols with the phosphorus derived from the seawater. The production of aerosols from the SML and SSW experiment contained less sodium content than those in the SUR experiment. However, the average total phosphorus concentration in the generated aerosols was expressed at the same level (~7 nmol m^{-3}). Therefore, comparing with sodium content, aerosols produced from SML experiment contained promisingly higher organic phosphorus. In addition, single chemical mass spectra of bubble generated particles also demonstrated that SML generated particles were enriched with organic carbon particles and it was produced in greater number in comparative to the SSW experiment and especially for submicron organic particles (D_a < 1 μm). The similar fractionation factor of organic phosphorus in the SML and SUR (a mixture of SML and SSW seawater) experiments indicated that the fractionation of organic phosphorus was specifically influenced by organic rich content in the SML.

When comparing the ratio concentration of total phosphorus to sodium between marine aerosols in the field measurement and the bubble bursting generated particles, the similar in the ratio number indicated that aerosols production from bubble bursting process had considerably contributed to certain amount of atmospheric phosphorus.

SML was able to concentrate all forms of phosphorus and demonstrated the significant enrichment towards particulate phosphorus. Beside the enrichment of substances from bulk seawater, *micro-biogeochemical response* to the natural and external perturbation increasing internal biological activity. Hence, more substances were aggregated within layer. As the media for bubble bursting process, SML influenced on the production of marine organic phosphorus aerosols, by suppressing the bigger particles formation and producing more organic aerosols into atmosphere. The presence of SML is not only the concentrated layer of various chemical substances, but it was also significant boundary for the biogeochemical process of phosphorus. The generated aerosols entrained with phosphorus from SML and bulk seawater can be dispersed in length and traveled for long distances, subsequently deposited into the surface ocean again, hence maintains the marine productivity by recycling between ocean and atmosphere.

Contents

1. Introduction

1.1. Sea-surface microlayer (SML)

Sea-surface microlayer (SML) is a boundary layer between two environmental compartments; atmosphere (fast response) and ocean (high heat capacity) where heat, energy and variety of materials can be exchanging [Donaldson and George, 2012]. This physical boundary layer covers about 70% of the earth surface, and has its significant roles in air–sea exchange of heat, gases and particles [Cunliffe et al., 2013; Wurl et al., 2006 and Liss and Duce, 1997] as well as in biogeochemical processes for material synthesis, transformation and cycling [Reinthaler et al., 2008; Wurl and Obbard, 2004; Liss and Duce, 1997; Wheeler, 1975].

The SML layer is distinguished by its differences in biological and physiochemical properties [Herdy, 1982] at which 50 μm depth has reported as a layer of sudden change where physical and chemical properties of seawater has found to change abruptly [Zhang et al., 2006]. Technically, SML thickness is measured extent from 1 to 1,000 μm depending on sampling devices, and prevailing metrological conditions [Wurl and Obbard, 2004, Stolle et al., 2011].

Various SML sampling devices were developed for SML collection in corresponding with research focuses and implications. Glass plates and drum rollers [Garret, 1965; Carlson et al., 1988] obtain typically 20 - 250 μm in depth are among the most common sampling devices [Zhang et al., 2003; Cunliffe et al., 2013]. In principle, when surface's device contacts with surface water, water adherence on sampling devices (glass, metal mesh and Teflon) was collected and determined as SML samples. The thickness was calculated based on sample volume and contact-surface area of the device and is varied by sampling devices and operations [Carlson, 1982, Liss and Duce, 1997].

1.1.1. SML structure

Recent study showed that SML components are relatively more complex and biologically involvement. Conventional view (**Fig. 1.1.1**) described SML as sub-strata of lipid layer over water associated organic substances layer and comprised mostly with polysaccharides, carbohydrates and proteins [Hardy, 1982]. However, the latest findings reviewed SML as hydrate gelatinous matrix (non - stratified) structure comprised with polymeric carbohydrates, proteins, and lipids [Cunliffe and Murrell, 2009; Wurl and Holmes, 2008]. Its condensed and derivative products are primarily derived from microbiological activities in bulk seawater.

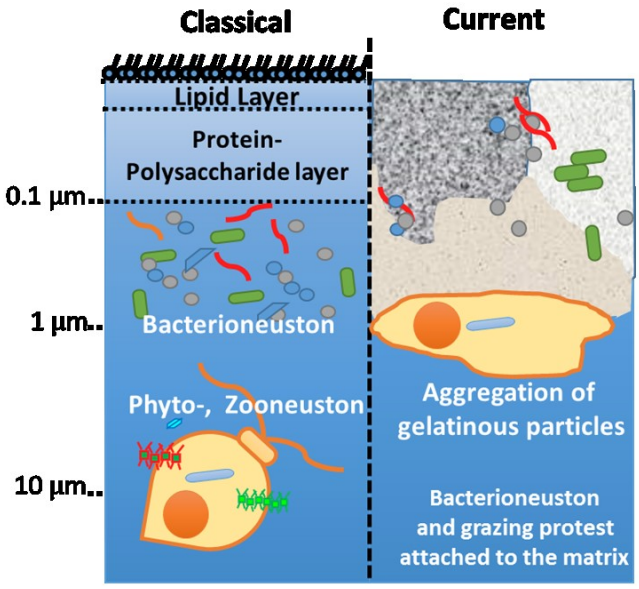

Fig. 1.1.1. Depth view structure of the sea-surface microlayer in the classical sub-layer concept (left side) and the current conceptual view (right side) [Cunliffe et al, 2011 and Hardy 1982].

1.1.2. SML source and its interfacial physical renewal and removal process

Substances in SML come from 2 sources. First, the upward flux that brought up substances from underlying water. Most materials derived as byproducts of biological activities such as respiratory or assimilation and are extensively associated with organic materials (see upward flux

of the buoyant particles; **Fig. 1.1.2**). The second source of materials is a downward flux in which particulate substances are deposited from the atmosphere [Frka et al., 2012; Duce et al., 1991]. Airborne particles are those originated from natural sources such as dust, pollen and plant materials or from anthropogenic sources such as fertilizers, waste and combustion products. Since, the former source are mostly surface affinity species; consequently, it can lowering surface tension and enduring the accumulation of atmospheric deposited materials in the SML. Particles dry deposition flux has reported to increase by 2-3 folds during low surface tension observed [Del Vento and Dachs, 2007].

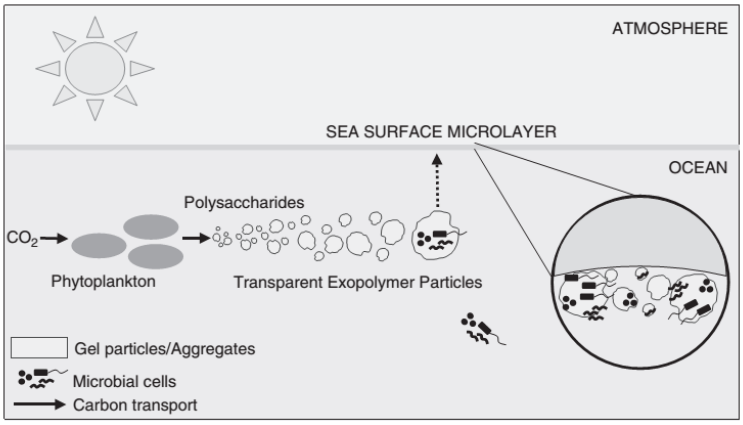

Fig. 1.1.2. Formation of buoyant particles; transparent exopolymer particles in bulk seawater [Cunliffe and Murrell, 2009]

SML layer can be dynamically modified by the near-surface turbulence such as wave breaking, share, convection, or raindrops. Micro-scale wave breaking (0.1–1 m in length, 2-3 cm in amplitude) produces convergence flow that leads to the intense renewal of subsurface water and is often occurred more widespread than white capping [Soloviev and Lukas, 2006]. Beside, substances from bulk seawater is brought up by diffusion, turbulent mixing and absorption on to bubble floatation and buoyant particles (**Fig. 1.1.3**) [Frka et al., 2012; Liss and Duce, 1997 Xhoffer et al., 1992].

On the contrary, wave dissipation, evaporation, microbial degradation, photo-oxidation, micellization and adsorption on sinking particles and bubble bursting are the removal processes that draw down substances from the SML [Gladyshev, 2002, Liss and Duce, 1997, Xhoffer et al., 1992, Hardy, 1982].

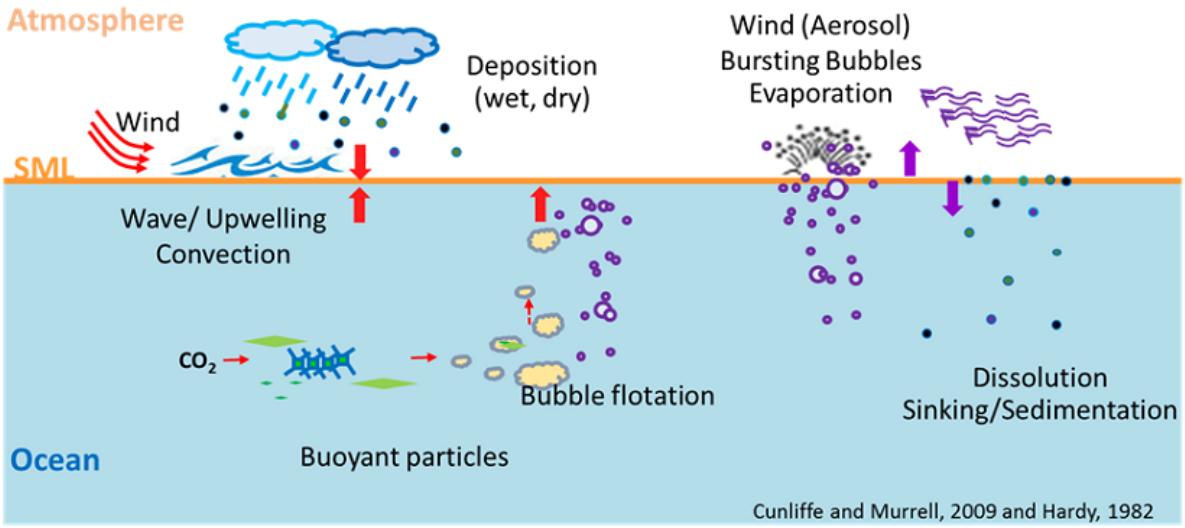

Fig. 1.1.3. The schematic diagram of physical interfacial processes influencing materials transportation at the interface; SML. Red arrows showed the renewal process in which supply substances and materials to the SML and the purple arrows showed the removal process [modified from Cunliffe and Murrell, 2009 and Hardy, 1982].

1.1.3. SML enrichment

Higher concentration of substances in the SML than those subsurface water is so called the enrichment. It is one of well acknowledged characteristics of the SML. The enrichment factor (EF) expresses in term of the concentration ratio of chemical in the SML over the sub-surface water or atmosphere [Liss and Duce, 1997].

SML is able to accumulate both dissolved and particulate substances to certain degree depending on chemical partitioning and surface stabilization. Generally, enrichment is determined

by its chemical phases and properties, e.g. speciation, solubility, surface active site for complex-ligand binding and organic composition [Hardy, 1982, Xhoffer et al., 1992; Hunter, 1980]. The surface active components can enhance the accumulation of atmospherically deposited materials including metals [Hardy et al., 1985] as well as to decrease the diffusive air–water exchange of gases together with other key factors such as wind stress, gas transfer velocity, surface wave slope [Liss and Duce, 1997; Frew et al., 2004].

Reported EF of materials were varied depending on its species, approximately from 1 to 3 in dissolved organic carbon, organic nitrogen and inorganic nutrient, and 3 - 38 and 2 – 100 for particulate organic carbons and particulate trace metals, respectively [Gladyshev, 2002; Liss and Duce, 1997; Hunter, 1980; Carlson, 1983 and Hardy, 1982]. These values suggested the selective accumulation for organic species and particle adsorption associated with surface active components [Liss and Duce, 1997; Cauwet, 1978]. High concentration of trace metals in the SML is the results from metal complexation with organic ligands and particulates [Wurl and Obbard, 2004].

Not only chemical enrichment, distinct assemblage of virus, bacteria (Bacterioneuston) and phytoplankton (Phytoneuston) in SML were reported and showed its adaptive strategy to survive in organic rich and intense light environment. An abundance of microbial community (in 2-4 order of magnitude) was reported to accumulate in the SML as a result of prevailing metrological conditions such as wind speed but not in association with particulate organic carbon contents [Stolle, et al., 2011; Franklin et al., 2005]. Another suggestions for microbial enrichment is that high production can be maintained under the increase of growth in the SML luxury resources with less predators [Aller, et al., 2005]. However, the observation of lower chlorophyll-a measurement during daytime is suggested to cause by passive accumulation of phytoplankton from advection [Joux et al., 2006]. This is except for the heterotrophic and autotrophic nanoflagellate that made its

rapid colonization on the surface as it is preferable to the intense light environment [Baastrup-Spohr and Staehr, 2009; Joux et al., 2006].

1.1.4. Bubble production and its related mechanisms to the SML formation

Bubbles are extensively contributed to the dynamic of air sea exchange of heat, energy and substances and are mediating the interfacial physiochemical interaction and geochemical cycling of substances in SML and surface water [Grammatika and Zimmerman, 2001]. It is generated either by wave braking at the depth of 0.5-3 m, precipitation or gaseous diffusion from biological process such as O_2 bubble from photosynthesis [Blanchard, 1989]. However, most bubbles in the ocean are produced by wave braking or white caps [Hultin et al., 2011].

At sea surface, air entrapment in seawater produced by wave braking creates bubble cloud that vertically reach surface [Blanchard, 1989]. Bubbles can disperse to depth by surface wave and turbulent mixing (**Fig. 1.1.4**). During it submerges, gas is slowly exchanged via bubble surface or forced by deeper pressure to compress and enclosed gas to solution [Grammatika and Zimmerman, 2001].

Bubble floatation as a scavenging process is very important for passive transportation of substances to sea surface. When bubbles rapture and burst, sea spray droplets are generated as jet droplets (larger-supermicron) and film droplets (smaller-submicron) [Blanchard, 1989]. These sea salt droplets as the primary marine aerosols are then suspended in the atmosphere [Lewis and Schwartz, 2004]. The observation of organic content in aerosols from bubble bursting experiment has suggested that SML has an influence on the surface-controlled process of bursting [Hultin et al., 2010]. Such marine aerosols consisting of sea salts and organic compounds are contributed to the global load and have the consequent impact to global climate [O'Dowd, et al., 2004]. Since, it has served also as cloud condensation nuclei (CCN), affecting the scatter of solar radiation and affecting

indirectly to global warning [IPCC, 2007]. In addition, the plume of bubble bursting can also cause disruption and removal of the SML [Hultin, 2010].

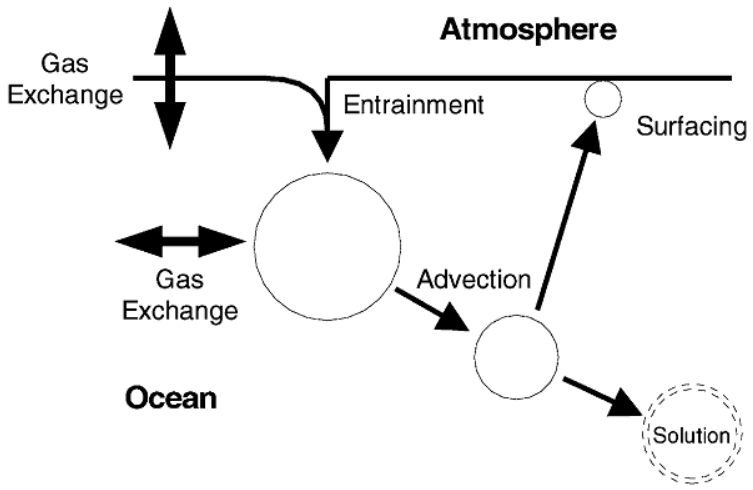

Fig.1.1.4. Air-sea exchanges; cycle of bubble formation and related process. Rate of bubble mediated mass transfer depends on the rate of bubble generation, advection and dispersion. [Grammatika and Zimmerman, 2001]

1.1.5. The SML distribution and its biogeochemical importance

Among the interfacial physical parameters, wind speed has been studied more extensively for its impact towards the persistence of SML. In nature, SML generally withstands to even at wind speed above the global average of 6.6 m s^{-1} [Wurl et al., 2011]. An increase of wind speed was related to the excess concentration of particulates in the SML [Lui and Dickhut, 2008]. Enrichments of dissolved organic carbons and amino acids has also reported in the SML even at wind speed exceeding 7.5 ms^{-1}. Moreover, even at higher wind speed regime (9.5 m s^{-1}), enrichment of surface active components in SML were detected [Wurl et al., 2011].

Data from the global average of wind speed in summer and winter (**Fig. 1.1.5**.) and the global ocean coverage of the SML (**Fig. 1.1.6**). It has been demonstrated that the Southern and North Atlantic Ocean during fall and winter are the only free surfactant (proxy of SML) coverage regions [Wurl et al., 2011].

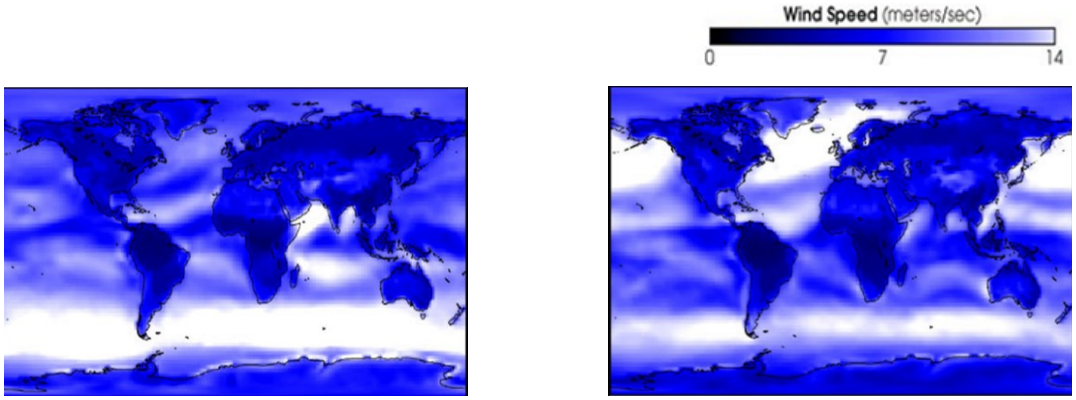

a) July b) January

Fig. 1.1.5. The global average wind speed (m s^{-1}) in (a) summer and (b) winter http://visibleearth.nasa.gov/v

In addition to wind speed, organic content in SML has influenced on its physiochemical properties by reducing short wave amplitude and developing critical wind speed [3-4 m s^{-1}; Liss and Duce, 1997]. A slope spectrum of small-scale waves and gas transfer velocity also attenuated [Frew, et al., 2004]. These developed condition has been reported in companion with a large scale biological productivity and an increase of dissolved organic carbon concentration [Frew, et al., 2004]. The study on air-sea CO_2 fluxes also suggested that natural surfactants (e.g. biological activities derived products) in SML could reduce the ocean CO_2 uptake and at least by 20% of the global net CO_2 flux under the moderate wind speed [Tsai and Lui, 2003].

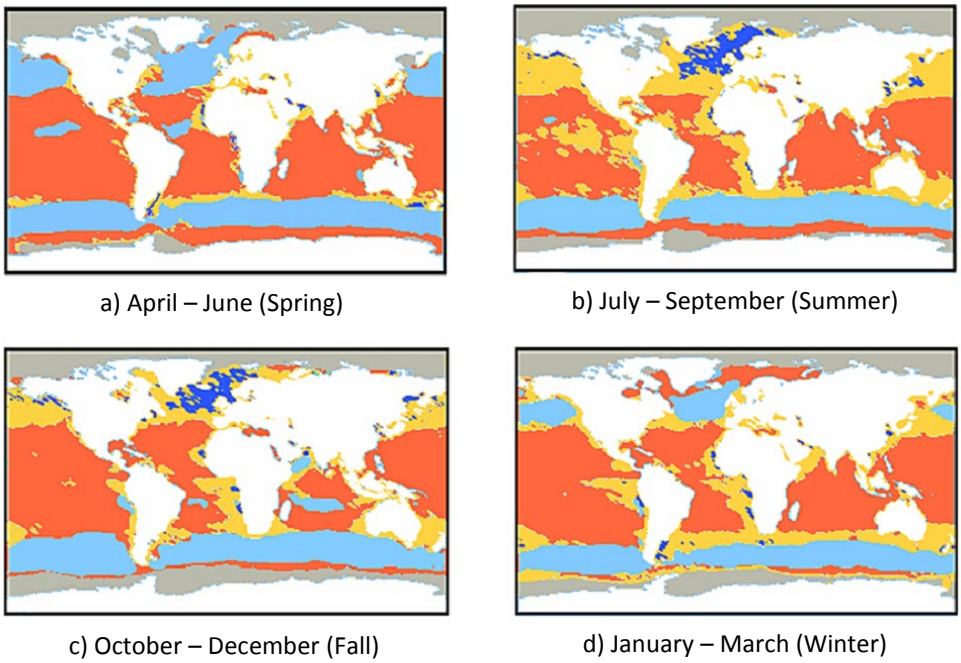

Fig. 1.1.6. Global distribution of SML surface coverage using enrichment factor of surfactant as the SML proxy and extrapolated with global maps of primary production.
Enrichment factor (EF) displayed in color as; Red for EF>2, Yellow for EF=1.5-2,
Dark blue for EF=1-1.5, and Light blue for non en enrichment (EF<1) [Wurl et al., 2011].

1.2. Phosphorus

1.2.1. Sources and s inks of phosphorus in ocean

Phosphorus is an essential element for living organisms and is required for the components of cellular and genetic materials. In ocean, main contributors of phosphorus are those terrestrial materials from the continental weathering processes and are transported to ocean via river (**Fig. 1.2.1**) [Ruttenberg, 2003]. Phosphorus in particulate phase exists mainly as apatite and phosphorus minerals. It incorporating with iron-manganese oxide/ hydroxides can rapidly remove by the sedimentation at the continental shelf [Paytan and McLaughlin, 2007]. Hence, loading of riverine phosphorus to ocean is mostly in dissolved forms. Dissolved phosphorus loading to ocean is

increased through the release of phosphate adsorbed on clay particles when salinity increased [Paytan and McLaughlin, 2007] and through anthropogenic inputs as river discharges (e.g. fertilizers, sewage, and paper and pulp manufacturing). Such anthropogenic inputs increase in double since pre-anthropogenic period and often lead to coastal eutrophication [Ruttenberg, 2003]. Later, dissolved phosphorus concentration is subsequently modified by sorption/desorption on the particle surface by salinity and redox condition changes, in addition to biological uptake and remineralization [Benitez-Nelson, 2000].

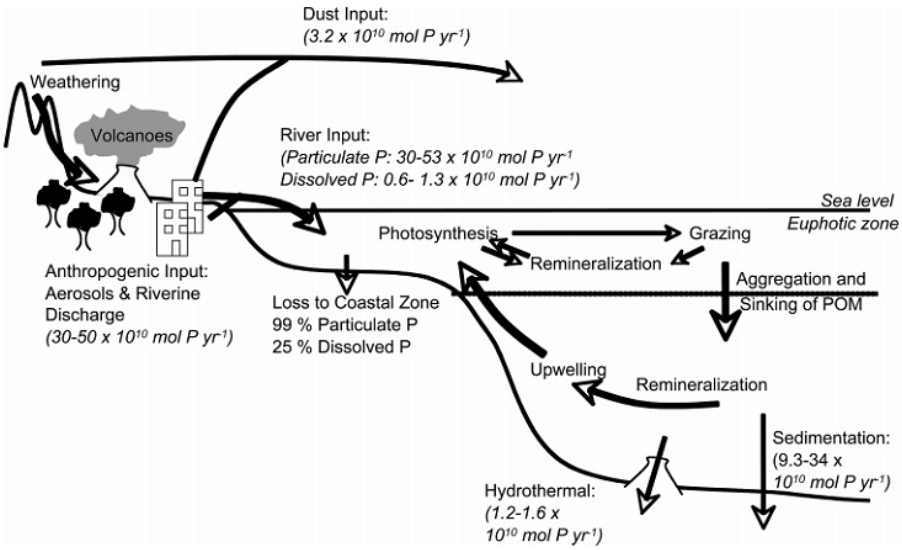

Fig. 1.2.1. The marine phosphorus cycle and flux (in italics)

[Paytan and McLaughlin, 2007]

Atmospheric deposition (**Fig. 1.2.2**) is the second most important phosphorus contribution to the net gain of ocean productivity of 560 Gg P a^{-1} with an estimate of 82% and 12% of total deposition from mineral aerosols and primary biogenic particles, respectively [Mahowald et al., 2008]. Phosphorus baring minerals often bound with Fe-oxides or associated with Ca and Al contain

similar phosphorus content like the earth's crust [0.09 wt%; Paytan and McLaughlin, 2007; Taylor, 1964]. However, concentration is variable depending on the soil types and its origins. Overall, total contribution of atmospheric source is less than 10% of riverine input [Graham and Duce, 1982] and are often low solubility and less bioavailability. Volcanic activity and hydrothermal process irregularly supplies additional reactive phosphorus to the ocean in forms of volcanic gases (condensed water soluble polyphosphate) and hot stream [Benitez-Nelson, 2000].

Particulate sedimentation on seafloor is the only process of the phosphorus oceanic sink. Phosphorus can be removed from water column by 1) organic matters burial, 2) phosphorus sorption and precipitation with iron hydroxides, 3) phosphorite burial and 4) hydrothermal process [Benitez-Nelson, 2000]. Sediment trap experiment showed that acid- insoluble organic phosphorus is the major deposition (40%) with the followings authigenic phosphorus (25%), and oxides associated phosphorus (21%) [Paytan, et al., 2003].

To date, an anthropogenic phosphorus inputs to the ocean via atmosphere by fertilizers, pesticides and biomass burning have increased [Paytan and McLaughlin, 2007; Mahowald, et al., 2008] and it estimates that the global inputs of atmospheric source is accounted for 15% of total phosphate [Mahowald, et al., 2008]. This number has yet fully accounted for phosphorus related to combustion emission that can make up to 50% for the global atmospheric source of phosphorus [Wang et al., 2014].

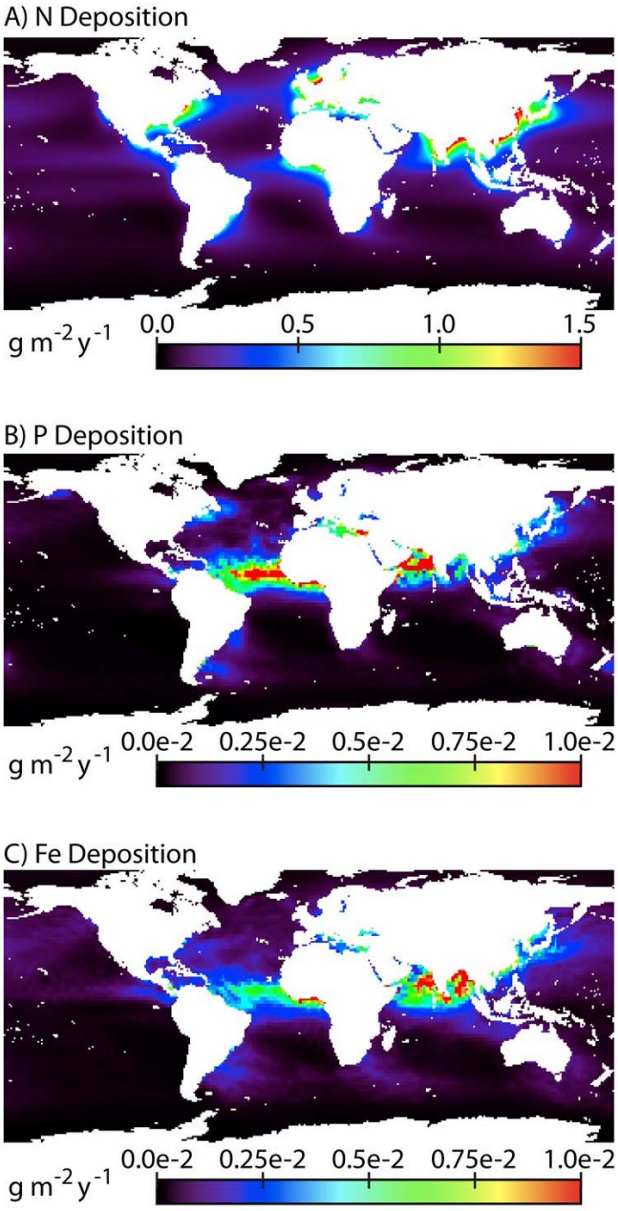

Fig. 1.2.2. The estimate global atmospheric deposition of limiting nutrients a) Nitrogen, b) Phosphorus and c) Iron [Okin et al., 2010]

1.2.2. Phosphorus composition and transformation in water column

Phosphorus in seawater exists in both organic and inorganic forms and either in dissolved or particulate phases and is segregated by the filtration procedure. Solution passed through a membrane filter (0.2-0.45 μm pore size) is defined as total dissolved phosphorus (TDS) which can further be characterized by its reactivity with phosphomolybdate complex to the soluble reactive phosphorus (SRP) and non-soluble reactive phosphorus (SNP). Interchangeably, dissolved organic phosphorus (DOP) is often utilized instead of SNP. SRP comprises dissolved inorganic compounds in which orthophosphate is the major constituent [Paytan and McLaughlin, 2007] (**Table 1.2.1**.) while, DOP is consisted notably of dissolved organic phosphorus and biological derived compounds such as monophosphate esters, nucleotides, nucleic acids, phospholipids, phosphonate and polyphosphate (the non-reactive inorganic compounds) [Benitez-Nelson, 2000; Strickland and Parson, 1972].

Particulate phosphorus mostly produces through biological process and recycled within water column [Lin, et al., 2012]. Total particulate phosphorus (TPP) can characterize to particulate inorganic phosphorus (PIP) and particulate organic phosphorus (POP). PIP comprises with the precipitates of 1) phosphorus minerals 2) phosphorus-adsorbed on biotic and abiotic particulates and 3) precipitates such as orthophosphate, pyrophosphate and polyphosphate in intracellular storage products [Yoshimura et al., 2007, Paytan and McLaughlin, 2007]. The organic particulate phosphorus, e.g. phosphorus esters, phosphorus diester, and phosphonate, were incorporated broadly with living and non-living organic matters [Paytan and McLaughlin, 2007].

Vertical profile (**Fig. 1.2.3**) of phosphorus shows the nutrient type profile with surface depletion and deep water enrichment of SRP. Dissolved phosphorus is taken up extensively by marine organisms. For particulate phosphorus, it is associated with biogenic particles or

incorporated into or adsorbed on to iron hydroxides. Remineralization of particulate phosphorus released dissolved phosphorus at depth and is recycled by upwelling. The turnover time of phosphorus in surface waters is considered to be very rapid and reported to less than a day to two weeks [Paytan and McLaughlin, 2007].

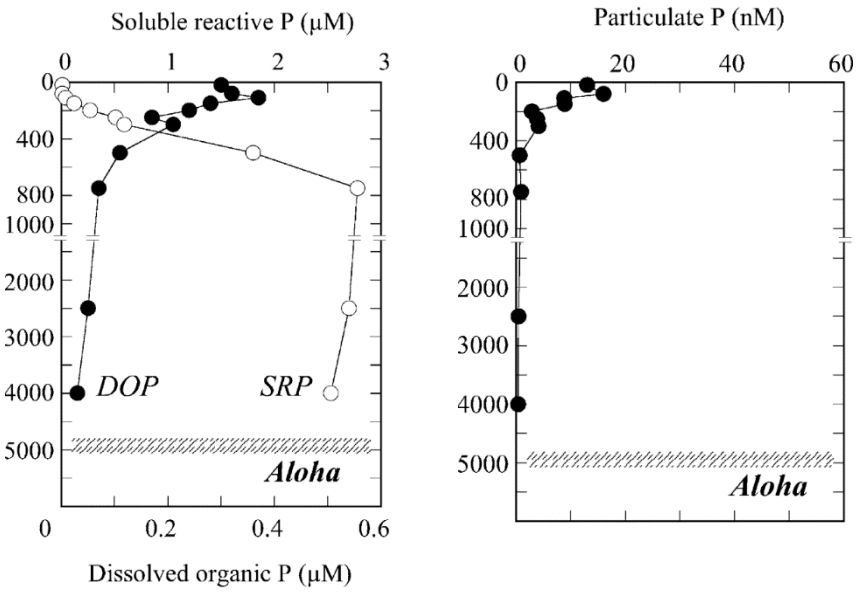

Fig. 1.2.3. Depth profile of soluble reactive phosphorus (SRP), dissolved organic phosphorus (DOP) and particulate phosphorus (PP) at Station Aloha near Hawaii (the shaded bars indicated sea floor) [Suzumura and Ingall, 2004]

The biological cycling and microbial reminerization are the primary pathways for phosphorus transformation. Reactive dissolved inorganic phosphorus is assimilated by phytoplankton and latterly altered and stored as the intercellular phosphorus compounds [Paytan and McLaughlin, 2007]. Polyphosphate and most dissolved organic phosphorus can be hydrolyzed by synthetic enzyme's marine bacteria and phytoplankton to sustain the phosphorus requirements, but in the different rates and efficiencies [Karl and Tien, 1997]. Much of this phosphorus transformation occurs in the upper water column and is involving extensively with biological

activities. Particulate phosphorus measured in the North Pacific water exhibited a good correlation with chlorophyll-a concentration, indicating its association with plankton cells [Yoshimura, et al., 2007]. In particular, the deviation of the Redfield ratio has attributed to surface adsorption of phosphorus rather than to biological processes, suggesting the scavenging phosphorus influences more on the interpretation of marine nutrient inventories [Sañudo-Wilhelmy, 2004].

Table. 1.2.1. Forms and distribution of phosphorus; in dissolved inorganic phosphorus (DIP), dissolved organic phosphorus (DOP) and particulate inorganic phosphorus (PIP) and particulate inorganic phosphorus (POP) in seawater from different ocean provinces. All displayed values were for surface water [Lin et al., 2012].

Study area	DIP (μM)	%DIP	DOP (μM)	%DOP	PIP (nM)	%PIP	POP (nM)	%POP
North Pacific Ocean								
Eastern	0.26	53	0.229	47	12.73	42	17.93	58
Equatorial	0.43	67	0.21	33				
Subtropical	0.01	3	0.3	97				
Subtropical	0.01–0.02	12–19	0.1–0.13	81–88	1–5	5–36	9–12	64–95
Subtropical-subarctic transition	0.05–0.17	25–50	0.14–0.17	50–75	1–7	6–21	17–58	79–94
Subarctic frontal zone	0.08–0.47	40–75	0.11–0.16	25–60	2–29	5–28	41–76	72–95
Northwest subarctic	1.01–1.42	85–91	0.14–0.22	9–15	5–14	9–17	51–110	83–91
Northeast subarctic	0.7–1.1	77–86	0.18–0.21	14–23				
Arctic Ocean								
Bering Sea	0.90 ± 0.47	89 ± 15	0.09 ± 0.11	11 ± 15	61 ± 62	79 ± 13	10 ± 7	21 ± 13
Chukchi–Beaufort seas	0.62 ± 0.10	82 ± 17	0.17 ± 0.17	18 ± 17	23 ± 8	83 ± 10	5 ± 4	17 ± 10
Atlantic Ocean								
Northeast	0.01	7	0.13	93				
North subtropical	0.009	10	0.08	90				
South subtropical	0.21	58	0.15	42				
Southern Ocean	1.07	83	0.216	17	27.61	67	13.48	33

1.3. The SML study prospective

The SML study has been limited by sampling procedures and devices. For different purposes of study, different sampling techniques is utilizing and the results are incomparable. The biogeochemical study on the SML aspects is even more scatted depending on the interests and often in non-continuity. Since, SML poses the wider effects to the global scale of air-sea exchanges of gas and energy and to the biogeochemical cycling of substances in the ocean. To understand the SML in its wider Earth system context, atmospheric deposition of terrestrial dust and organic

particles is further suggested to be studied in cooperative with SML by the parallel sampling initiatives [Cunliffe et al., 2013]. To date this approach has yet fulfilled because of the different time constrained of each sampling techniques. Recent study informed that salinity has affected on SML composition, molecular structure and optical properties [Lechtenfeld et al., 2013]. This addressed the needs of the study on the environmental condition affected molecular structure of SML formation.

1.4. Objective and goals

In this study, phosphorus is selected for the observation of an interaction of substances between atmosphere and ocean. The initiative work comes from the observation of the relatively uniform concentration of phosphorus in marine aerosols over the remote North Pacific Ocean [Graham and Duce, 1979; Furutani et al., 2010]. With disregarding to the source distances, it is suggested to the alternative source of phosphorus that moderating such consistency. The high organic component and particulate matters in SML and its interfacial position between these two environmental compartments has suggested and called for the interest point of this study.

In this study, I attempt to compare the concentration and composition of suspended particulate phosphorus in aerosols and in seawater. The objectives of this study are

1) Determine the difference of composition and forms of phosphorus in the atmospheric and oceanic suspended particulate matters including the SML

2) Characterize chemical composition of particles by size in SML and SSW sample observed the enrichment event during the research cruise in the Eastern Equatorial Pacific Ocean and the possible causes contributed to such event

3) Understand the mechanism of bubble bursting experiment, its sea to air fractionation for phosphorus and the influences of SML towards the formation of atmospheric phosphorus

2. Material and Method

2.1. Research expeditions

Three expeditions were conducted in this study with two open ocean cruises on the R/V Hakuho Maru and near coastal cruise on the R/V Tansei Maru. The following are the cruise tracks and description of each research expedition in different geographic provinces.

1) The Subtropical Western North Pacific cruise (SWNP-2010)

This cruise was carried out in spring time during May 18th-June 4th, 2010 in the Subtropical Western North Pacific (SWNP) on the survey transect line 137°E from 30°N (St. 02) to 15°N (St. 05) at 5° interval. The transect featured the oligotrophic water of the North Pacific Subtropical Gyre where phosphorus, nutrients and surface chlorophyll-a in seawater presented in relatively low concentration. In this cruise, 5 SML samples from St.02, St.04 and St.05) and 19 aerosol samples and 6 blanks were collected (**Fig. 2.1.1**). This line transect has reported the influences of the atmospheric input of anthropogenic substances from inland industry. The mean concentration of atmospheric phosphorus in this region was measured at 0.24 nmol m^{-3} (Furutani et al., 2010). Wind speed recorded during SML sampling was ranged at 3 - 6.1 m s^{-1} and chlorophyll-a concentrations were at 0.01 - 0.05 µg L^{-1}.

2) The Coastal Sea around the Ryukyu Islands cruise (CRI-2010)

This cruise was carried out in summer time during September 25th - October 3rd, 2010 off the coast around the Ryukyu Islands. The cruise started from Kagoshima port, sailed east and turned to the direction for Naha then made left return around Okinawa Island and cruised back to Nagasaki port. On this cruise, 3 SML samples at St. 04, St. 07 and St. 09 (**Fig. 2.1.2**) and 7 aerosol samples with 3 blanks were collected. Wind speed recorded during the sampling was relatively low and

ranged at 1.5-2.6 m s^{-1}. The surface chlorophyll-a concentration were 0.03 and 0.02 µg L^{-1} at St.04 and St.07 and increased to 0.15 µg L^{-1} at St.09.

3) The Eastern Equatorial Pacific Cruise cruise (EEP-2012)

This cruise was carried out in winter time during the survey transect at the Eastern Equator Pacific from 95.5°W (St. 01) to 140°W (St. 10) during January 29th - February 19th, 2012. Five SML samplings were conducted at 5 stations (**Fig. 2.1.3**) and 10 surface SPM samples were collected. This cruise was part of the Equatorial Pacific Ocean and Stratospheric/Troposphere Atmosphere Study (EqPOS) campaign to find the biogeochemical linkages between ocean and atmosphere in the Eastern Equatorial Pacific (EEP), the remote area characterized with less anthropogenic impacts from the continent, features a High Nitrate, Low Chlorophyll-a (HNLC) condition, and was the largest source of oceanic CO_2 emission to the atmosphere. Wind speed recorded during the sampling was at 1.1-4.4 m s^{-1}. Surface chlorophyll-a concentration were ranged at 0.15 - 0.37 µg L^{-1}.

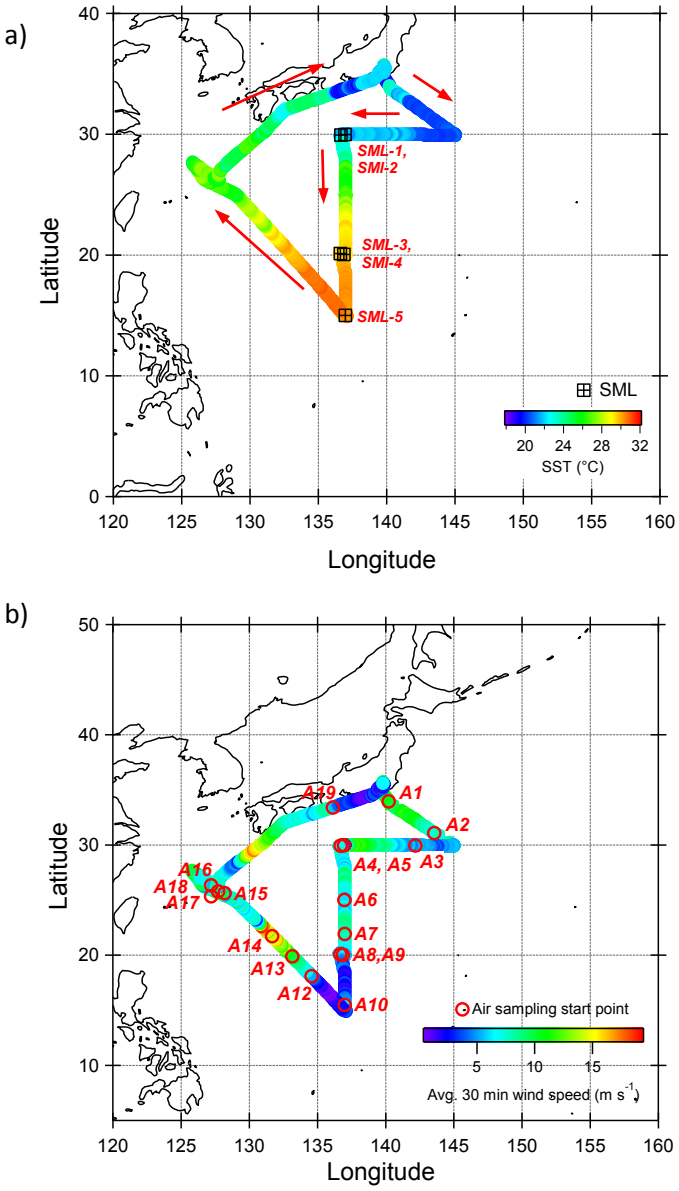

Fig. 2.1.1. Ship track of Subtropical Western North Pacific (SWNP-2010) on the R/V Hakuho Maru demonstrated in a) sea surface temperature (°C) with the SML (black open square) sampling location and b) an average wind speed 30 min (m s^{-1}) with the start point of each air sampling (open circle).

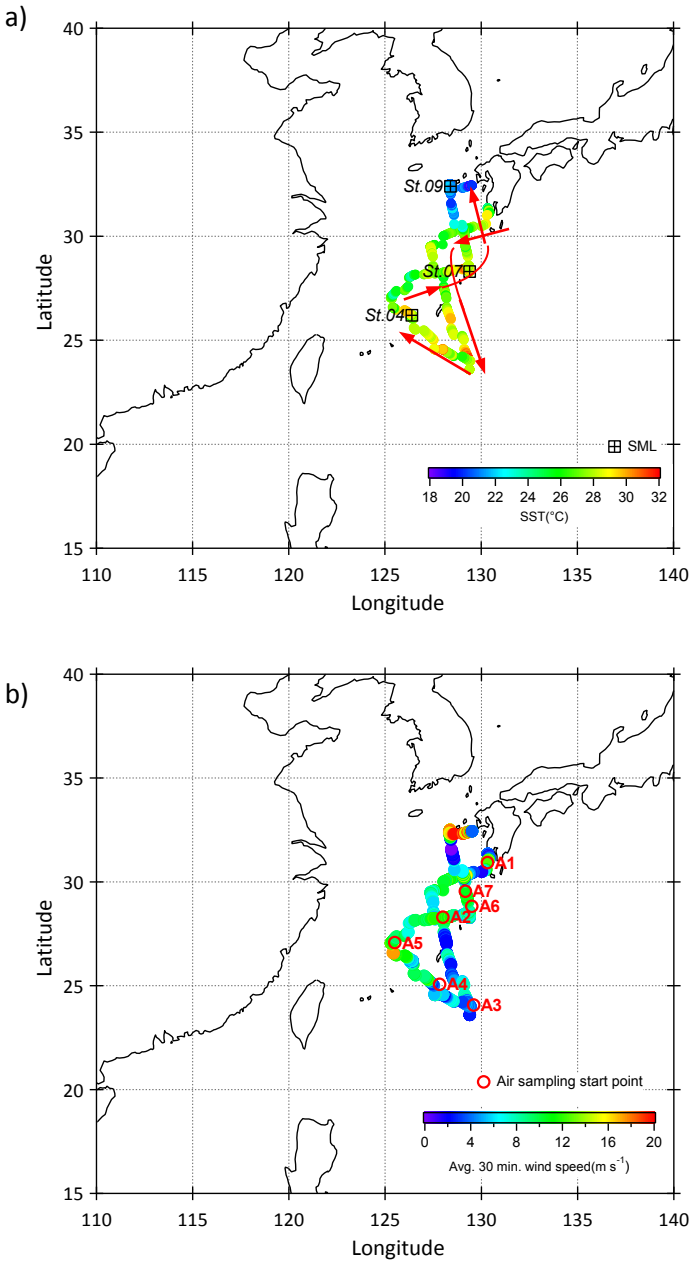

Fig. 2.1.2. Ship track off the Coastal Sea around the Ryukyu Islands (CRI-2010) on the R/V Tansei Maru demonstrated in a) sea surface temperature (°C) with the SML (black open square) sampling location and b) an average wind speed 30 min (m s^{-1}) with the start point of each air sampling (open circle).

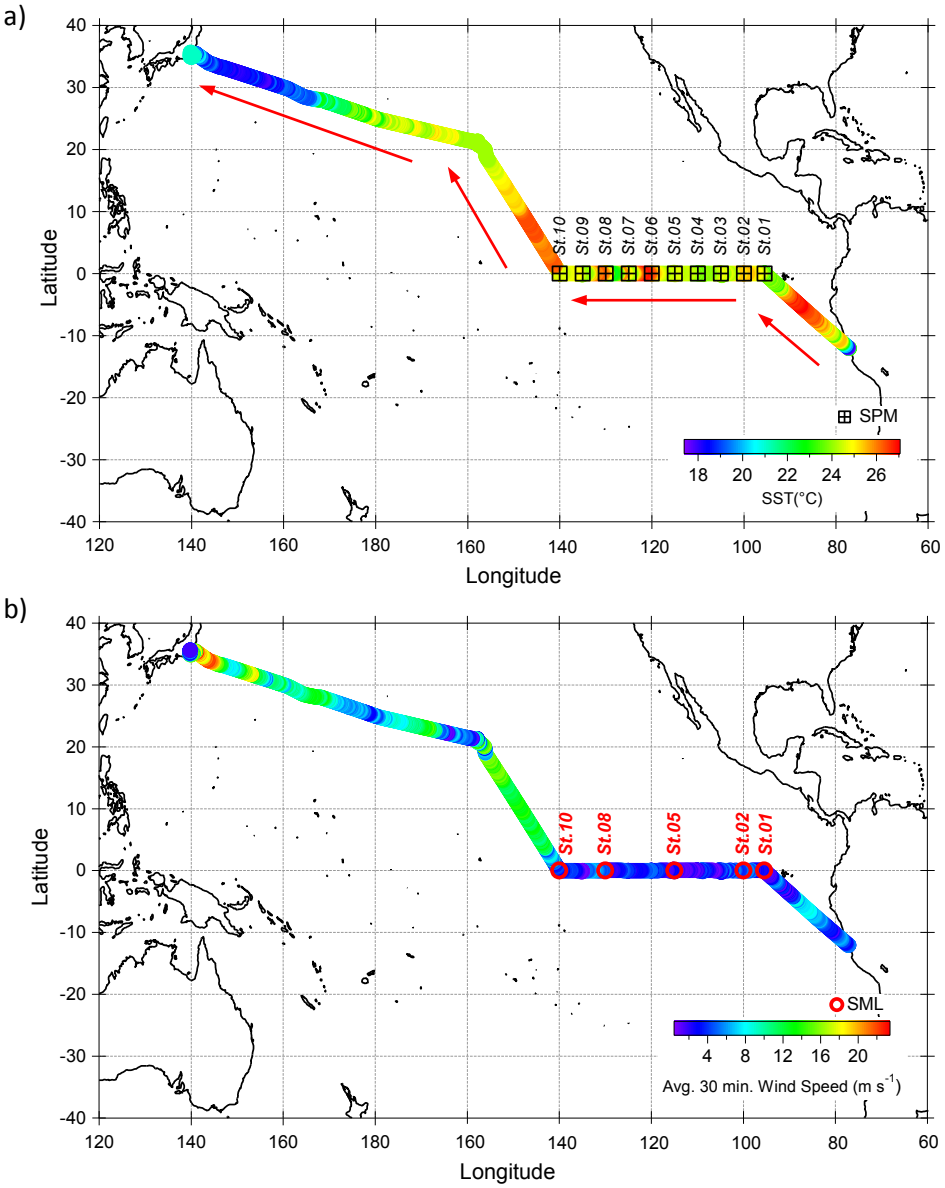

Fig. 2.1.3. Ship track of the Eastern Equatorial Pacific Cruise (EEP-2012) on the R/V Hakuho Maru demonstrated in a) sea surface temperature (°C) with the surface SPM (black square) sampling location and b) an average wind speed 30 min (m s^{-1}) with the SML (red open circle) sampling location

2.2. Environmental Sampling

In this study seawater including surface microlayer (SML) sample were collected and filtered through a 0.4 um membrane filter and a glass filter. Filters and filtrates were kept frozen for the phosphorus analysis. Particulate phase particle retained on a membrane filter was analyzed for the elemental composition by an energy dispersive X-ray fluorescence spectrometer (ED-XRF, Kimoto electric, Model MXF-01). The atmospheric particles were collected by a high volume sampler on quartz filters that were kept frozen in the sealed plastic bags until further analysis. Details on each environmental sampling described in **Table 2.2.1**.

2.2.1. Sea-surface microlayer (SML) sampling

Sea-surface microlayer (SML) sampling was performed in pair with subsurface water (SSW, at 1.5m depth by sinking an empty cleaned narrow mouth bottle with a weight) under calm sea surface condition on a small work boat with a distance approximately 500 m upstream and upwind from the mother research vessels i.e., R/V Hakuho Maru or R/V Tansai Maru (**Fig. 2.2.1**).

SML samples were collected by two sampling methods; a glass plate (SML-GP) and a Polymethyl Methacrylate (PMMA) rotating drum (SML-D) which have been suggested for one of the best scientific SML sampling practices [Cunliffe et al, 2013]. Based on a principle, about 20 - 150 µm of surface seawater adhered to the samplers' surface due to the different of viscous retention [Liss and Duce, 1997]. The glass plate sampler (surface area of 0.18 m^2) vertically immersed into seawater and withdrawal with an approximate speed of 20 cm s^{-1} [Harvey and Burzell, 1972], the adhesive surface seawater retained on the glass plate was wiped with a polypropylene wiper and collected into pre-acid washed polypropylene bottles. The collected volume divided by the total surface of collection resulted in the thickness layer.

The in-house PMMA rotating drum sampler (**Fig. 2.2.1**) with surface area of 0.79 m^2 was operated manually with an approximate rotating speed of 6 rpm [Harvey, 1966], adhesive seawater retained on the drum surface was wiped out with a polypropylene wiper into collection bottles. The collected volume divided by the total surface area of collection resulted in the thickness layer.

To prevent a contamination from atmospheric side, most part of the rotating drum was covered with a polypropylene hood. Prior sampling, rotating drum and glass plate ware kept covered with a cleaned polypropylene sheet to prevent a contamination from particles or dust. In every sampling, the first sample was utilized to rinse the devices and discarded.

After sampling, all parts of sampling devices contacted with sampling water were rinsed thoroughly with Milli-Q water (>18 MΩ cm–1; Millipore Co.) and dried in oven and kept under in a clean polypropylene box to prevent the contamination from particles and dust, while rest of the sampling devices and other related equipment were rinsed vigorously with freshwater, air dried and covered with a clean sheet until for the next experiment.

Determination of SML thickness

SML thickness (σ) can be calculated by divided the obtained sampling volume over the total surface area (obtained by the surface area of sampling devices multiply by the number of drum rotating or glass plate dipping). From these two methods; SML-D and SML-GP, the SML thickness calculated from 3 cruises were ranged between 20 – 47, 23-56 and 31-56 μm, for SWNP-2010, CRI-2010 and EEP-2012, respectively. The summary of sample locations, meteorological parameter and SML thickness displayed in **Table 2.2.2** and details of each SML samples in term of number of dipping or rotating and total volume of SML samples were given in the **Table 2.2.3**. The mentioned numbers of the thickness was in the same range with the 'physical and chemical properties' layer of sudden change (50±10 μm) [Zhang et al., 2003]. However, the deviation of thickness can be

differently resulted from the efficiency of collection devices and meteorological conditions. It is reviewed that the thickness of SML especially SML-GP was affected with the wind speed and have less significant influence from water temperature and salinity [Carlson, 1982; Cunliffe and Wurl, 2014; and reference therein].

Table 2.2.1. Summary of the sampling procedures for different environmental media from 3 research cruises; SWNP-2010, CRI-2010 and EEP-2012.

Environmental Media	**Method**			
	Collection method	**Samples**	**Analysis**	**Cruises**
Atmospheric suspended particles	High volume air sampler	Quartz Filters 90 mm in diameter	Phosphorus and XRF	SWNP-2010 and CRI-2010 for 24 h- cycle
	Bubble bursting experiment	Membrane and glass filters (47 mm diameter)	Phosphorus and XRF	EEP-2012
Sea surface microlayer (SML) pairing with subsurface water (SSW)	Drum and glass plate on the small boat	Particulate on glass and membrane filters and filtrate seawater (0.4 µm pore size)	Phosphorus and XRF	SWNP-2010 at St.02, St.04 and St.05 CRI-2010 at St.04, St.07 and St.09 EEP-2012 at St.01, St.02, St.05, St.08 and St.10
		Filtrate and unfiltered seawater	MAGIC-SRP	
Surface water and at depth	On board bucket sampling for surface	Particulate on glass and membrane Filters and filtrate seawater (0.4 µm pore size)	Phosphorus, Ion chromatography and XRF	EEP-2012 at St.01, St.02, St.05, St.08 and St.10 for 0m, 5m, 10m, 50m, 100m, 200 m and surface chlorophyll maximum depth (SCM)
		Filtrate and unfiltered seawater	MAGIC-SRP	

a) SML sampling by rotating drum

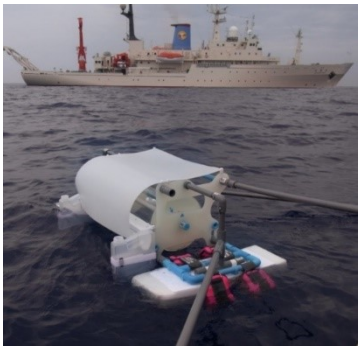

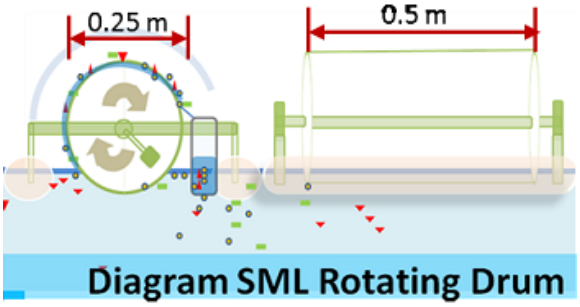

b) SML sampling by glass plate

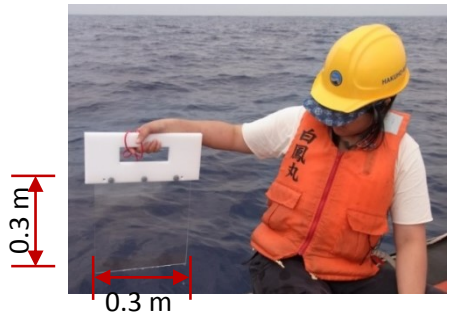

c) SSW sampling by bottle at depth 1.5 m

d) on board bucket water sampling

Fig. 2.2.1. Photos during the sample collection and diagram of sea-surface microlayer by a) rotating drum (SML-D), b) glass plate (SML-GP) and subsurface water (SSW) sampling on c) small boat (at 1.5 m depth) and d) on board with clean bucket water sampling (at 0.3 m depth)

Table 2.2.2. Summary of the SML thickness and meteorological variables on the SWNP-2010, KT-10-21 and EEP-2012

Station	Date	Start	Stop	Location	Water (°C)	Air (°C)	WS ($m\ s^{-1}$)	Salinity (psu)	Chl-a($\mu g\ L^{-1}$)	Thickness (μm)							
SWNP-2010										SML-Drum				SML-Glassplate			
SML-1;St.02	21-May-10	11:00	11:33	30°N 137°E	21.5	23.3	3.0	34.7	0.05	n/a				46.9	45.6	27.8	41.7
SML-2;St.02	22-May-10	12:33	13:22	30°N 136.6°E	21.9	22.5	4.2	34.7	0.05	27.1	31.7			32.4	31.0		
SML-3;St.04	25-May-10	8:39	9:48	20°N 137°E	29.2	29.6	6.1	34.9	0.01	24.1	20.3			32.3			
SML-4;St.04	26-May-10	14:18	14:42	20°N 136.6°E	29.4	29.5	4.3	34.9	0.01	27.9	25.3			32.2			
SML-5;St.05	27-May-10	12:18	13:10	15°N 137°E	30.4	30.5	4.3	34.7	0.02	32.3	32.9			41.1			
CRI-2010																	
SML-1;St.04	29-Sep-10	10:00	10:50	26.2°E 126.4°E	28.4	27.5	2.4	34.2	0.03	25.3	27.9	22.8		55.6			
SML-2;St.07	1-Oct-10	9:30	10:10	28.3°E 129.4°E	28.6	27.0	2.6	34.1	0.02	44.3	42.2	48.1	45.6	44.4	50.6		
SML-3;St.09	2-Oct-10	10:20	11:43	32.4°E 128.4°E	26.4	24.2	1.5	33.0	0.15	38.0	42.2	43.0	43.0	50.9			
EEP-2012																	
St.1	2-Feb-12	8:34	9:35	0°N 95.5°W	23.1	25.9	2.9	34.6	0.17	36.8	39.4			45.6			
St.2	3-Feb-12	10:36	11:52	0°N 100°W	24.5	26.5	2.4	33.8	0.15	36.9	36.7	31.7	38.0	45.6			
St.5	7-Feb-12	11:48	12:53	0°N 115°W	24.7	25.9	1.1	34.9	0.20	36.1	30.6	31.1	35.9	32.2			
St.8	11-Feb-12	9:23	10:58	0°N 130°W	24.1	25.1	2.7	34.7	0.20	39.2	38.5	41.1		48.3			
St.10	13-Feb-12	9:00	10:20	0°N 140°W	23.6	24.8	4.4	35.1	0.37	43.9	39.0			55.6			

WS = average wind speed for 30 min during all course of sampling

n/a =not measure

Table 2.2.3. Sample volume (mL), total surface area of collection (m^2) and calculated SML thickness (µm) of SML drum (SML-D) and glass plate (SML-GP) samples from the SWNP-2010, CRI-2010 and EEP-2012

Sampling Location		Date	Sampling No.	No. Dip / Round	Total Volume (mL)	Total Surface (m^2)	Total Volume (m^3)	Thickness (µm)
SWNP-2010								
St.02	30°N, 137°E	May 21, 2010	SML-GP#1	45	380	8.10	0.00038	46.9
		11:00-11:33	SML-GP#2	50	410	9.00	0.00041	45.6
			SML-GP#3	50	375	9.00	0.00038	41.7
			SML-PMMA	50	250	9.00	0.00025	27.8
St.02	30°N, 136.6°E	May 22, 2010	SML-GP#1	60	350	10.80	0.00035	32.4
		12:33-13:22	SML-GP#2	60	335	10.80	0.00034	31.0
			SML-D#1	60	1500	47.40	0.00150	31.6
			SML-D#2	70	1500	55.30	0.00150	27.1
St.04	20°N, 137°E	May 25, 2010	SML-GP#1	100	582	18.00	0.00058	32.3
		08:39-09:48	SML-D#1	50	950	39.50	0.00095	24.1
			SML-D#2	50	800	39.50	0.00080	20.3
			SML-D#3	50	1000	39.50	0.00100	25.3
St.04	20°N, 136.6°E	May 26, 2010	SML-GP#1	100	250	18.00	0.00025	13.9
		14:18-14:42	SML-D#1	50	850	39.50	0.00085	21.5
			SML-D#2	50	850	39.50	0.00085	21.5
			SML-D#3	50	900	39.50	0.00090	22.8
St.05	15°N, 137°E	May 28, 2010	SML-GP#1	100	740	18.00	0.00074	41.1
		12:18-13:10	SML-D#1	80	2040	63.20	0.00204	32.3
			SML-D#2	40	1040	31.60	0.00104	32.9
CRI-2010								
St.04	26.2°N, 126.4°E	Sept 29, 2010	SML-GP#1	100	1000	18.00	0.00100	55.6
		10:00-10:50	SML-D#1	100	2000	79.00	0.00200	25.3
			SML-D#2	100	2200	79.00	0.00220	27.8
			SML-D#3	100	1800	79.00	0.00180	22.8
St.07	26.2°N, 126.4°E	Oct 1, 2010	SML-GP#1	75	600	13.50	0.00060	44.4
		09:30-10:10	SML-GP#2	100	910	18.00	0.00091	50.6
			SML-D#1	60	2100	47.40	0.00210	44.3
			SML-D#2	60	2000	47.40	0.00200	42.2
			SML-D#3	50	1900	39.50	0.00190	48.1
			SML-D#4	50	1800	39.50	0.00180	45.6
St.09	32.4°N, 126.8°E	Oct 2, 2010	SML-GP#1	120	1100	21.60	0.00110	50.9
		10:20-11:43	SML-D#1	60	1800	47.40	0.00180	38.0
			SML-D#2	60	2000	47.40	0.00200	42.2
			SML-D#3	50	1700	39.50	0.00170	43.0
			SML-D#4	50	1700	39.50	0.00170	43.0
EEP-2012								
St.01	0°N, 95.5°E	Feb 2, 2012	SML-GP#1	100	820	18.00	0.00082	45.6
		08:34-09:35	SML-D#1	124	3600	97.96	0.00360	36.7
			SML-D#2	62	1930	48.98	0.00193	39.4
St.02	0°N, 100°E	Feb 3, 2012	SML-GP#1	100	820	18.00	0.00082	45.6
		11.48-12:52	SML-D#1	120	3500	94.80	0.00350	36.9
			SML-D#2	60	1740	47.40	0.00174	36.7
			SML-D#3	60	1500	47.40	0.00150	31.6
			SML-D#4	60	1800	47.40	0.00180	38.0
St.05	0°N, 115°E	Feb 7, 2012	SML-GP#1	100	580	18.00	0.00058	32.2
		10:36-11:52	SML-D#1	120	3420	94.80	0.00342	36.1
			SML-D#2	60	1450	47.40	0.00145	30.6
			SML-D#3	120	2950	94.80	0.00295	31.1
			SML-D#4	60	1700	47.40	0.00170	35.9
St.08	0°N, 130°E	Feb 11, 2012	SML-GP#1	100	870	18.00	0.00087	48.3
		10:36-11:52	SML-D#1	120	3716	94.80	0.00372	39.2
			SML-D#2	120	3650	94.80	0.00365	38.5
			SML-D#3	120	3895	94.80	0.00390	41.1
St.10	0°N, 140°E	Feb 13, 2012	SML-GP#1	150	1500	27.00	0.00150	55.6
		10:36-11:52	SML-D#1	60	2080	47.40	0.00208	43.9
			SML-D#2	120	3695	94.80	0.00370	39.0

Note: Surface area (m^2) of SML-D = 0.79 (Drum sampler)
SML-GP = 0.18 (Glass Plate)

2.2.2. Surface seawater sampling

Surface water (SUR) collection on board by clean bucket was performed together with CTD operation. Water at a specific depth was also collected with Niskin bottles (**Table. 2.1.1.**). All seawater samples including SML were filtered either with pre-combusted (550°C; 5 h) glass filters (GF/F Whatman, 0.7 μm) for particulate phosphorus (TPP) analysis or membrane filters (Nuclepore® Whatman, 0.4 μm) for element analysis with an energy dispersive X-ray fluorescence spectrophotometer (ED-XRF, Kimoto Electric, Model MXF-01). Unfiltered and filtered water samples were collected in pre acid-cleaned (10% HCl) polypropylene bottles and stored at -20 °C until the analysis of total dissolved phosphorus (TDP) and soluble reactive phosphorus (SRP).

2.2.3. Aerosols sampling

Aerosols samples were collected on the pre-combusted (at 550 °C for 5 h) quartz fiber filters (2500QAT-UP, 90 mm in diameter, PALLFLEX Products Co.) during two cruises on SWNP-2010 and CRI-2010 by a high-volume (11 $m^3 h^{-1}$) virtual impactor air sampler (Kimoto Electric, Model AS-900). On board, the air sampler was set up in the front of the upper deck (at 17 m above the sea level) and a wind-sector controller was connected to control the direction of the receiving air mass and to avoid contamination from ship's exhaust during the aerosols sampling. This air sampler is able to collect fine (D < 2.5 μm) and coarse modes (D > 2.5 μm) particles on the same filter. The sampling time was set for 24 h-cycle with the total air sampling volume between 120 - 264 m^3.

After the collection, the sampled filter was placed in the polyethylene seal-plastic bag immediately and kept frozen (-20 °C) for further chemical analysis. At every 3 cycles of sampling, field blank was deployed by leaving the filter in the sampler for 5 min under the idle mode and kept the blank filters as the same manner with the samples.

Prior using, a filter holder were soaked overnight in the nutrient-free detergent (Contaminon B, Wako Pure Chemical Industries) rinsed and then soaked in the 1N hydrochloric acid (HCl) solution for another 24 h, then rinsed with Milli-Q water 3 times and dried in oven. After the cleaning process, the pre-combusted quartz fiber filters were loaded on to this holder in the clean (laminar flow) room.

2.2.4. Bubble bursting experiment

The bubble bursting experiment is the additional experiment conducted on board only on the EEP-2012 cruise. This experiment was aimed to collect the fresh atmospheric particulates ejected from different seawater during the air bubbling process. Surface water (denoted as SUR and collected by the bucket sampling on the vessel); collected from St.02, St.05, St.08 and St.10. SML and SSW samples collected from St.05, St.08 and St.10.

The particles from the bubble bursting process were collected on to pre-combusted quartz filters (47mm diameter) for phosphorus analysis and for water soluble ionic species. The bubble injection rate was set up to 400 mL min^{-1} at depth of 20 cm from the surface water level. The bubbling time has set for 1.5 h per cycle. The air flow injected in the bubbling system was filtered with a HEPA unit, and set the flow rate for 15 L min^{-1} or the final air volume of 0.135 m^{-3}. Sample seawater of 3.5 L was utilized for each experiment.

2.3. Sample treatment and analysis

2.3.1. Sample handling and storage

Filtration equipment and containers were cleaned with a nutrient free detergent and acid washing (10% HCl) and rinse with ultrapure water and air dry. The sample bottles were rinsed twice

with the sample water prior using. The membrane filter were flashed with 100 mL of distilled water 3 times before filtration [APHA, AWWA-WEF, 1998]. For glass filters (GF/F, 47 mm in diameter, Whatman) the pre-combustion at 550 °C for at least 1 h was required to remove organic contamination [Solorzano and Sharp, 1980].

Filtrate and unfiltered seawater samples collected for the phosphorus analysis were kept at -20°C without any preservation. The storage time recommended for seawater is no longer than 140-210 days [Worsfold, et al., 2005].

2.3.2. Determination of phosphorus in environmental samples

The quantitative analysis of phosphorus is based on the colorimetric measurement of the blue compounds that latterly reduced from the phosphomolybdate heteropoly from the reaction of an acidified molybdate reagent with phosphate [Grasshoffe et al., 1999], as the following.

$PO_4^{3-} + 12MoO_4^{2-} + 27H^+ \rightarrow H_3PO_4(MoO_3)_{12} + 12H_2O$

$H_3PO_4(MoO_3)_{12}$ + Reducing Agent $\rightarrow$ Phosphomolybdum Blue [Mo(VI) -> Mo(V)]

The blue phosphomolybdic complex can be stable for an hour with no influence on salinity [Grasshoff et al., 1999]. However, sample contains more than 350 µM of silicate or arsenate ions can interfere and surplus the color intensity [Grasshoff et al., 1999].

Schematic diagram (**Fig. 2.3.1**) showed the operational definition of the phosphorus fractions and the overview of phosphorus analyses in aquatic systems. At the laboratory, filtrates samples were thawed, mixed and prepared in triplicate. Soluble reactive phosphorus (SRP) was determined by the MAGIC-SRP method which included the pre-concentration step by the magnesium induced co-precipitation prior the colorimetric measurement of the molybdate-phosphate complexes [Karl and Tien, 1992; Lomas et al., 2010]. By pH induction (with the addition

of 1M NaOH at 1:40 v/v ratio), SRP was co-precipitated and formed brucite pellets ($Mg(OH)_2$). Supernatant was discarded after centrifugation and the precipitate was re-dissolved with 0.1 M HCl solution, then treated with conventional molybdenum blue colorimetric method [Murphy and Riley, 1962; Strickland and Parson, 1972].

This precipitation and pre-concentration is enabled phosphorus measurement to the nano-molar level (at 2 nM; in Lomas et al., 2010 study). In this study with the concentration factor of 5, the method detection limit of MAGIC-SRP was determined as three times of the standard deviation of the lowest molybdenum blue standard (0.2 µM) at 4.0 ± 1.4 nM. For total dissolved phosphorus (TDP), filtered seawater were pre-oxidized with boracic acid-persulfate oxidation solution (5 g of $K_2S_2O_8$ and 3 g of H_3BO_3 in 100 mL of 0.375 M NaOH) at 1:10 reagent to sample volume ratio and placed in autoclave at temperature of 120 °C for 30 min prior MAGIC-SRP analysis [Liu et al., 2010]. Dissolved organic phosphorus (DOP), then calculated by the subtraction of TDP with SRP.

For total particulate phosphorus (TPP) analysis, glass fiber filter and quartz filter were sectioned and ashed overnight at 550 °C. Later, the residuals were dissolved in 1 mL of 1 N HCl and diluted to 20 mL with Milli-Q water and latterly shaken well for 30 min [Chen et al., 1985; Chen et al., 2006]. Then, the solution was concentrated, filtered, analyzed by the molybdenum blue colorimetric method [Strickland and Parsons, 1972]. With 10 time concentration factor, the detection limit of the TPP analysis determined as three times of the standard deviation of the lowest molybdenum blue standard (0.15 µM) and was 2 ± 0.7 nM. Particulate inorganic phosphorus (PIP) or the extractable inorganic phosphate was measured after the filter extraction with 1 N HCl without ashing process. This procedure was also applied for the atmospheric samples. For the sampling time of 24 h duration, the detection limit of the analysis was 0.03 nmol m^{-3} for the air volume of 264 m^{-3}.

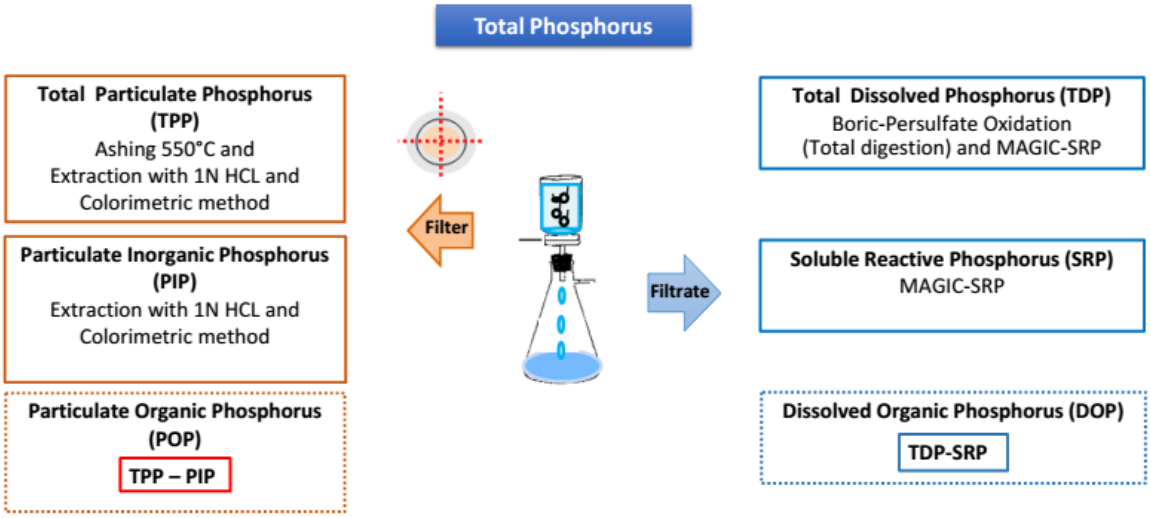

Fig. 2.3.1. Schematic diagram of the phosphorus analysis in dissolved and particulate forms. Rectangular frame expressed the method of phosphorus aalysis [Strickland and Parsons, 1972; Grasshoff et al., 1999 and Chen et al., 2006]

2.3.3. Determination of elemental composition by XRF spectrometry

X-ray fluorescence (XRF) spectrometry is an elemental analysis technique measured the x-ray produced under the excited state when atom releases the excess energy and falls to ground state. The X-ray fluorescent radiation is the energy characteristic of each atom and can be used to identify for the element [Iwamoto, 2008]. This radiation is analyzed by sorting the energies of photons (counting per second) or the intensity in which is proportional related to the amount of each element presented in materials. By comparing the intensity with a known elemental concentration of certified standards, concentration is obtained quantitatively.

In this study, sample filters were analyzed by an energy dispersive X-ray fluorescence spectrometer (ED-XRF, Kimoto electric, Model MXF-01) with an operating accelerating voltage of 20 kV and a beam current at 2 mA. The collection time is set for 500 sec per sample [Iwamoto et

al., 2009]. The palladium X-ray tube is used for the x-rays generation and the toroidal graphite is selected as a secondary target for light elements, such as Al and Si.

The certified material, a simulated Asian mineral Dust (CJ-2; National Research Center for Environmental Analysis and Measurement, China) was applied for the calibration purpose. By suspending this standard in ultrapure water with known amount and aliquot of solution is filtered to load on the filters (Nuclepore® Whatman) and the calibration curves is calculated based on the elemental intensity and the elemental concentration of standards. The detection limit determined by 3 times of the signal to noise ratio was displayed in **Table 2.3.1**.

The particulate phosphorus measured in the XRF-analysis exhibited less sensitivity when compared with the colorimetric method. In certain case, the results from the XRF analysis were utilized inevitably thus, the deviation of the XRF measurement was compared with the colorimetric method and shown in **Fig. 2.3.2**.

Table 2.3.1. Detection limits of the suspended particulate elements measured in 1L of SML seawater. 2-3 L of seawater was applied to increase the sensitivity for the routine SPM analysis.

	Detection limit	
	(nM)	(ng/L)
Al	38 ± 12.6	1024 ± 341
Ca	8 ± 1.8	297 ± 74
Cl	8 ± 1.9	274 ± 69
Fe	2 ± 0.5	84 ± 28
Ti	2 ± 0.5	71 ± 23
Si	12 ± 4.0	334 ± 111
S	10 ± 3.1	258 ± 86
P	4 ± 1.2	107 ± 36

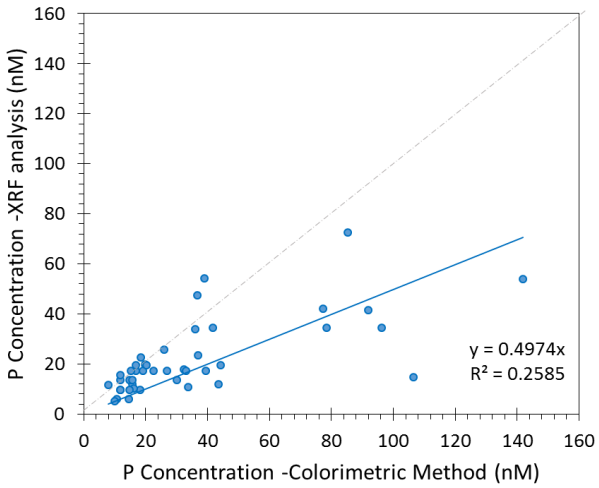

Fig. 2.3.2. Comparison of the particulate phosphorus concentration between the colorimetric method and the XRF method.

2.3.4. Determination of water soluble fraction of the ionic species in the aerosols

Major cations (Na^+, K^+, Mg^{2+}, and Ca^{2+}) and anions (F^-, Cl^-, Br^-, NO_3^- and SO_4^{2-}) in atmospheric particulate from the bubble bursting experiment were measured by an ion chromatography (IC; Dionex-320, Thermo Scientific Dionex) using a CS16 cation exchange column with a CG16 guard column for cation analysis and an AS17 anion exchange column with an AG17 guard column for anion analysis. Methanesulfonic acid (MSA) was used as the eluent for the cation analysis while, potassium hydroxide was applied as the eluent in the anion analysis.

Filter samples were sectioned and re-suspended with the Milli-Q water and extracted with the ultra-sonication. The extracted solution then, filtered with a PTFE syringe filter (Millipore Co.) and analyzed for cations and anions. For seawater, samples was diluted (about 10 times) prior the analysis. The detection limits calculated as three times of the standard deviation of the procedural blanks as shown in the following **Table 2.3.3.**

Table 2.3.3. The detection limits of the ionic species

Method detection limit					
Cation	µg/L	µM	Anion	µg/L	µM
Na^+	4.03	0.18	F^-	4.24	0.22
K^+	4.54	0.12	Cl^-	4.24	0.12
Mg^{2+}	2.35	0.10	Br^-	0.88	0.01
Ca^{2+}	6.10	0.15	NO_3^-	3.79	0.06
			SO_4^{2-}	2.36	0.02

3. Total and particulate phosphorus in ocean, atmosphere and its interface; sea-surface microlayer

3.1. Introduction

Phosphorus is an essential bioactive element that has its biological function in energy storage cells, and component in bio-molecules. In aquatic environment, phosphorus functions as a macronutrient and co-limiting factor for water productivity. Main input of phosphorus to the ocean is through the riverine path as the soluble phosphorus from the weathering process. Dissolved form is the major phosphorus constituent in open ocean and makes up to about 90% of total phosphorus [Karl and Tien, 1997]. Both dissolved inorganic and organic phosphorus is extensively utilized by various microorganisms depending on its bioavailability and its uptake-mechanism that are different among the assemblages [Paytan and McKaughlin, 2007]. In the open ocean, the input from the riverine source is diminished, the supply from the atmospheric deposition is become necessity.

Unlike carbon and nitrogen that have the stable gaseous phase, phosphorus is transported principally as particles in the atmosphere [Graham and Duce, 1979] and mineral bearing phosphorus aerosols is accounted for 82 % of the total atmospheric deposition [**Table 3.1.1**, Mahowald et al., 2008]. However, under the ongoing anthropogenic perturbation, phosphorus related to biomass and fuel combustion emission comprised mostly in the inorganic forms is becoming a massive burden to the global atmospheric phosphorus [Wang, et al., 2014].

Over the remote air of the North Pacific Ocean, the study has shown the relatively low atmospheric phosphorus and its consistent concentration (0.07 – 0.09 nmol m^{-3}, Furutani et al., 2010) without regard to its source distances (**Fig. 3.1.1)**. This suggested that more than 50% of phosphorus supply to atmosphere had yet known sources of origin [Furutani et al., 2010]. Alternately, sea water has purposed as the source for atmospheric phosphorus [Graham and Duce,

1979]. From bubble bursting experiment [Graham et al., 1979], it is found that organic phosphorus are enriched in air droplets and its enrichment was depended upon its surface organic contents and wind velocity; suggesting that SML can also be a source provided phosphorus to the ejected droplets.

Table 3.1.1. The global sources of atmospheric phosphorus [Mahowald et al., 2008]

	Total P (Tg P a^{-1})	PO_4 (Tg P a^{-1})
Dust	1.150	0.115
Primary biogenic particles	0.164	0.082
Biomass burning	0.025	0.012
Fossil Fuels	0.024	0.012
Biofuels	0.021	0.010
Volcanoes	0.006	0.003
Sea salts	0.0049	0.0049
Total	1.39	0.24
Percent anthropogenic	4.8	14.3

[a]Less than 10 μm.

As areceiving media, substances in SML is entirely supplied from the underlying subsurface water and from the atmospheric deposition. Phase partitioning of dissolved and particulate phosphorus are subsequently modified by various interfacial physical process as well as microbiological activities including biomass production and degradation [Frka et al., 2012; Liss and Duce, 1997; Xhoffer et al., 1992]. However, net photosynthesis in the SML has reported to be less significant. Instead, the respiration rate was elevated and is related to the organic-rich condition [Reinthaler et al., 2008; Hardy and Apts, 1989].

Herein, we presented the results of the differences of phosphorus composition in sea-surface microlayer (SML) samples in comparing with the underlying seawater together with the atmospheric and oceanic particulates phosphorus in the same sampling area. This field study is try

to gain the understanding about the influence of SML towards oceanic biogeochemical cycle of phosphorus and the contribution of SML to the atmospheric phosphorus and vice versa.

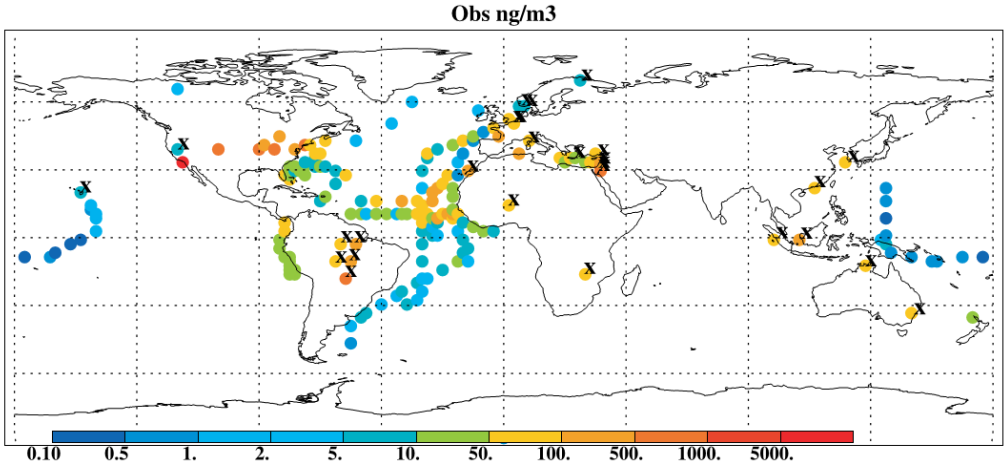

Fig. 3.1.1. Global distribution of the atmospheric phosphorus in term of total particulate phosphorus (Total.P) in ng m^{-3} [Mahowald et al., 2008]

3.2. Distribution of phosphorus in sea-surface microlayer, subsurface water and atmosphere

3.2.1. Distribution of phosphorus in SML and subsurface water

The average phosphorus concentrations by forms are shown in **Table 3.2.1** and the summary of phosphorus composition in the SML and subsurface water (SSW) from 3 cruises; as follows.

SWNP-2010 cruise

During SWNP-2010 cruise, seawater of the subtropical Pacific region was characterized with its low nutrient concentration. On the average (n = 5), concentrations of total phosphorus in sea-

surface microlayer collected by glass plate (SML-GP) and drum (SML-D) and subsurface water (SSW) were 0.42, 0.36 and 0.36 µM, respectively. Dissolved organic phosphorus (DOP) had contributed to the largest phosphorus fraction in surface seawater and was accounted for about 52% - 76% of total phosphorus. The second largest pool was soluble reactive phosphorus (SRP) and shared about 17% - 42%. The remaining total particulate phosphorus (TPP) comprised only about 5 - 9% (**Fig. 3.2.1** and **Fig.3.2.2**). Within particulate phosphorus pool, particulate inorganic phosphorus (PIP) concentration was more dominant than that of particulate organic phosphorus (POP). When comparing among the SML samples, SML-GP showed to contain higher concentration for both total phosphorus and major DOP fraction (**Table 3.2.1**).

CRI-2010 cruise

In CRI-2010 cruise, seawater samples were collected in the coastal sea around the Ryukyu Islands; subtropical region in the Western North Pacific. Concentration of total phosphorus were relatively low. On the average (n=3), total phosphorus concentration were 0.28, 0.23 and 0.21 µM, in SML-GP, SML-D and SSW, respectively (**table 3.2.1**). The largest phosphorus pool in SML was DOP and comprised about 52% - 65% of the total. In SSW, SRP was a major fraction and occupied about 51% of total. The remaining TPP was accounted for more than 10 - 15 % of the total (**Fig. 3.2.1** and **Fig.3.2.2**). In particulate forms, PIP content measured from SML and SSW were quite similar, but POP concentration were clearly higher in the SML than the SSW.

EEP-2012 cruise

For EEP-2012 cruise, seawater samples were collected from the High Nitrate, Low Chlorophyll-a (HNLC) region in upwelling zone of the Eastern Equatorial Pacific (EEP). Concentration of total phosphorus were 3-fold higher than the other two cruises. On the average (n=4, excluded the sample from St. 01) concentrations of total phosphorus were 1.54, 1.69 and

1.50 µM, in the SML-GP, SML-D and SSW, respectively. DOP and SRP comprised more than 98% of total phosphorus and its proportions in seawater were almost at equal. DOP was slightly higher in the SML and instead, SRP was higher in the SSW. For TPP proportion, it makes up to even less than 2% of the total phosphorus (**Fig. 3.2.1** and **Fig.3.2.2**).

High concentration of particulate phosphorus in the SML was addressed in EEP-2012 cruise due to very low concentration in SSW samples. Especially at St.01 (0°N, 95.5°W), where the highest concentration of particulate phosphorus was detected (**Fig.3.2.2**). TPP measured at St. 01 rose to the same µM level like the dissolved phosphorus concentration and pose the significant shift of phosphorus composition(TPP = 0.59 and 1.29 µM in SML-GP and SML-D, respectively).

Overall, total dissolved phosphorus was made up to approximately 90% of total phosphorus in seawater for both the SML and SSW samples in all 3 cruises. SRP and DOP were varied in its proportion but make up to almost 90% of total phosphorus in SML and SSW. In SWNP-2010, DOP was accounted for the dominant phosphorus fraction in both SML and SSW. For CRI-2010, DOP was dominated in the SML while SRP was the major composition in the SSW. For EEP-2012, both DOP and SRP fractions were equally make up to the largest pool of phosphorus in seawater. For particulate phosphorus, it is made up to about 5-13 % of total phosphorus in SWNP-2010 and CRI-2010. The open ocean EEP-2012 cruise contained less TPP concentration and its composition was only 2 % of the total phosphorus.

Table 3.2.1. Phosphorus concentration in sea-surface microlayer (SML) and subsurface water (SSW), demonstrated for dissolved and particulate phosphorus in terms of soluble reactive phosphorus (SRP), total dissolved phosphorus (TDP), particulate inorganic phosphorus (PIP) and total particulate phosphorus (TPP) from 3 cruises; SWNP-2010, CRI-2010 and EEP-2012.

Cruise	Station	Sample types	Depth*	Dissolved P		Paritculate P	
				SRP (µM)	TDP (µM)	PIP (nM)	TPP (nM)
SWNP-2010	SML-1;St.02	SML-GP	40.5	0.07 ± 0.06	0.34 ± 0.08	42.3 ± 9.0	50.7 ± 18.9
		SML-D	not sample				
		SSW	1.5	0.04 ± 0.07	0.17 ± 0.27	28.2 ± 13.5	33.8 ± 13.4
	SML-2;St.02	SML-GP	31.7	0.20 ± 0.06	0.41 ± 0.07	28.2 ± 34.9	33.8 ± 22.0
		SML-D	29.4	0.20 ± 0.12	0.30 ± 0.25	15.3 ± 6.5	18.3 ± 7.7
		SSW	1.5	0.07 ± 0.06	0.41 ± 0.14	28.2 ± 13.5	33.8 ± 11.4
	SML-3;St.04	SML-GP	28.2	0.07 ± 0.01	0.29 ± 0.10	28.2 ± 9.0	33.8 ± 18.9
		SML-D	20.3	0.08 ± 0.03	0.31 ± 0.11	26.5 ± 3.6	31.8 ± 7.7
		SSW	1.5	0.07 ± 0.07	0.37 ± 0.15	20.1 ± 8.8	24.1 ± 3.8
	SML-4;St.04	SML-GP	32.2	0.07 ± 0.01	0.41 ± 0.31	28.2 ± 9.0	33.8 ± 18.9
		SML-D	26.6	0.15 ± 0.02	0.32 ± 0.25	11.4 ± 3.6	13.7 ± 5.7
		SSW	1.5	0.04 ± 0.02	0.29 ± 0.14	20.1 ± 9.9	24.1 ± 7.2
	SML-5;St.05	SML-GP	41.1	0.12 ± 0.05	0.41 ± 0.06	17.6 ± 9.0	21.1 ± 18.9
		SML-D	32.6	0.17 ± 0.02	0.41 ± 0.25	7.8 ± 4.6	18.8 ± 5.7
		SSW	1.5	0.07 ± 0.07	0.41 ± 0.15	14.1 ± 8.8	16.9 ± 3.8
	average ± sd	SML-GP	34.7	0.11 ± 0.04	0.37 ± 0.12	28.9 ± 14.2	34.6 ± 19.5
		SML-D	27.2	0.15 ± 0.05	0.34 ± 0.22	15.3 ± 4.6	20.7 ± 6.7
		SSW	1.5	0.06 ± 0.06	0.33 ± 0.17	22.1 ± 10.9	26.6 ± 7.9
CRI-2010	SML-1;St.04	SML-GP	55.6	0.15 ± 0.08	0.24 ± 0.08	7.0 ± 1.9	36.3 ± 8.1
		SML-D	26.2	0.06 ± 0.07	0.19 ± 0.07	12.3 ± 10.0	30.3 ± 3.1
		SSW	1.5	0.15 ± 0.05	0.24 ± 0.06	5.7 ± 2.5	17.6 ± 1.0
	SML-2;St.07	SML-GP	50.6	0.01 ± 0.05	0.24 ± 0.14	25.5 ± 3.0	42.8 ± 13.5
		SML-D	46.2	0.15 ± 0.03	0.24 ± 0.03	16.0 ± 3.7	48.4 ± 11.0
		SSW	1.5	0.15 ± 0.04	0.24 ± 0.03	5.1 ± 2.3	15.8 ± 0.9
	SML-3;St.09	SML-GP	50.9	0.01 ± 0.08	0.24 ± 0.08	6.5 ± 2.7	33.6 ± 14.6
		SML-D	41.4	0.01 ± 0.05	0.14 ± 0.03	4.5 ± 0.4	24.6 ± 5.1
		SSW	1.5	0.01 ± 0.04	0.10 ± 0.09	10.7 ± 3.1	18.0 ± 7.7
	average ± sd	SML-GP	46.6	0.06 ± 0.07	0.24 ± 0.10	13.0 ± 2.5	37.5 ± 12.0
		SML-D	34.7	0.06 ± 0.05	0.14 ± 0.04	8.2 ± 4.7	25.8 ± 6.4
		SSW	1.5	0.08 ± 0.04	0.14 ± 0.06	5.4 ± 2.7	12.8 ± 3.2
EEP-2012	SML-St.01	SML-GP	45.7	0.84 ± 0.14	-	243.4 ± 32.5	587.8 ± 129.9
		SML-D	38.1	0.85 ± 0.30	-	547.7 ± 43.5	1286.2 ± 43.5
		SSW	1.5	0.88 ± 0.09	-	6.4 ± 0.6	18.0 ± 11.9
	SML-St.02	SML-GP	45.6	0.45 ± 0.02	1.09 ± 0.00	6.8 ± 4.0	9.6 ± 2.5
		SML-D	35.8	0.57 ± 0.16	1.09 ± 0.00	9.4 ± 9.0	12.9 ± 10.1
		SSW	1.5	0.35 ± 0.06	0.87 ± 0.32	2.7 ± 2.0	3.7 ± 3.3
	SML-St.05	SML-GP	32.2	0.97 ± 0.05	1.78 ± 0.00	8.0 ± 0.0	25.8 ± 14.7
		SML-D	33.4	1.14 ± 0.03	2.07 ± 0.08	10.5 ± 5.7	41.6 ± 0.0
		SSW	1.5	1.14 ± 0.03	2.12 ± 0.16	6.3 ± 5.7	9.3 ± 1.5
	SML-St.08	SML-GP	48.3	0.95 ± 0.04	1.89 ± 0.48	6.6 ± 4.1	15.6 ± 13.5
		SML-D	39.6	1.10 ± 0.08	2.35 ± 0.48	4.5 ± 0.5	10.9 ± 6.6
		SSW	1.5	1.03 ± 0.15	2.01 ± 0.32	2.7 ± 1.6	9.5 ± 3.2
	SML-St.10	SML-GP	55.6	0.57 ± 0.02	1.32 ± 0.00	6.6 ± 4.4	25.7 ± 15.8
		SML-D	41.4	0.66 ± 0.03	1.15 ± 0.08	11.5 ± 2.9	30.2 ± 24.3
		SSW	1.5	0.52 ± 0.06	0.98 ± 0.16	3.1 ± 2.8	14.8 ± 0.0
	average ± sd	SML-GP	46.6	0.74 ± 0.03	1.52 ± 0.12	7.0 ± 3.1	19.2 ± 11.6
		SML-D	34.7	0.87 ± 0.08	1.67 ± 0.16	9.0 ± 4.5	23.9 ± 10.3
		SSW	1.5	0.76 ± 0.08	1.50 ± 0.24	3.7 ± 3.0	9.3 ± 2.0

*depth in µm for glass plate (SML-GP) and drum (SML-D) and m for SSW

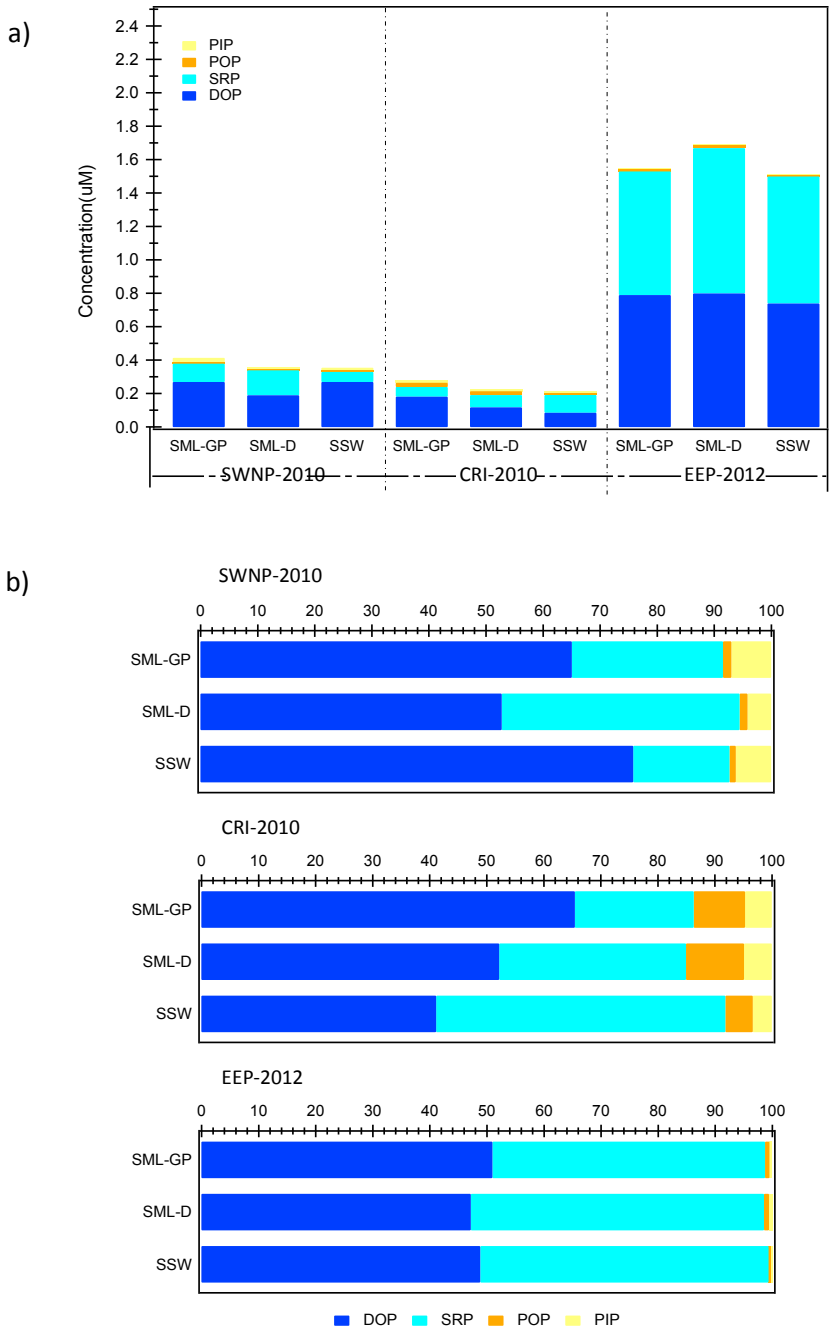

Fig. 3.2.1. a) The average concentration of phosphorus by forms; soluble reactive phosphorus (SRP), dissolved organic phosphorus (DOP), particulate inorganic phosphorus (PIP) and particulate organic phosphorus (POP) in SML-GP (Glass plate), SML-D (Drum) and subsurface water (SSW) samples and b) percentage of phosphorus composition in 3 cruises; SWNP-2010, CRI-2010 and EEP-2012.

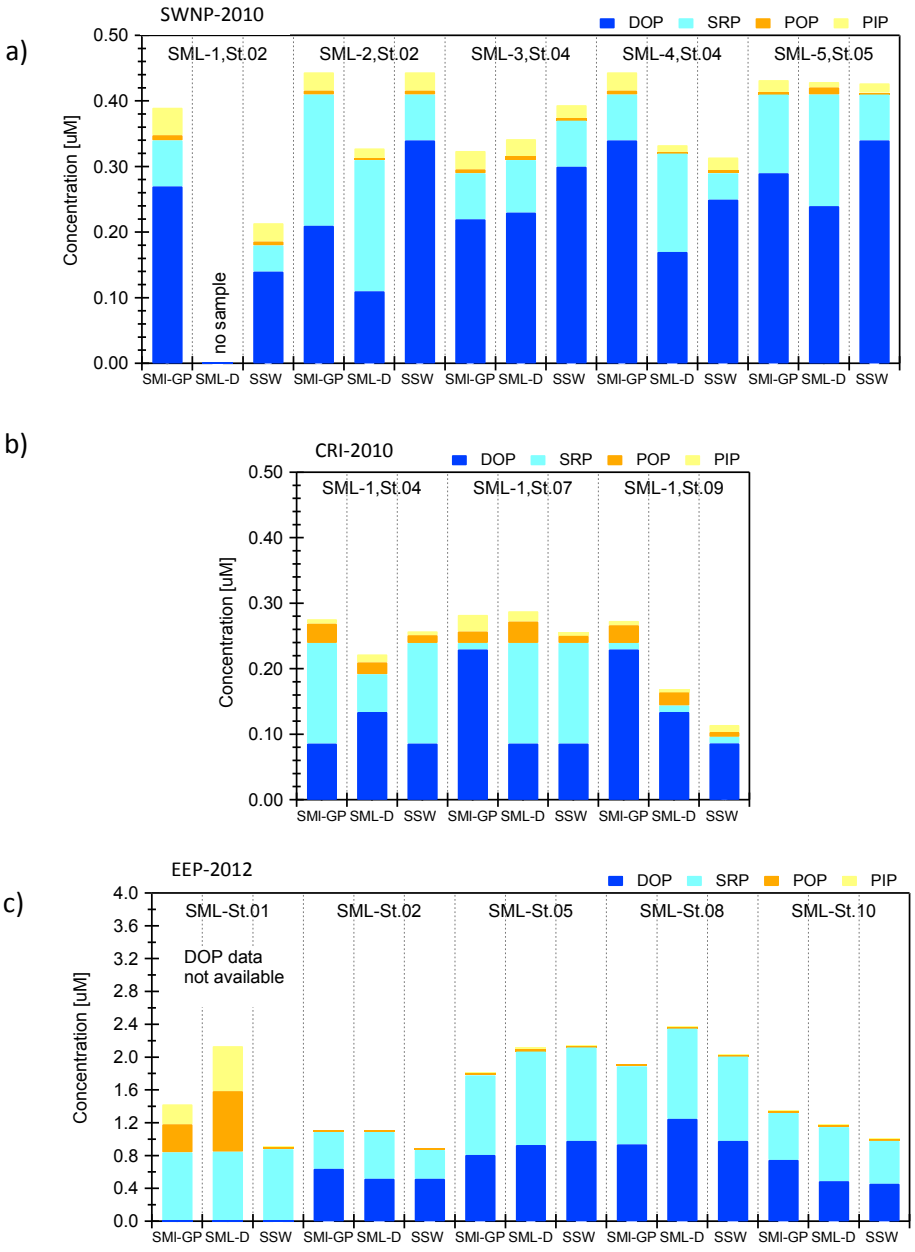

Fig.3.2.2. Concentration of phosphorus distributed in dissolved organic phosphorus (DOP), soluble reactive phosphorus (SRP), particulate inorganic phosphorus (POP), and particulate inorganic phosphorus (PIP) in sea-surface microlayer (SML-D and SML-GP) and subsurface seawater (SSW). Samples were taken from a) SWNP-2010, b) CRI-2010, and c) EEP-2012.

3.2.2 Distribution of phosphorus in marine aerosols

Total particulate phosphorus (Total.P) in marine aerosols were measured after ashing and extraction with HCl solution. Particulate inorganic phosphorus (PIP) was obtained from the analysis of the filter-HCl extractable solution. The particulate organic phosphorus (POP) calculated by the subtraction of PIP from Total.P and presented in **Tables 3.3.1** as the % org phosphorus. Concentration of atmospheric phosphorus from 19 and 7 aerosol samples taken during the SWNP-2010 and CRI-2010 displayed with the 7 day backward trajectories of the air mass at the SML sampling points (**Fig. 3.2.3** and **Fig. 3.2.4)**.

Total phosphorus concentration in aerosol samples were relatively lower in SWNP-2010 than the CRI-2010 (**Table 3.2.2**). The average concentration of Total.P in SWNP-2010 and CRI-2010 cruises were 0.15 $\pm$ 0.06 and 0.19 $\pm$ 0.07 nmol m^{-3}, respectively. These were similar with Total.P number in previous study that reported as an average of Total.P over the Western North Pacific region at 0.24 $\pm$ 0.14 nmol m^{-3} (n=21) [Furutani et al., 2010]. The organic phosphorus contained in aerosols were accounted for 40% and 30% in the SWNP-2010 and CRI-2010.

There was a decrease in Total.P along with the ship track cursing from 30°N to 15°N on the 137°E transect in SWNP-2010 cruise (**Fig. 3.2.3**). Total.P increased again when the ship cruised toward the northwest to Japan with the increase of PIP fraction in aerosol samples. Most particulate phosphorus was mostly resided in fine mode particles (aerosols with diameter, D_a less than 2.5 µm) and comprised about 68% of total phosphorus. Concentration of PIP was relatively consistent in CRI-2010 cruise and ranged from 0.05 - 0.16 nmol m^{-3} (**Fig. 3.2.4**). While POP concentration exhibited from less than detection limits (sample A5) to 0.26 nmol m^{-3}. Like in SWNP-2010 cruise, particulate phosphorus in CRI-2012 was also resided majorly in fine-mode in which accounted for 62.85% of total phosphorus.

Phosphorus containing aerosols in the Western North Pacific region were mostly presented in fine particle mode. The observation of a decrease of Zn and Fe content in marine aerosols with a percentages of fine particles in marine air from the Western North Pacific to Central North Pacific region had indicated that this fine particles were originated from anthropogenic and crustal sources [Furutani et al., 2010]. The size-resolved fractionation study of particulate phosphorus in marine aerosols showed a seasonal variation of fine and coarse fractions of PIP and POP and demonstrated that phosphorus particles from local anthropogenic sources are associated extensively with the fine-mode aerosols [Chen et al., 2008]. Thus, atmospheric phosphorus in the Western North Pacific region was more influenced by the continental source.

Since atmospheric phosphorus in marine air of the Western North Pacific region were originated mostly from the continental source and with the different sampling procedure between SML and aerosols collection, these results were unable to directly compare of phosphorus composition. The following section, enrichment of phosphorus in the SML was discussed solely in comparative with subsurface water. Instead, enrichments of phosphorus in aerosol samples were further described in the bubble bursting experiment (chapter 5).

Table 3.2.2. Concentration (nmol m^{-3}) of atmospheric phosphorus measured during SWNP-2010 and CRI-2010 cruises in total phosphorus (Total.P) and total inorganic phosphorus (TIP). The content of organic phosphorus and Total.P in fine particles were presented in the percentages as % Org.P and % Fine, respectively.

Sample	Latitude	Longitude	Start Date	Stop Date	Air Volume m^3	Conc.(nmol m^{-3})		%Total	%Fine
						PIP	TotalP	OrgP	(Da < 2.5 μm)
SWNP-2010									
A1	33.57N	140.13E	5/18/10 10:13	5/19/10 9:21	253.3	0.05	0.09	46.59	71.57
A2	31.05N	143.34E	5/19/10 9:34	5/20/10 8:52	241.0	0.05	0.09	46.59	71.57
A3	29.57N	142.11E	5/20/10 9:00	5/21/10 8:58	268.7	0.04	0.14	68.00	42.88
A4	29.58N	136.57E	5/21/10 9:26	5/22/10 8:50	218.5	0.15	0.23	34.28	61.31
A5	29.56N	136.42E	5/22/10 8:58	5/23/10 8:51	237.8	0.05	0.15	67.96	64.39
A6	25.00N	136.59E	5/23/10 8:58	5/24/10 8:56	184.8	0.06	0.12	46.59	71.57
A7	21.56N	137.00E	5/24/10 9:12	5/25/10 8:50	235.1	0.05	0.09	46.59	71.57
A8	20.02N	136.52E	5/25/10 8:57	5/26/10 8:48	247.9	0.05	0.09	46.59	71.57
A9	20.05N	136.41E	5/26/10 8:53	5/27/10 8:55	242.1	L.D.	0.09	100	71.57
A10	15.29N	137.00E	5/27/10 9:14	5/28/10 8:53	228.6	0.08	0.10	13.31	71.57
A11	16.15N	136.01E	5/28/10 8:57	5/28/10 20:53	127.5	0.09	0.17	46.59	71.57
A12	18.05N	134.34E	5/28/10 8:59	5/29/10 8:54	129.5	0.09	0.17	46.59	71.57
A13	19.53N	133.09E	5/29/10 8:58	5/29/10 20:44	124.6	0.15	0.18	13.31	71.57
A14	21.43N	131.40E	5/29/10 8:47	5/30/10 8:57	132.8	0.14	0.22	35.04	53.63
A15	25.37N	128.12E	5/30/10 9:11	5/30/10 20:59	125.4	0.09	0.17	46.59	71.57
A16	26.20N	127.12E	5/30/10 21:03	5/31/10 8:49	87.5	0.13	0.17	19.95	53.63
A17	26.20N	127.12E	5/31/10 8:54	5/31/10 20:51	84.2	0.23	0.26	13.31	71.57
A18	26.47N	127.43E	5/31/10 20:55	6/1/10 8:51	119.8	0.16	0.18	13.31	71.57
A19	33.24N	136.08E	6/1/10 20:53	6/3/10 8:52	389.5	0.07	0.07	9.86	80.55
				Total mean		0.10	0.15	40.06	67.72
				Standard deviation		0.06	0.06	16.81	6.28
CRI-2010									
A1	30.56N	130.19E	9/25/10 18:26	9/26/10 18:24	237.02	0.16	0.16	0	53.55
A2	28.18N	128.00E	9/26/10 18:30	9/27/10 18:04	247.23	0.10	0.20	51.26	67.34
A3	24.04N	129.36E	9/27/10 18:10	9/28/10 17:50	224.63	0.11	0.11	0	81.31
A4	25.04N	127.50E	9/28/10 17:55	9/29/10 18:07	241.77	0.05	0.20	76.96	67.16
A5	27.05N	125.30E	9/29/10 18:12	9/30/10 17:55	282.30	0.13	0.26	50.76	62.50
A6	28.50N	129.30E	9/30/10 18:00	10/1/10 18:00	258.73	0.09	0.09	0	81.72
A7	29.54N	129.17E	10/1/10 18:06	10/2/10 13:12	269.04	0.09	0.28	67.51	62.45
				Total mean		0.10	0.19	30.44	64.85
				Standard deviation		0.03	0.07	19.73	10.21

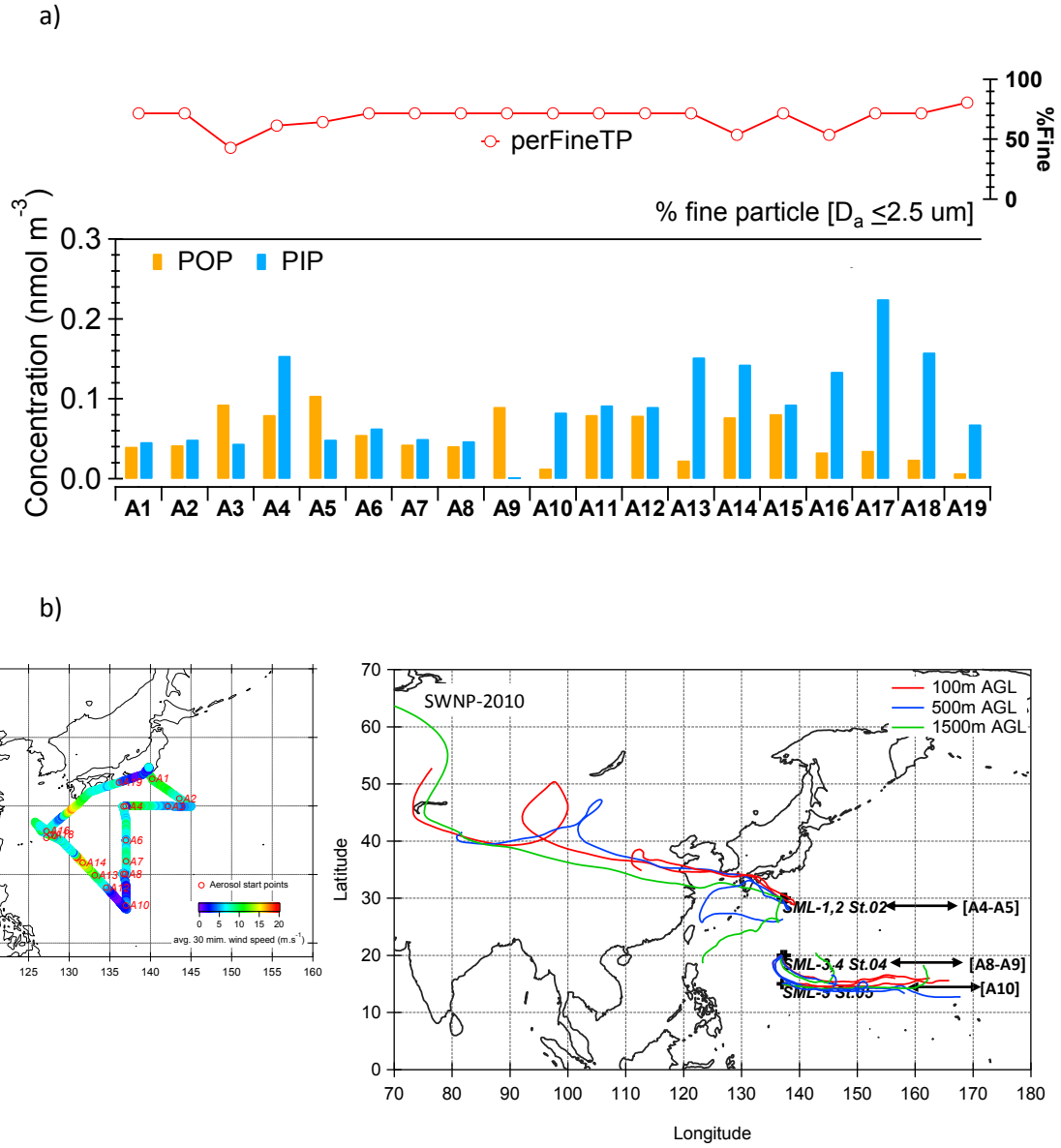

Fig. 3.2.3. (a) Concentration of atmospheric phosphorus measured during in the Subtropical Western North Pacific cruise (SWNP-2010). Blue bar represented concentration of particulate inorganic phosphorus (PIP) and orange bar represented for particulate organic phosphorus (POP). (b) atmospheric sampling location comparing with the 7-day air mass trajectory at points of SML sampling. Red - open circle in the above panel represented the fraction of Total.P in fine mode aerosols ($D_a \leq$ 2.5µm).

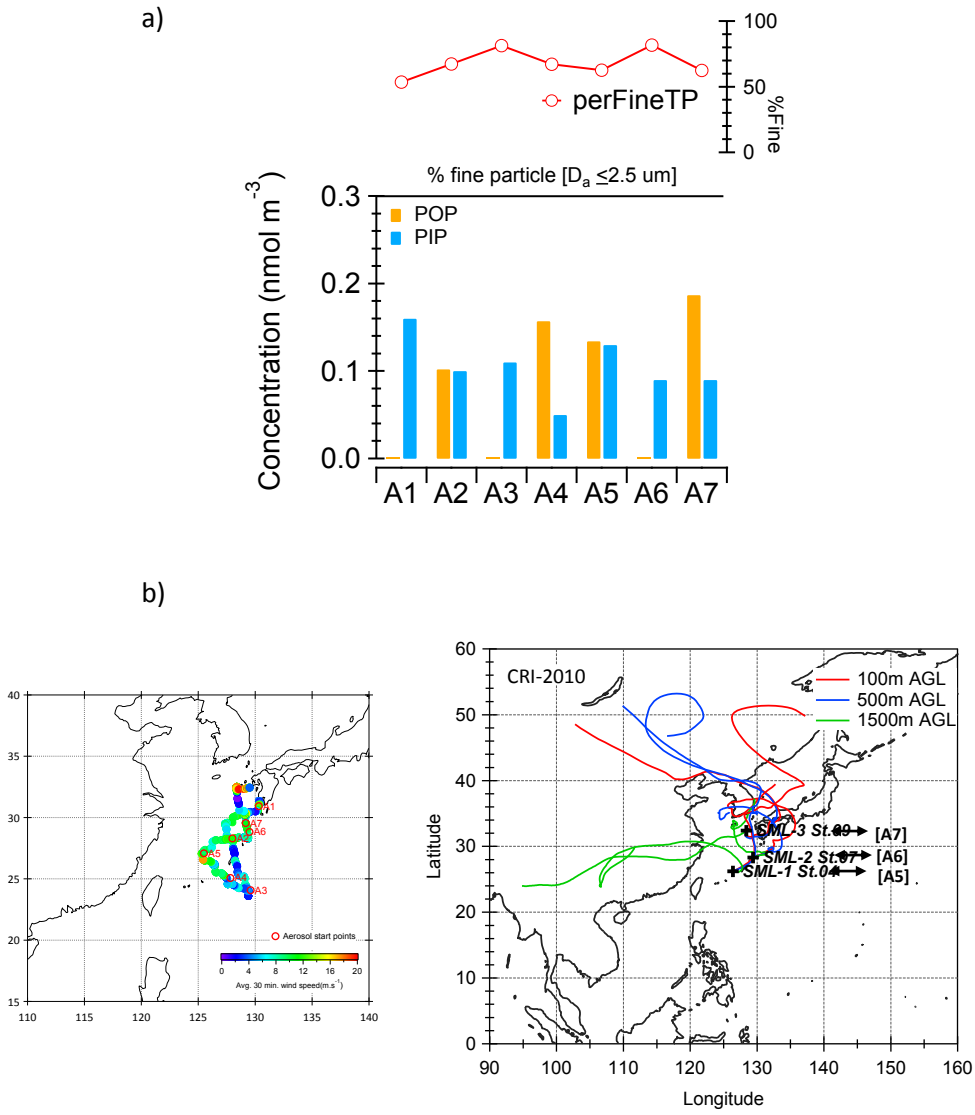

Fig. 3.2.4. (a) Concentration of atmospheric phosphorus measured during in the Coastal Sea around the Ryukyu Islands (CRI-2010). Blue bar represented concentration of particulate inorganic phosphorus (PIP) and orange bar represented for particulate organic phosphorus (POP). (b) atmospheric sampling location comparing with the 7-day air mass trajectory at points of SML sampling. Red - open circle in the above panel represented the fraction of Total.P in fine mode aerosols ($D_a \leq$ 2.5µm).

3.3. Enrichment of phosphorus in SML

Enrichment factor (EF) is expressed as the ratio concentration of the interest chemical in the SML over the SSW (**Eq. 3.1**., Liss and Duce, 1997). Typically, a degree of enrichment is depending on the methods of collection and is influenced by geographical locations and physical process e.g. wind and wave actions (**Fig. 2.1.2-3**). The enrichment is indicated when EF is greater than 1.

$$\mathrm{EF}x = \frac{[X]sml}{[X]ssw} \qquad \textbf{[Eq. 3.1.]}$$

When sampling with two different methods, the surface excess concentration (SEC) is considerably used for the comparison purpose. SEC is expressed as the excess concentration of SML over the underlying SSW in the same thickness dimension. The equation demonstrated in **Eq. 3.2** [Liss and Duce, 1997].

$$\mathrm{SEC}x = ([X]sml - [X]ssw)x\mathrm{SML}thickness \qquad \textbf{[Eq. 3.2.]}$$

In general, phosphorus tends to enrich in the SML layer with the EF of 1-3 for the dissolved forms and slightly higher in the particulate phosphorus to 1 - 7 [Hillbricht-ilkowska and Kostrzewska-szlakowska, 2004]. Enrichment of soluble phosphorus as phosphate was reported in the same level with the other nutrient species at EF of 1-3 [Reinthaler et al, 2008; Gladyshev, 2002].

3.3.1. Enrichment and surface excess concentration of phosphorus in glass plate and drum samples

In this study the enrichment factor (EF) from glass plate (SML-GP) displayed slightly higher in number of concentration than those of the drum sampler (SML-D) in dissolved phosphorus forms. The SML-GP thickness was also exhibited much thicker layer (**Table 3.2.1, Table 3.3.1** and **Fig. 3.3.1**). SML-D, displayed greater EF for the particulate phosphorus. The surface excess concentration (SEC)

of SML-GP samples also exhibited much higher excess phosphorus concentration. High SEC for dissolve phosphorus was exhibited in the EEP-2012, while CRI-2010 exhibited the highest excess concentration of particulate phosphorus (**Table 3.3.2**).

3.3.2. Enrichment of phosphorus and its concentration in SML and SSW

In most SML samples, enrichment of total dissolved phosphorus (TDP) was not expressed (EF_{TDP} = 1; **Fig.3.3.1**), but for SRP and DOP fraction, enrichment factor showed a large variation. Under low productivity seawater of the Subtropical Western North Pacific region (SWNP-2010 cruise), SRP enrichment was displayed in relatively high enrichment at a factor of 1.1 - 4.1 and was higher than those DOP (EF_{DOP} = 0.6 – 2.0). This was because SRP depleted in water column (SRP_{SML}= 0.11-0.15 µM and SRP_{SSW} = 0.06 µM). The depleted nutrient in seawater was resulted to low productivity thus, low enrichment of particulate phosphorus observed (TPP_{SML}= 21-35 nM, EF_{TPP} = 0.5 - 1.5, **Fig. 3.2.1**, **Fig. 3.3.1 and Table 3.3.1**).

In CRI-2010 cruise, DOP was more dominant in the SML and accounted for 60-70% of total phosphorus (**Fig.2.3.1** and **Fig. 2.3.2**) while SRP was more dominant in SSW. This cruise showed higher enrichment of DOP (EF_{SRP} = 0.1 - 1, EF_{DOP} = 1 - 2.7). For particulate phosphorus, it showed moderately high enrichment to a factor of 5 due to the biological complex of coastal water and the faster biogeochemical response and the quicker material turnover rate. Previous studies have addressed that enrichment of phosphorus is closely related with particulate organic matter (POM) in providing surface for sorption/adsorption process [Danos, 1983; Liss duce, 1997] and an anion binder for phosphate [Cauwet, 1978]. High enrichment of POP and PIP in the CRI-2010 was likely resulted from those phosphorus sorption/adsorption onto POM.

For a High Nitrate, Low Chlorophyll-a (HNLC) seawater in the Eastern Equatorial Pacific (EEP-2102 cruise), neither SRP nor DOP found the enrichment factor greater than 1. Concentration

of both SRP and DOP in SML and SSW did not show any differences (SRP_{SML} = 0.74 - 0.87 µM, DOP_{SML} = 0.78 - 0.87 µM). Under the HNLC condition, surplus nutrients like phosphorus did not drawdown from bulk seawater, hence, low to non-enrichment resulted. However, enrichment of particulate phosphorus was considerably high due to the very lower background concentration (TPP_{SML}= 19-1280 nM, EF_{TPP} = 0.95-72) and the production of particulate phosphorus.

Table 3.3.1. Summary for average, minimum and maximum number of enrichment factors (EF) for total dissolved phosphorus (TDP), total particulate phosphorus (TPP), soluble reactive phosphorus (SRP), dissolved organic phosphorus (DOP), particulate inorganic phosphorus (PIP) and particulate organic phosphorus (POP) for SML-GP and SML-D samples from 3 cruises; SWNP-2010, CRI-2010 and EEP-2012.

Enrichment Factor		TDP	TPP	SRP	DOP	PIP	POP
SWNP-2010	Glass plate	1.2	1.3	1.9	1.1	1.3	1.3
		[0.8-2]	[1-1.5]	[1-2.7]	[0.6-2]	[1-1.5]	[1-1.5]
	Drum	0.9	0.9	2.5	0.6	0.8	1.5
		[0.7-1.1]	[0.5-1.3]	[1.1-4.1]	[0.3-0.8]	[0.5-1.3]	[0.5-3.9]
CRI-2010	Glass plate	1.5	2.2	0.7	2.1	2.8	2
		[1.0-2.5]	[1.9-2.7]	[0.1-1]	[1-2.7]	[0.6-5]	[1.6-3.7]
	Drum	1.1	2.1	0.8	1.3	1.9	2.4
		[0.8-1.5]	[1.4-3.1]	[0.4-1]	[1-1.6]	[0.4-3.1]	[1.5-3]
EEP-2012	Glass plate	1.1	8.3	1.1	1.1	9.3	8.3
		[0.8-1.4]	[1.6-32.7]	[0.9-1.3]	[0.8-1.6]	[1.3-38]	[1.3-29.7]
	Drum	1.1	17.0	1.2	1.1	19.2	16.1
		[1-1.3]	[1.2-71.5]	[1-1.6]	[0.9-1.3]	[1.6-85.6]	[1-63.7]

[minimum - maximum]

Table 3.3.2. Summary for average, minimum and maximum number of surface excess concentration (SEC) of phosphorus by all forms for SML-GP and SML-D samples from 3cruises; SWNP-2010, CRI-2010 and EEP-2012.

Surface Excess Concentration		TDP(µM)	TPP(nM)	SRP (µM)	DOP (µM)	PIP (nM)	POP (nM)
SWNP-2010	Glass plate	1.7	240.2	1.7	0.0	48.0	288.3
		[-2.2-6.8]	[0-684]	[0-3.9]	[-3.9-5.3]	[0-570]	[0-114]
	Drum	-0.7	-137.0	1.9	-2.7	33.8	-103.2
		[-3.1-0.7]	[-455-156]	[0.2-3.6]	[-6.7-0]	[-379-130]	[-76-265]
CRI-2010	Glass plate	2.4	1060.0	-2.4	4.9	769.2	136.0
		[0-10]	[793-1370]	[-7.3-4.6]	[0-7.3]	[-217-1030]	[-80-190]
	Drum	0.2	704.0	-0.8	1.1	564.4	704.7
		[-1.3-2.0]	[247-1508]	[-2.5-0]	[0-2]	[-257-505]	[158-1004]
EEP-2012	Glass plate	2.4	427.2	-0.7	3.2	154.7	272.5
		[-10.9-18.9]	[273-26040]	[-5.5-4.6]	[-5.5-16.1]	[54-10832]	[87-15209]
	Drum	5.3	420.6	3.3	2.1	158.6	262.0
		[-1.7-13.5]	[57-48317]	[0-7.9]	[-1.7-10.7]	[70-20624]	[-13-27693]

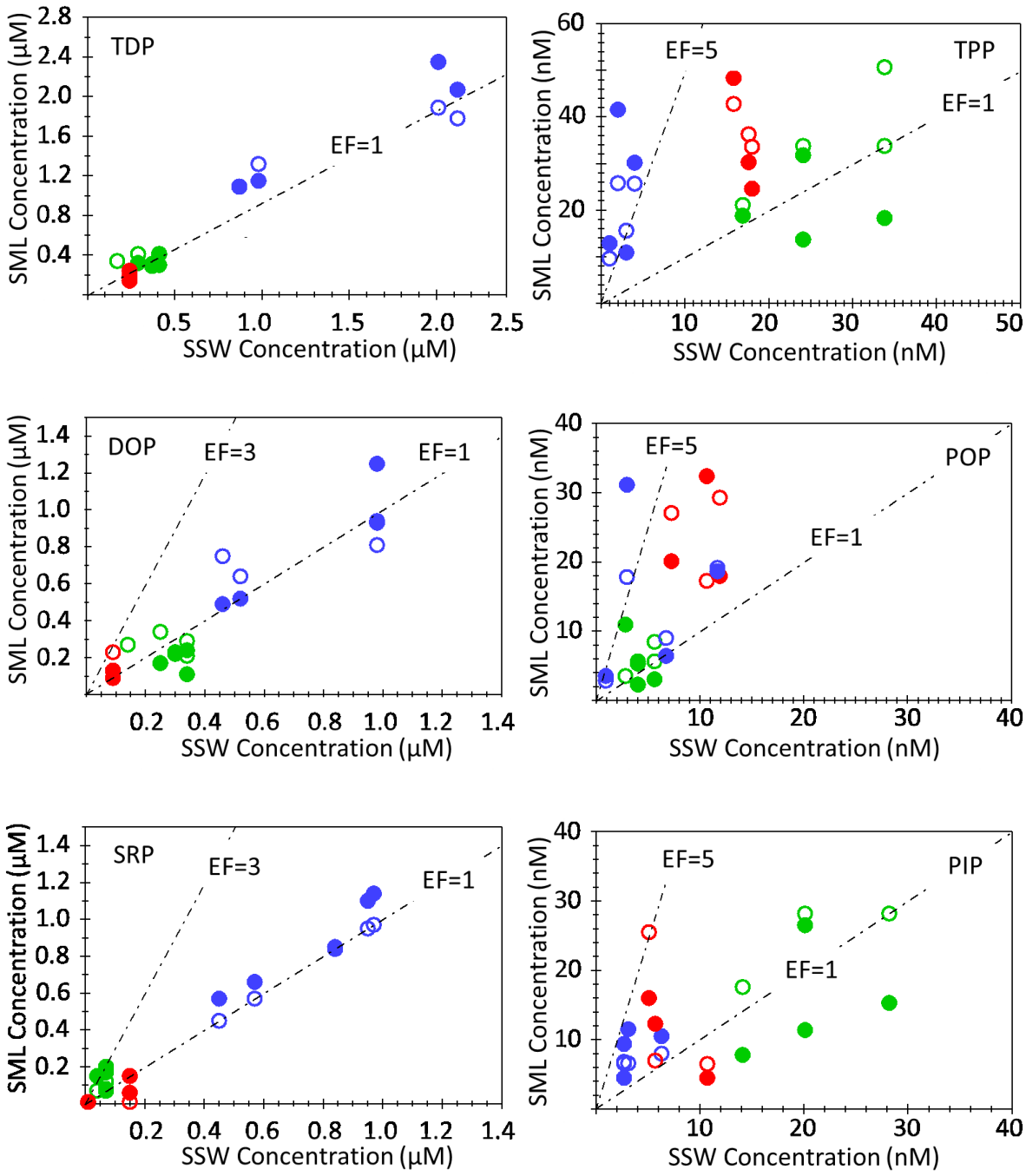

Fig. 3.3.1. Relationship between the concentration of phosphorus in SML and SSW, in the left panel for total dissolved phosphorus (TDP), dissolved organic phosphorus (DOP) and soluble reactive phosphorus (SRP) and in the right panel for total particulate phosphorus (TPP), particulate organic phosphorus (POP) and particulate inorganic phosphorus (PIP). EF>1 indicated the enrichment of phosphorus in SML over SSW in 3 cruises; SWNP-2010, CRI-2010 and EEP-2012.

3.3.3. Enrichment factor and its relation to wind speed and chlorophyll-a

Previous work show the effect of wind speed towards the enrichment of surfactant [Wurl et al., 2011].In biological productive seawater, it was shown also an enrichment of surfactant. Enrichment of TDP and TPP plotted against wind speed and surface chlorophyll-a concentration (as an indicator of productive seawater (**Fig. 3.3.2)**. TDP and TPP enrichment tended to decrease with an increasing wind speed. For an increase of chlorophyll-a concentration, only CRI-2010 sample showed an inverse trend. Since data sets was too small, it was evitable to conclude the increase of productivity in the Coastal Sea decreased the TTP enrichment.

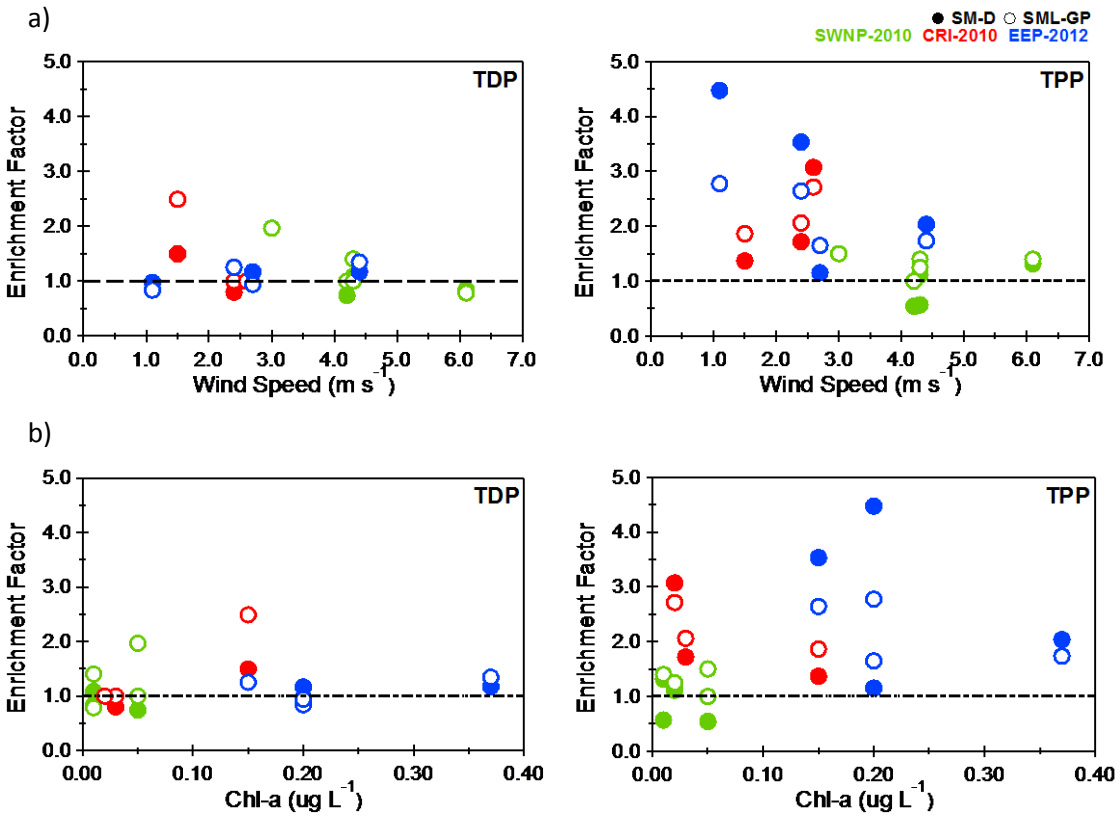

Fig. 3.3.2. Scatter plot of a) winds speed (m s^{-1}) and b) surface chlorophyll-a concentration (µg L^{-1}) with the enrichment factors of total dissolved phosphorus (TDP) and total particulate phosphorus (TPP) in 3 cruises, SWNP-2010, CRI-2010 and EEP-2012. Dashed line represent the EF=1.

In term of organic phosphorus as DOP and POP, scatter plots of enrichment factor with the wind speed showed a similar decreasing trend with an increase of wind speed, but more announced in the POP fraction. However, relation of chlorophyll-a and enrichment was not found in the organic phosphorus (**Fig. 3.3.3**).

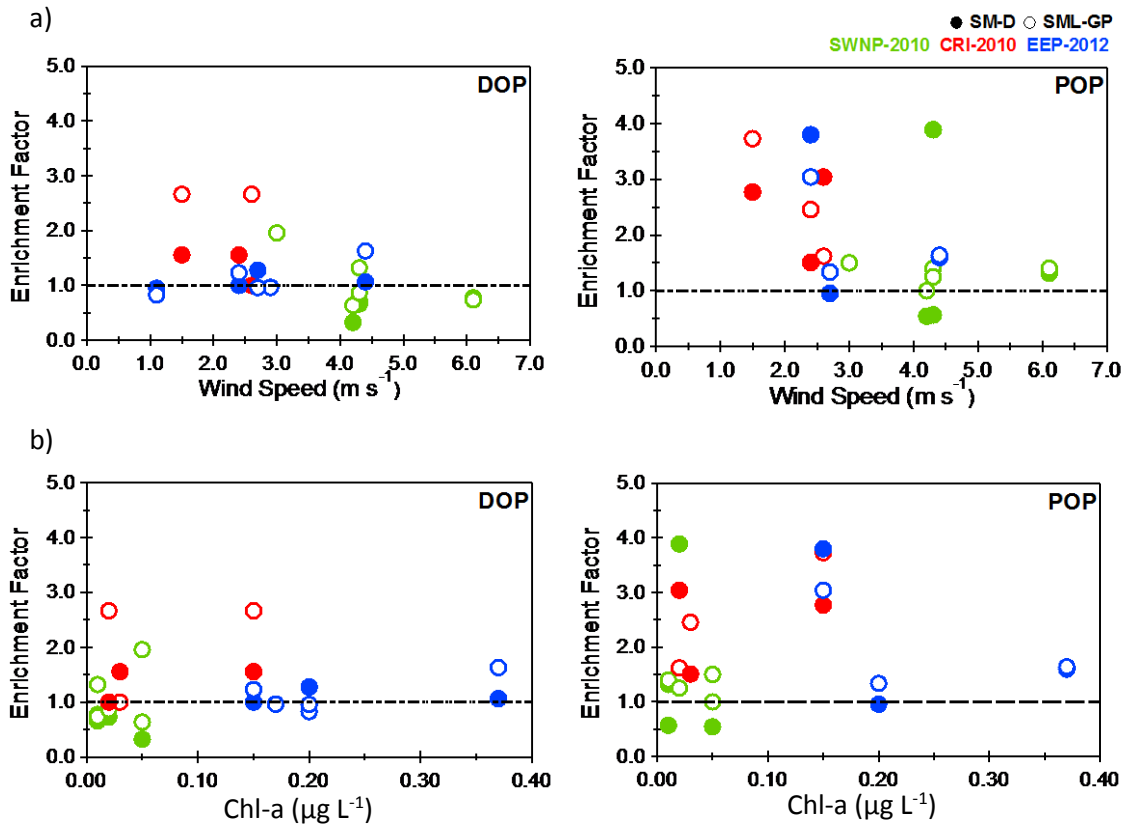

Fig. 3.3.3. Scatter plot of a) winds speed (m s^{-1}) and b) surface chlorophyll-a concentration (µg L^{-1}) with the enrichment factors of dissolved organic phosphorus (DOP) and particulate organic phosphorus (POP) in 3 cruises, SWNP-2010, CRI-2010 and EEP-2012.

Dashed line represent the EF=1.

3.4. Vertical distribution of phosphorus and suspended particulate matter in Eastern Equatorial Pacific (EEP-2012)

3.4.1. Vertical distribution of phosphorus in EEP-2012

Phosphorus as phosphate has been observed for non- homogeneity in concentration at sea surface boundary since 1967. Goering and Wallen investigated the first half meter of the surface water and demonstrated that the highest concentration of phosphate was at the first 5 cm. Under low phosphate condition, the maxima phosphate was delineated at depth of 30 cm [Goering and Wallen, 1967]. To date, extended knowledge has revealed to the importance of the SML position in the global scale. However, the dynamic changes of its biological and chemical composition within its layer brought up the difficulty in studying SML chemical composition. Since materials in SML were generating from the bulk seawater and the atmosphere, vertical profile can provide informative link and relative cause for the adverse changes of chemical composition in the SML, and vice versa.

In this section the vertical profiles of phosphorus and it distribution by forms in the first 200 m of water column were displayed in comparison with SML phosphorus composition. **Fig. 3.4.1** demonstrated the vertical distribution of phosphorus in 5 sampling stations in the Eastern Equatorial Pacific (EEP-2012). The concentration of phosphorus, its organic content and enrichment factor were presented in **Table 3.4.1, Table 3.4.2**, respectively. Since seawater in the Eastern Equatorial Pacific region (3°N – 3°S, 90 -140°W) reported the maximum biological productivity in corresponding with the equatorial divergence and upwelling [Pennington et al., 2006]. Near the equator, wind-driven surface causes the lift of thermocline towards euphotic zone and increase the productivity rate with nourished water. Contour profile of phosphorus in EEP-2012 demonstrated also the relaxation trend toward St. 10 where high concentration of particulate phosphorus found

at deeper water (**Fig. 3.4.2**). An increase of particulate phosphorus pool had followed the peak of sub-surface chlorophyll-a maxima (**Fig.3.4.3**)

SRP showed a typical nutrient profile with the lowest surface concentration and increased at depths (**Fig. 3.4.1**). Still, SRP in the SML was slightly higher than in the underlying SSW. For DOP, the highest concentration presented at the near surface or in the SML and slowly decreased with depths to 200 m. This was exception for the DOP at St. 08 where the DOP maxima was observed at 45 m (DOP = 2.16 μM). This DOP peak was found in corresponding with the sub-surface chlorophyll-a maximum depth (at 50 m, Chl-a = 0.35 μg L^{-1}) and the POP peak. Note that, DOP concentration was slightly higher in St.08 than other station while the SRP level remained the same.

For particulate phosphorus, PIP concentration was decreased with the increased depth. POP at St. 01 and St. 05 showed the highest concentration at the SML. The remaining St .02, St. 08 and St. 10 demonstrated the highest POP at the depth of subsurface maximum chlorophyll-a (at ~50 m, **Fig. 3.4.1** and **Fig. 3.4.3**). At St.10 (140°W), there were a considerable peak of POP and PIP in the top 50 m of water column. The change in the vertical profile of phosphorus from St.08 to St.10 were observed also in the SRP and DOP concentration. Since, a direct and/or an indirect link between the particulate phosphorus and chlorophyll-a concentration has been reported in the Pacific Ocean before [Yoshimura et al, 2007; Suzumura and Ingall, 2004], the particulate peak observed in here was likely related to the biological production and transformation of phosphorus in water column. In addition, the strongest upwelling signals for the equatorial upwelling region has been reported at around St. 10 [Gordon et al., 1997] where the peak of particulate phosphorus was demonstrated. From the 7-day back trajectory air mass, at St.10 also showed the different direction of air parcel travelled to the sampling station (**Fig. 3.4.4**).

Interestingly, the highest concentration of particulate phosphorus (TPP = 0.24-0.74 μM) at St. 01 where SRP profiles displayed the normal distribution, was not likely to reflect the above

enrichment process. Detailed analysis on the single particles of SML and SSW at St. 01 was performed to confirm the biogeochemical response towards the micro- environmental changes in SML (in Chapter 4).

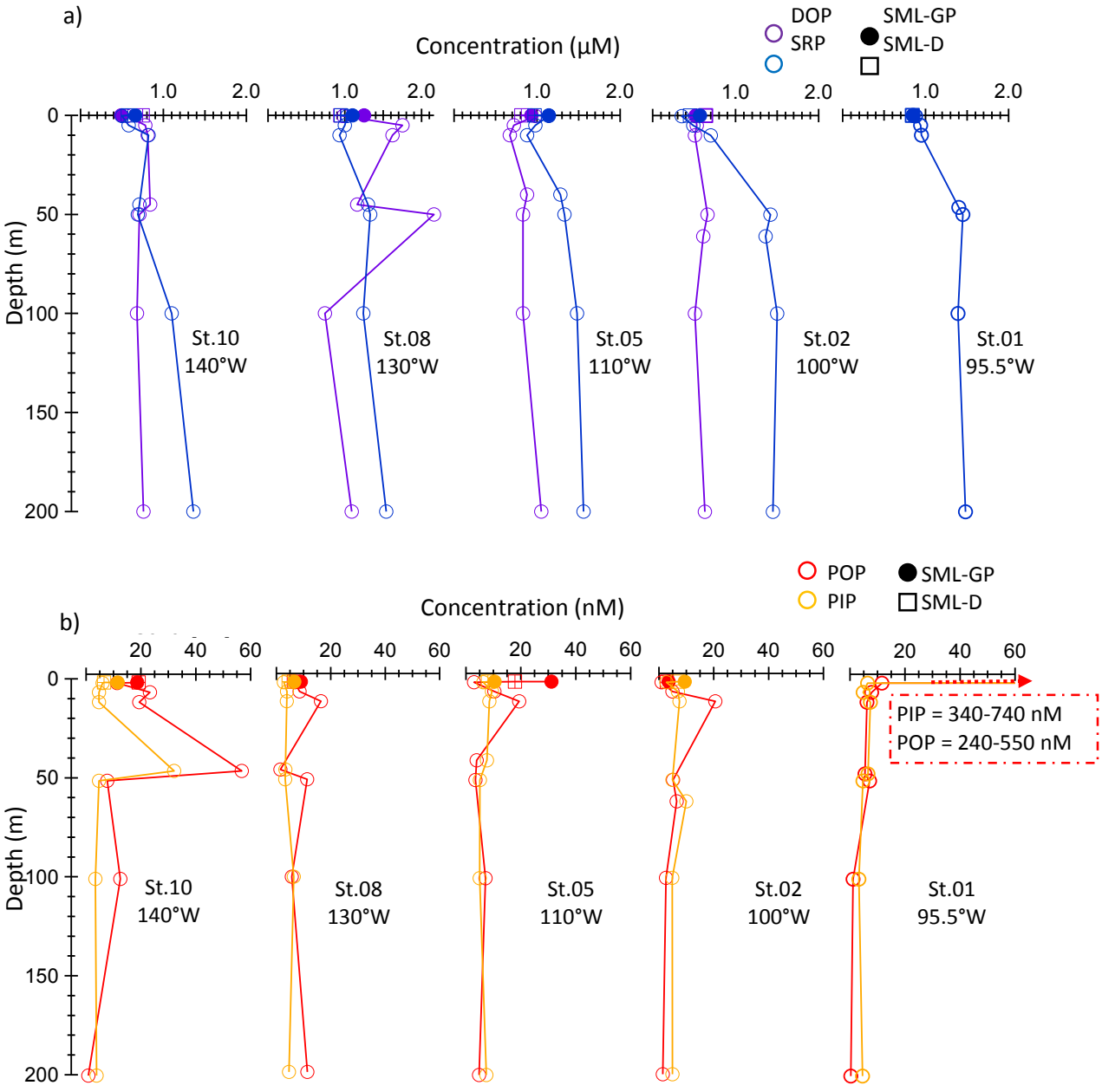

Fig.3.4.1. Vertical profiles of phosphorus in soluble reactive phosphorus (SRP), dissolved organic phosphorus (DOP), particulate inorganic phosphorus (PIP) and organic phosphorus (POP) from SML to 200 m, in five stations of EEP-2012. Note that the DOP data at St.01 was not available.

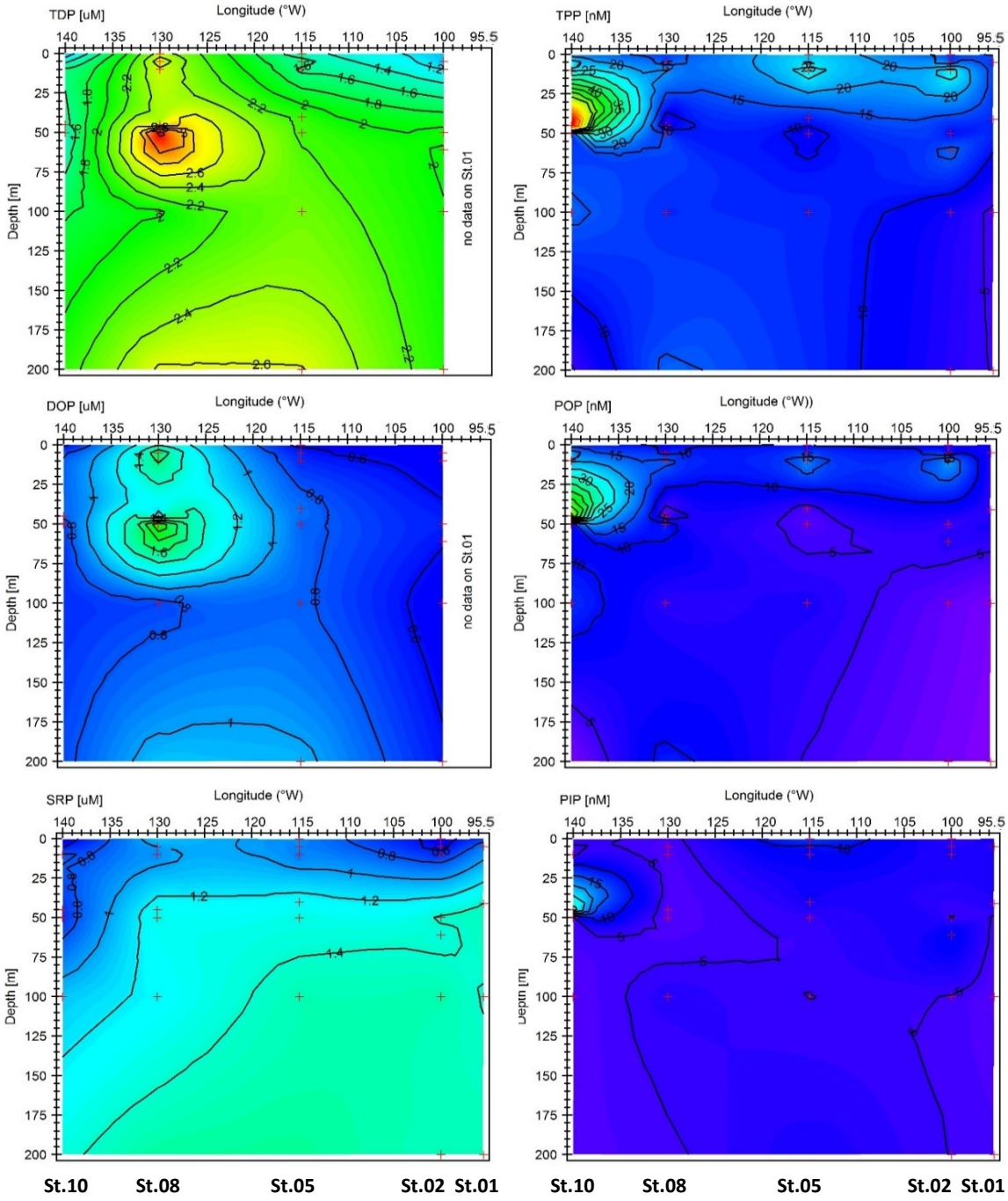

Fig.3.4.2. Concentration contour of phosphorus in µM for total dissolved phosphorus (TDP) , dissolved organic phosphorus (DOP) and soluble reactive phosphorus (SRP) in left panel and concentration in nM for total particulate phosphorus (TPP), particulate organic phosphorus (POP) and particulate inorganic phosphorus (PIP) in right panel on the Equatorial line transect from 95.5 °W – 140 °W in EEP-2012

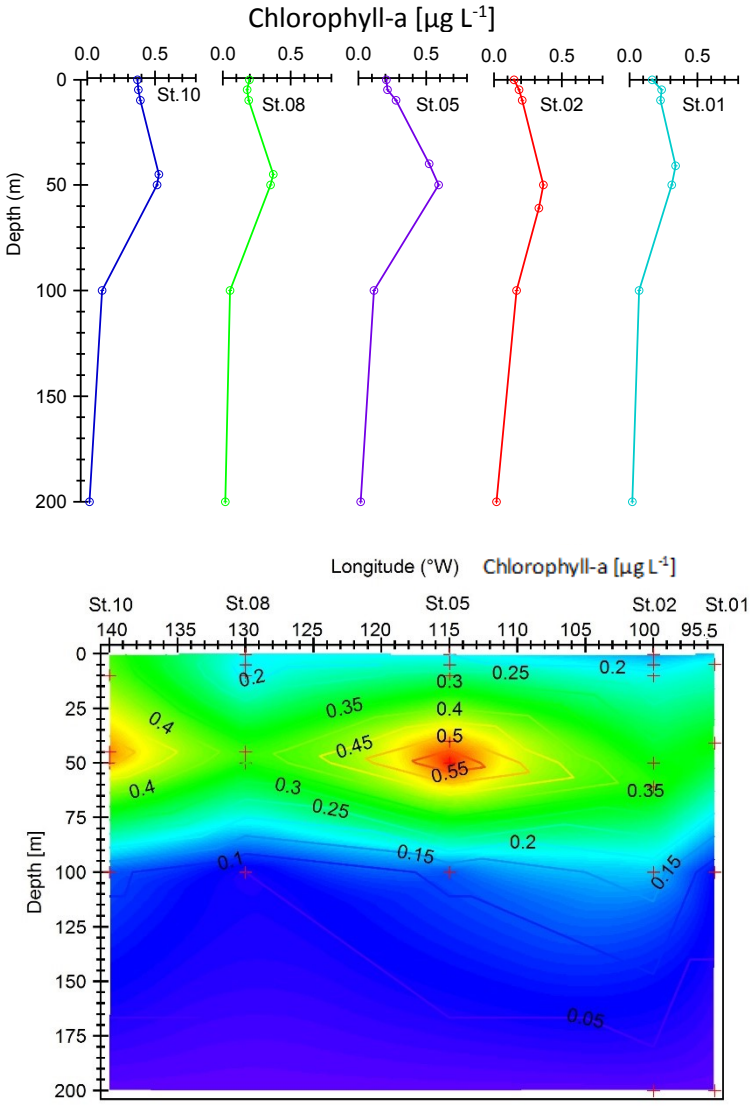

Fig.3.4.3. Vertical profile and counter concentration of chlorophyll-a [µg L^{-1}] in EEP-2012

Table 3.4.1 Distribution of phosphorus in µM for total dissolved phosphorus (TDP) and soluble reactive phosphorus (SRP) and in nM for total particulate phosphorus (TPP) and particulate inorganic phosphorus (PIP) from SML to 200 m in 5 sampling stations in EEP-2012. The organic phosphorus presented as the percentage of total dissolve phosphorus and total particulate phosphorus in %DOP and %POP), respectively.

Sampling Description		Depth	Chl-a.	Dissolved Phousphorus (µM)			Particulate Phousphorus (nM)		
		(m)	µg/l	SRP	TDP	%DOP	PIP	TPP	%POP
ST.01: 0°N, 95.5°W	SML-GP	0.000046		0.84 ± 0.14			243.4 ± 32.5	587.8 ± 129.9	58.6
Date: Feb 2, 2012	SML-D	0.000038		0.85 ± 0.30			547.7 ± 43.5	1286.2 ± 43.5	57.4
	SSW	1.5	0.17	0.88 ± 0.09	no	no	6.4 ± 0.6	18.0 ± 11.9	64.4
		5	0.23	0.94 ± 0.09			4.77 ± 3.5	12.63 ± 7.5	62.2
		10	0.23	0.95 ± 0.16	d	d	7.43 ± 3.2	13.58 ± 8.2	45.3
		41	0.34	1.40 ± 0.10	a	a	6.53 ± 2.8	12.00 ± 7.2	45.6
		50	0.31	1.45 ± 0.08	t	t	4.70 ± 0.3	11.80 ± 5.6	60.2
		100	0.07	1.39 ± 0.00	a	a	3.20 ± 1.9	4.27 ± 0.4	25.0
		200	0.02	1.48 ± 0.12			4.53 ± 1.1	4.85 ± 0.5	6.6
St.02: 0°N, 100°W	SML-GP	0.000046		0.45 ± 0.02	1.09 ± 0.00	58.7	6.8 ± 4.0	9.6 ± 2.5	29.4
Date: Feb 3, 2012	SML-D	0.000036		0.57 ± 0.16	1.09 ± 0.00	47.7	9.4 ± 9.0	12.9 ± 10.1	27.5
	SSW	1.5	0.15	0.35 ± 0.06	0.87 ± 0.32	59.8	2.7 ± 2.0	3.7 ± 3.3	25.5
		5	0.18	0.49 ± 0.03	1.02 ± 0.06	52.0	6.91 ± 6.2	11.85 ± 6.8	41.7
		10	0.21	0.70 ± 0.12	1.21 ± 0.20	42.1	7.49 ± 5.5	28.07 ± 7.3	73.3
		50	0.33	1.36 ± 0.15	1.97 ± 0.29	31.0	10.01 ± 9.1	16.44 ± 0.0	39.1
		61	0.36	1.42 ± 0.03	2.08 ± 0.06	31.7	4.89 ± 1.9	10.01 ± 9.1	51.1
		100	0.17	1.50 ± 0.06	2.01 ± 0.23	25.4	4.87 ± 1.9	7.42 ± 7.2	34.3
		200	0.02	1.45 ± 0.07	2.08 ± 0.13	30.3	4.94 ± 1.9	6.30 ± 0.1	21.6
St.05: 0°N, 115°W	SML-GP	0.000032		0.97 ± 0.05	1.78 ± 0.00	45.5	8.0 ± 0.0	25.8 ± 14.7	69.0
Date: Feb 7, 2012	SML-D	0.000033		1.14 ± 0.03	2.07 ± 0.08	44.9	10.5 ± 5.7	41.6 ± 0.0	74.9
	SSW	1.5	0.20	1.14 ± 0.03	2.12 ± 0.16	46.2	6.3 ± 5.7	9.3 ± 1.5	31.9
		5	0.21	0.98 ± 0.12	1.70 ± 0.13	42.4	9.46 ± 9.2	19.78 ± 12.7	52.2
		10	0.28	0.88 ± 0.09	1.55 ± 0.00	43.2	8.55 ± 4.9	27.97 ± 0.0	69.4
		40	0.52	1.28 ± 0.17	2.16 ± 0.35	40.7	7.61 ± 6.9	11.53 ± 5.6	34.0
		50	0.59	1.33 ± 0.16	2.16 ± 0.26	38.4	5.10 ± 4.9	8.55 ± 4.9	40.3
		100	0.11	1.48 ± 0.09	2.31 ± 0.26	35.9	4.97 ± 4.7	12.08 ± 5.3	58.9
		200	0.02	1.56 ± 0.19	2.61 ± 0.35	40.2	7.41 ± 6.7	12.16 ± 6.7	39.1
St.08: 0°N, 130°W	SML-GP	0.000048		0.95 ± 0.04	1.89 ± 0.48	49.7	6.6 ± 4.1	15.6 ± 13.5	57.7
Date: Feb 11, 2012	SML-D	0.000040		1.10 ± 0.08	2.35 ± 0.48	53.2	4.5 ± 0.5	10.9 ± 6.6	58.9
	SSW	1.5	0.20	1.03 ± 0.15	2.01 ± 0.32	48.8	2.7 ± 1.6	9.5 ± 3.2	71.3
		5	0.18	1.00 ± 0.02	2.75 ± 0.12	63.6	3.89 ± 1.1	12.41 ± 8.3	68.7
		10	0.19	0.93 ± 0.25	2.55 ± 0.41	63.5	3.83 ± 1.2	20.20 ± 5.5	81.0
		45	0.37	1.30 ± 0.20	2.46 ± 0.64	47.2	3.28 ± 2.0	4.72 ± 1.2	30.6
		50	0.35	1.33 ± 0.08	3.49 ± 0.39	61.9	3.26 ± 2.0	14.57 ± 8.0	77.7
		100	0.05	1.24 ± 0.04	1.98 ± 0.14	37.4	6.39 ± 4.0	12.08 ± 5.7	47.1
		200	0.02	1.54 ± 0.21	2.63 ± 0.29	41.4	4.59 ± 2.8	15.98 ± 5.4	71.2
St.10: 0°N, 140°W	SML-GP	0.000056		0.57 ± 0.02	1.32 ± 0.00	56.8	6.6 ± 4.4	25.7 ± 15.8	74.4
Date: Feb 13, 2012	SML-D	0.000041		0.66 ± 0.03	1.15 ± 0.08	42.6	11.5 ± 2.9	30.2 ± 24.3	61.8
	SSW	1.5	0.37	0.52 ± 0.06	0.98 ± 0.16	46.9	3.1 ± 2.8	14.8 ± 0.0	78.9
		5	0.38	0.58 ± 0.08	1.36 ± 0.17	57.4	4.69 ± 3.6	27.97 ± 11.0	83.2
		10	0.39	0.82 ± 0.02	1.63 ± 0.17	49.7	4.69 ± 2.8	24.08 ± 5.5	80.5
		45	0.53	0.71 ± 0.03	1.55 ± 0.11	54.2	32.08 ± 5.5	88.84 ± 19.4	63.9
		50	0.51	0.69 ± 0.00	1.40 ± 0.13	50.7	4.69 ± 3.6	12.41 ± 7.5	62.2
		100	0.11	1.10 ± 0.00	1.78 ± 0.23	38.2	3.38 ± 1.7	15.87 ± 5.4	78.7
		200	0.02	1.36 ± 0.13	2.12 ± 0.30	35.8	3.78 ± 1.1	4.59 ± 1.2	17.6

Table 3.4.2 Enrichment factor of phosphorus by forms; total dissolved phosphorus (TDP), dissolved organic phosphorus (DOP), soluble reactive phosphorus (SRP), total particulate phosphorus (TPP), particulate organic phosphorus (POP) and particulate inorganic phosphorus (PIP) in EEP-2012 ($EF=P_{SML}/P_{SSW}$)

	Enrichment Factor (EF)					
	TDP	DOP	SRP	TPP	POP	PIP
SML-GP						
St. 01	no data	no data	0.96	32.66	29.69	38.03
St. 02	1.25	1.23	1.29	2.64	3.04	2.50
St. 05	0.84	0.83	0.85	2.78	6.01	1.26
St. 08	0.94	0.96	0.92	1.65	1.34	2.43
St. 10	1.35	1.63	1.10	1.74	1.64	2.10
SML-D						
St. 01	no data	no data	0.97	71.45	63.66	85.58
St. 02	1.25	1.00	1.63	3.53	3.80	3.44
St. 05	0.98	0.98	1.00	4.47	10.50	1.65
St. 08	1.17	1.28	1.07	1.15	0.95	1.65
St. 10	1.17	1.07	1.27	2.04	1.64	3.68

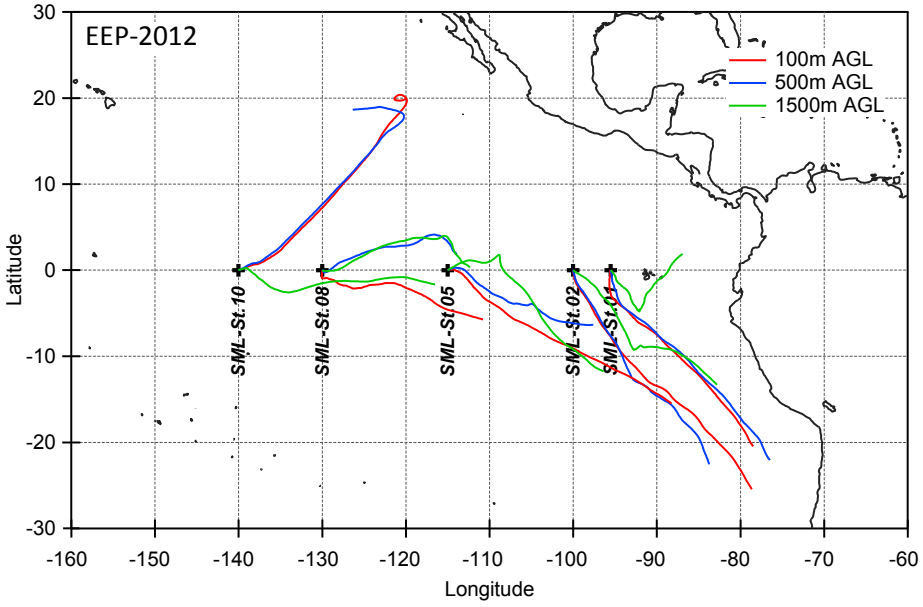

Fig.3.4.4. Seven day backward trajectory of the air mass at the SML sampling stations in EEP-2012.

3.4.2. Vertical distribution of suspended particles in EEP-2012

Particles in water column can be characterized into fine suspended particles with considerably negligible settling velocity acting like standing stocks and sinking particles consisting of fecal pellets and aggregates that are responsible for the vertical transportation of material to deeper water [McCave, 1984]. Suspended particulate matter (SPM) consisting of various materials from plankton, bacteria, detritus, clay and particulate organic matter, has its important role in biogeochemical cycling of carbon and other elements in the ocean [McCave, 1984]. It produces in-situ by the biogenic sources e.g., opal and carbonate [Iwamoto et al., 2009] or externally through the riverine and atmospheric deposition. SPM has its long resident time in the column and presents with the large surface to volume ratio enabling the modification of the chemical composition in seawater by sorption and desorption process [Iwamoto and Uematsu, 2014].

Physical and chemical properties of SPM provided the information of the biological activity in water mass and it behavior can also relate to the biogeochemical process in the ocean, for example biogenic Si and Ca and crustal particles e.g. Al, Ti and Fe [Iwamoto and Uematsu, 2014]. The production, sinking and decomposition of biogenic particles are important to characterize the distribution of trace elements within the oceans [Wakeham and Canuel, 1988]. The release of particulate-bound elements can occur either by ion exchange processes with surface-b ound element or dissolution of element-bound to labile (e.g. organic) constituents [Fowler and Knauer, 1986]. As such processes can also occur in the SML despite the fact that SML is a small reservoir with the temporal stability. Conversion of dissolved organic materials to particulate matters, conversion of low-molecular-weight materials in to higher molecular weight substances, and photochemical transformation are the available interfacial processes enabling the modification of elemental composition in the SML [Liu and Dickhut, 1998]. For trace elements in SPM, it often

expresses the SML enrichment factor in the similar degree with particulate phosphorus and particulate organic matter, in range of 1-38 [Liss and Duce, 1997].

Water mass in the EEP-2012 relies its maximum biological productivity with the equatorial upwelling that brought up the nourish water to surface in which iron and silicon are the trace nutrients restrained the regional productivity to lower than expected [Pennington et al., 2006, Brzezinski et al., 2011]. The vertical distribution of particulate trace elements, Al, Si, Ca, and Fe were displayed here in comparison with the concentration in the SML to provide additional details for the biogeochemical process in water mass.

From previous section, **Fig.3.4.3** showed the vertical distribution of chlorophyll-a from surface to 200 m depth along the equatorial transect from 140°W to 95.5°W. The highest concentrations were found below sub-surface at the sub-surface chlorophyll a maximum layer (40-61 m) and at St. 05 showed the highest subsurface chlorophyll-a maximum concentration.

For particulate Si (pSi), the vertical profile showed the highest concentration at surface and decreased with depths (**Fig. 3.5.1.a**). In corresponding to the highest chlorophyll-a peak, it was found that the surface water (including SML, SSW and SUR) at St. 05 exhibited the highest pSi concentration in comparative with other stations. The average EF_{pSi} was 3.7 (n=5) and showed the decrease trend from St. 01 to St. 10 following the increase of pSi in the subsurface water (**Table 3.5.1 and 3.5.2**). The low but maximum surface lithogenic silica concentration observed by Adjou et al. (2011) has confirmed that the particulate Si input from the atmosphere by wind-driven has lesser impact in the Eastern Equatorial Pacific region and mostly produces in-situ.

For particulate Ca (pCa), the maximum concentration observed at 100 - 200 m depth; ranging from 0.1 - 0.26 µmol Ca L^{-1} (**Table 3.5.1** and **Fig. 3.5.2.b**). The maximum of pCa at depth had pointed to the incorporation of Ca with the detrital and fecal materials. The formation of pCa at

deeper layer has caused by the stratified upwelled water (density interface) that prevented the particles from sinking [Kindler et al., 2010; Lal and Lerman, 1970]. For surface water, SML exhibited much higher concentration of pCa and EF_{pCa} was ranging from 1.8 - 4 (**Table 3.5.2**). The highest surface pCa concentration was found at St. 02 (SML = 0.54 and SUR = 0. 17 µmol Ca L^{-1}). Under the rich organic content in the SML layer, pCa can occur possibly as by the incorporation with particulate organic matter.

Particulate Al (pAl), as the representative of the lithogenic particles; for the riverine input or the atmospheric deposition. The highest concentration of pAl was constrained at the surface water ($\underline{\geq}$.20 nmol Al L^{-1}, **Fig. 3.5.1.c**). In SUR sample, an increase of pAl was found from St. 01 towards St. 10, ranging from 19.3 to 59.4 nmol Al L^{-1}. While in the SML, concentration of pAl was doubled but did not show any differences except at St. 08. The average EF_{Al} was 2.6 and the lowest EF was observed at St. 10 where the pAl level in water column was relatively high.

Particulate Ti (pTi) and Fe (pFe) are both tracers of mineral particles and the indicators for the atmospheric deposition in open ocean. The concentration profile of pTi and pFe were similar with pAl where high concentration exhibited at surface water and decreased in subsurface water to the non-detection limit level (**Table 3.5.1** and **Fig.3.5.1.d**). Mean enrichment of pTi and pFe were at the factors of 9.5 and 6.1, respectively. The highest concentration of pTi was found in SML at St. 05. The highest pFe concentration was observed at St. 01 along with the highest particulate phosphorus observed.

Table 3.4.3. Concentration of particulate silicon (pSi), calcium (pCa), aluminum (pAl), iron (Fe) and titanium (Ti) in surface water (SML, SSW and SUR) of EEP-2012. The enrichment factor displayed as the concentration ratio between the SML and SSW.

Station	depth	Concentration (μM)		Concentration (nM)		
		pSi	pCa	pAl	pFe	pTi
Drum (depth= μm)						
SML-St.01	38.08	2.94	0.54	137.5	81.0	45.8
SML-St.02	35.81	1.08	0.14	105.8	25.0	17.7
SML-St.05	33.41	3.19	0.16	107.2	42.2	70.5
SML-St.08	39.60	0.63	0.13	43.8	45.4	20.9
SML-St.10	41.43	2.56	0.24	111.5	38.1	23.6
Average	37.67	2.08 ± 0.98	0.24 ± 0.12	101.2 ± 23.0	46.3 ± 13.9	35.7 ± 18.0
SSW (depth= m)						
SSW-St.01	1.50	0.48	0.14	47.2	7.2	7.8
SSW-St.02	1.50	0.19	0.06	18.6	4.8	2.3
SSW-St.05	1.50	1.37	0.09	106.8	15.2	3.8
SSW-St.08	1.50	0.19	0.05	26.9	9.0	3.6
SSW-St.10	1.50	2.58	0.06	70.4	L.D.	L.D.
Average	1.50	0.96 ± 0.81	0.08 ± 0.03	53.96 ± 27.7	9.0 ± 3.1	4.4 ± 1.7
Surface water (Bucket sampling on board)						
SUR-St.01		0.20	0.06	19.3	22.3	22.7
SUR-St.02		0.23	0.17	23.1	2.3	1.3
SUR-St.05		0.70	0.05	27.7	0.4	0.6
SUR-St.08		0.29	0.04	14.7	4.8	1.3
SUR-St.10		0.53	0.04	59.4	1.2	2.9
Average		0.39 ± 0.18	0.07 ± 0.04	28.84 ± 12.2	6.2 ± 6.4	5.8 ± 6.8
Enrichment Factor (EF=SML/SSW)						
St.01		6.1	3.9	2.9	11.3	5.9
St.02		5.5	2.4	5.7	5.3	7.7
St.05		2.3	1.8	1.0	2.8	18.3
St.08		3.4	2.7	1.6	5.0	5.9
St.10*		1.0	4.0	1.6	n.a.	n.a.
Average		3.7 ± 1.7	3.0 ± 0.8	2.6 ± 1.4	6.1 ± 2.6	9.5 ± 4.4

Table 3.4.4. Concentration of particulate silicon (pSi), calcium (pCa), aluminum (pAl), iron (Fe) and titanium (Ti) from surface water to 200 meter depth in EEP-2012.

Longitude	Depth	Concentration [μM]		Concentration [nM}		
		pSi	pCa	pAl	pFe	pTi
95.5°W	SML-D	2.94	0.54	137.5	81.0	45.8
(St.01)	SSW	0.48	0.14	47.2	7.2	7.8
	SUR	0.20	0.06	19.3	22.3	22.7
	50	0.02	0.05	1.9	0.5	n.d.
	100	0.04	0.11	2.2	0.5	1.3
	200	0.03	0.07	1.5	0.7	n.d.
100°W	SML-D	1.08	0.14	105.8	25.0	17.7
(St.02)	SSW	0.19	0.06	18.6	4.8	2.3
	SUR	0.23	0.17	23.1	2.3	1.3
	10	0.04	0.07	2.6	1.1	n.d.
	50	0.03	0.05	1.9	0.4	n.d.
	61	0.03	0.17	3.7	0.9	n.d.
	100	0.06	0.24	2.6	0.9	n.d.
	200	0.05	0.09	2.6	1.4	n.d.
115°W	SML-D	3.19	0.16	107.2	42.2	70.5
(St.05)	SSW	1.37	0.09	106.8	15.2	3.8
	SUR	0.70	0.05	27.7	0.4	0.6
	50	0.08	0.16	1.9	0.5	n.d.
	100	0.06	0.25	2.6	1.3	n.d.
	200	0.05	0.11	1.5	0.4	n.d.
130°W	SML-D	0.63	0.13	43.8	45.4	20.9
(St.08)	SSW	0.19	0.05	26.9	9.0	3.6
	SUR	0.29	0.04	14.7	4.8	1.3
	10	0.02	0.06	1.5	n.d.	n.d.
	45	0.10	0.13	1.5	n.d.	n.d.
	50	0.11	0.11	1.5	0.4	n.d.
	100	0.08	0.10	1.9	0.7	n.d.
	200	0.06	0.26	1.9	0.5	n.d.
140°W	SML-D	2.56	0.24	111.5	38.1	23.6
(St.10)	SSW	2.58	0.06	70.4	1.0	2.0
	SUR	0.53	0.04	59.4	1.0	2.9
	50	0.13	0.16	3.3	0.4	n.d.
	100	0.03	0.10	1.1	n.d.	n.d.
	200	0.06	0.14	2.6	0.9	an

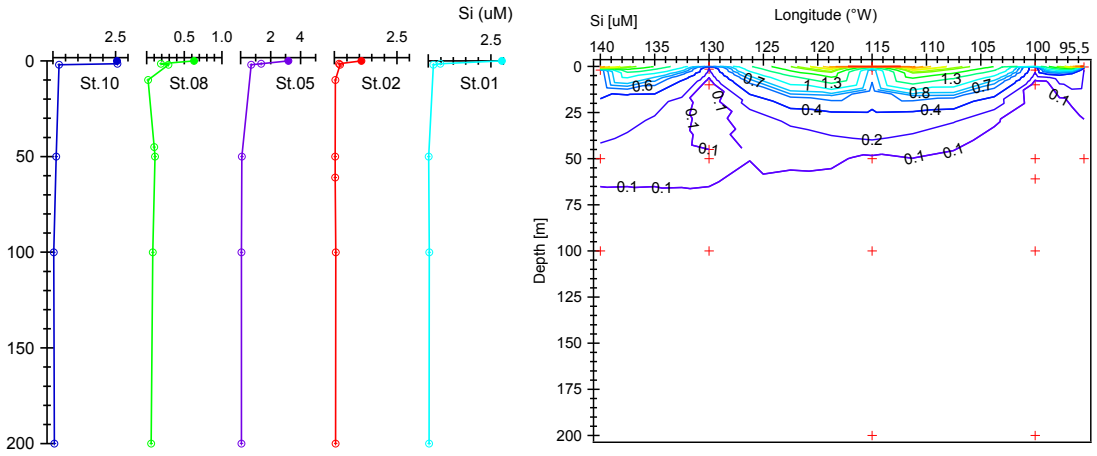

Fig.3.4.4.a. Vertical profile of particulate Si (pSi) in µmol Si L^{-1} and concentration contour of pSi in the Equatorial line transect from 95.5°W-140°W in EEP-2012.

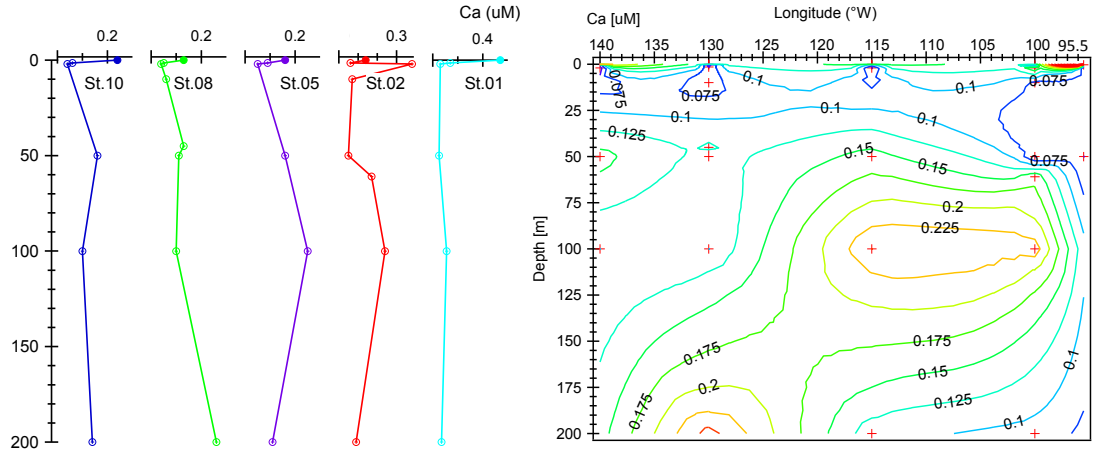

Fig.3.4.4.b. Vertical profile of particulate Ca (pCa) in µmol Ca L^{-1} and concentration contour of pCa in the Equatorial line transect from 95.5°W-140°W in EEP-2012.

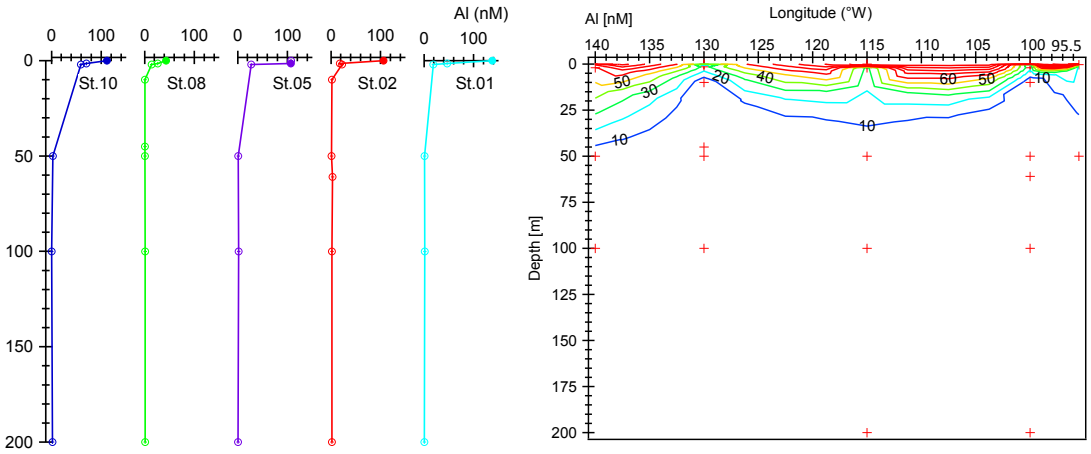

Fig.3.4.4.c. Vertical profile of particulate Al (pAl) in nmol Al L^{-1} and concentration contour of pAl in Equatorial line transect from 95.5°W-140°W in EEP-2012.

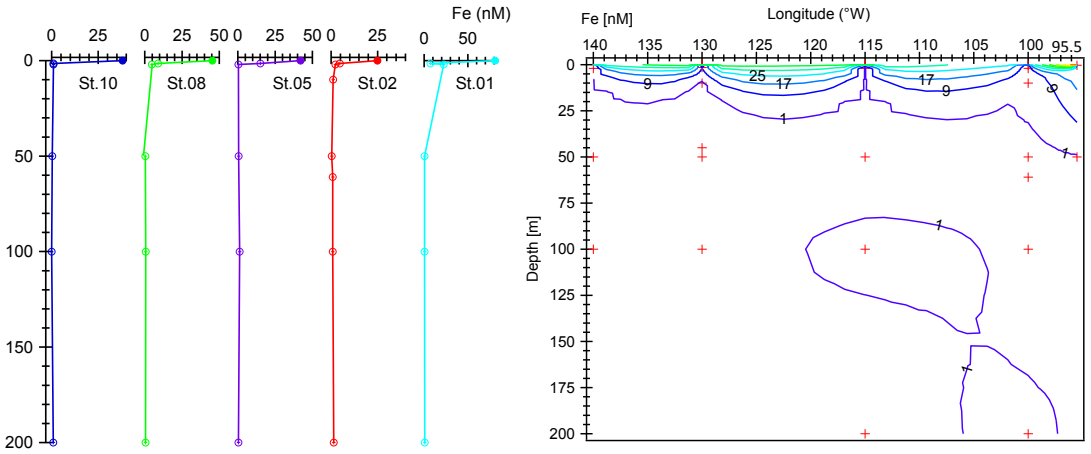

Fig.3.4.4.d. Vertical profile of particulate Fe (pFe) in nmol Fe L^{-1} and concentration contour of pFe fin the Equatorial line transect from 95.5°W-140°W in EEP-2012.

3.5. Biogeochemical importance of phosphorus in the SML

In bulk seawater, the partitioning between dissolved and particulate phosphorus is governed by the adsorption/desorption on particle surfaces, biological uptake and remineralization [Paytan and McLaughlin, 2007, Lin et al., 2012]. For SML, phosphorus composition may exhibit differently varying on the temporal changes in the physical and biogeochemical process at the interface and/or within the water column. The physical process as such micro-scale wave braking and wind speed induced the removal and renewal of surface substances and modify the chemical composition. However, biological by-products in water column brought up to sea surface and accumulated in the SML increasing substances concentration and surface active area for the reaction.

Even though, upward transportation controlled the accumulation of substances in the SML, biogeochemical process has been massively influenced by microorganism [Cunliffe et al., 2011]. The reminerization of dissolved organic matter and the breakdown of particulate organic matter by microbial activity were likely to occur within the SML. This has been suggested from the observation of the elevated hydrolytic activity in the SML that increase the turnover rate of organic carbon [Cunliffe et al., 2013]. Microbial assemblage with the specific enzyme to break down polymeric substances and the opportunistic species that can rapidly response to the high nutrient condition were found as an active microbial community in the SML [Obernosterer et al., 2008].

Likewise, phosphorus can be processed and transformed to the bioavailable forms by ranges of microbiological activity within the SML. Hydrolytic process can potentially release substantial amount of nutrients including phosphate into seawater. This has observed from the accumulating of such phosphorus at the cell surface [Björkman and Karl, 1994]. Since phosphorus regeneration and cycling ultimately in the eutrophic zone, the upward transportation and the accumulation of organics and phosphorus in the SML can be recycled effortlessly. Up to date the

upward biological flux of organic matter has yet determined even in carbon cycling [Cunliffe et al., 2013]. The measurement of the ascending flux in-situ comparing with bottle incubation is suggesting for future study, since there is no consensus in the SML results from the bottle study of the high respiration rate and an inhibition result of SML biomass production study [Obernosterer et al., 2008]. The study of such specific biogeochemical activity that occur within the organic rich SML can be important to emphasize the role of SML in sustaining the phosphorus recycling process especially for the open ocean and phosphorus-limited productivity region.

Summary

Same as bulk seawater, total dissolved phosphorus (TDP) was a major phosphorus pool in the SML and accounted for about 90% of total phosphorus in SWNP-2010 and CRI-2010 and 98% in the EEP-2012. Level of TDP was higher in a High Nitrate, Low Chlorophyll-a (HNLC) seawater (~ 0.9 - 2 µM; EEP-2012) than the oligotrophic seawater (0.1-0.4 µM; SWNP-2010 and CRI-2010). Concentration of particulate phosphorus were reported at about 21-38 nM in the SML and 12-26 nM in the SSW, in SWNP-2010 and CRI-2010. In the EEP-2012, particulate phosphorus concentration was similar to aforementioned number but lower in the SSW (4 – 18 nM). Enrichment factor (EF) is reported as the ratio concentration of substances in the SML over SSW. EF of TDP, SRP and DOP reported in this study ranged from 0.7-2.5, 0.1-4.1 and 0.3-2.7, respectively. For particulate phosphorus, except for the SWNP-2010, particulate organic phosphorus was more dominant in the SML. The low background concentration of particulate phosphorus (<20 nM in the SSW) contributed to higher enrichment factor among these particulate pool and varied from 0.5 to 72.

Enrichment of phosphorus by forms was associated with its relative low concentration in SSW. Aside from physical enrichment process induced by wind and wave action, the water characteristic driven by the biological activity was also important. Thes enrichment tended to

decrease with the increase wind speed. However, the difference of surface chlorophyll-a concentration (as the trophic state of seawater indicator) did not show clearly a reverse trend of the decrease of enrichment with increase chlorophyll-a concentration, in this study.

Vertical profile of phosphorus in EEP-2012 demonstrated particulate phosphorus peak at depth of the subsurface chlorophyll-a maximum (St.10, 140°W) where previously reports the strong upwelling signal around this area [Gordon et al., 1997]. Profile of particulate Al and Fe presented its highest concentration in the SML, indicating the external input of nutrients from the atmosphere, enhancing the biological productivity, increasing enrichments of particulate Si, Ca and phosphorus in the SML.

Phosphorus in the SML supplied from the upward transportation of substances in bulk seawater and from the atmospheric deposition. It is suggested that SML is not only the media of substance enrichment, microbial activity within the SML are able to alter, breakdown and transform and regenerate bioactive element like phosphorus and reintroduce into the biogeochemical process. The further study on the rate of upward transportation is suggested to clarify how important of the microbial food web in the SML for the recycling of phosphorus which is important to sustain the productivity in certain phosphorus limited ocean region.

4. Enrichment of particulate phosphorus in a sea-surface microlayer over the Eastern Equatorial Pacific Ocean

4.1. Introduction

Sea-surface microlayer (SML) is a thin interfacial layer lying between atmosphere and ocean and is distinguished by its differences in biological and physiochemical properties from the subsurface water (SSW). SML varies from 1 to 1,000 μm as a result of different collection devices/methods and meteorological conditions [Cunliffe et al., 2013; Zhang et al., 2006], such as wave breaking and wind velocity. The presences of SML as the surface organic film has well recognized to pose the influences in controlling the transportation of heat, gases, liquid, and solids in air–sea exchange process [Cunliffe et al., 2013; Liss and Duce, 1997] such as reduction of gas transfer velocity and role of energy barrier at the interface. It also acts as the modulating media for materials synthesis, transformation and cycling in biogeochemical process within the SML [Wheeler, 1975].

SML is a mixture of organic materials complied with a hydrated gelatinous matrix of carbonate, protein, and lipids [Wurl and Holmes; 2008]. Such materials have been supplied from the underlying SSW and atmospheric deposition [Frka et al., 2012; Joux et al., 2006; Duce et al., 1991]. The layer is latterly modified and altered by the biogeochemical production or degradation within [Joux et al., 2006; Frka et al., 2012] and is well known for the accumulation of chemical substances. Reported enrichment of chemicals has exhibited well with organic binding substances such as, particulate organic carbons and particulate trace metals [Liss and Duce, 1997; Hardy, 1982]. In case of phosphorus, the enrichment of soluble phosphorus as phosphate was reported at the same level with other nutrient species by the enrichment factor of 2-3 [Reinthaler et al, 2008, Gladyshev, 2002].

Not only chemical enrichment, distinct assemblage of bacteria (Bacterioneuston) and phytoplankton (Phytoneuston) in SML were also reported [Cunliffe et al., 2013; Joux et al., 2006]. The abundance of microbial community (in 2-4 order magnitude) was reported in responding to prevailing metrological condition but not associated with particulate organic carbon content [Stolle et al., 2011].

SML showed its non-equilibrium and substantial changes that was influenced by several physiochemical and biological processes both from water column and atmosphere. As the microhabitat, it is expected that the biogeochemical processes taken place in SML and can be affected by a slight external nutrient input, such as a deposition of atmospheric substances. Since, SML is a thin layer with a markedly small volume, it is worth considering the occurrence of such a mutual biogeochemical link and its variation within the SML. This study reported the observation of biogeochemical responses altering the chemical properties changes within SML and the possible causes of this effects emphasizing the importance of SML as the layer of biogeochemical dynamics.

4.2. Enhancement of phosphorus and particulate elements

The observations were conducted on board the R/V Hakuho Maru during 29 January - 19 February 2012 in the Eastern Equatorial Pacific (EEP-2012) as part of the Equatorial Pacific Ocean and Stratospheric/Troposphere Atmosphere Study campaign that aimed to understand the biogeochemical linkages between ocean and atmosphere in the Eastern Equatorial Pacific where is the remote area with less anthropogenic impact from the continent, keeping the High Nitrate Low Chlorophyll-a (HNLC) condition [Kaupp et al., 2011] and the largest oceanic CO_2 emission to atmosphere [Calvo et al., 2011].

SML samples were collected with a glass plate (SML-GP) and a Polymethyl Methacrylate (PMMA) rotating drum (SML-D) along with the collection of sub-surface water (SSW; at depth 0f 1.5

m). The sampling locations were demonstrated with chlorophyll-a concentration in **Fig. 4.2.1** and physical parameters were listed in **Table 4.2.1**. On shipboard, surface water samples (SUR; refer to the subsurface water sampling on board by clean bucket with approximate depth of 0.3 m) were collected during the CTD casting with Niskin bottles at depths of 5 m, 10 m, 50 m, 100 m and 200 m. The composition of phosphorus in dissolved and particulate fractions was reported in **Table 4.2.2** with particulate elements and those enrichment factors.

Table 4.2.1. Sampling stations and environmental conditions during the SML collection in EEP-2012

Station	Location	Date	Time	σ_{avg} (μm)	T_{water} (°C)	T_{air} (°C)	WS (m/s)
St.01	0˚N 95.5˚W	Feb 02,2012	08:34-09:36	41 ± 5	23.1	25.9	2.9
St.02	0˚N 100˚W	Feb 03,2012	10:36-11:52	36 ± 5	24.5	26.5	2.4
St.05	0˚N 115˚W	Feb 07,2012	12:48-13:53	33 ± 3	24.7	25.9	1.1
St.08	0˚N 130˚W	Feb 11,2012	09:23-10:58	40 ± 5	24.1	25.1	2.7
St.10	0˚N 140˚W	Feb 13,2012	09:00-10:20	41 ± 9	23.6	24.8	4.4

σ_{avg} is the average thickness of the SML samples,

WS is the 10 min average wind speed during the sampling

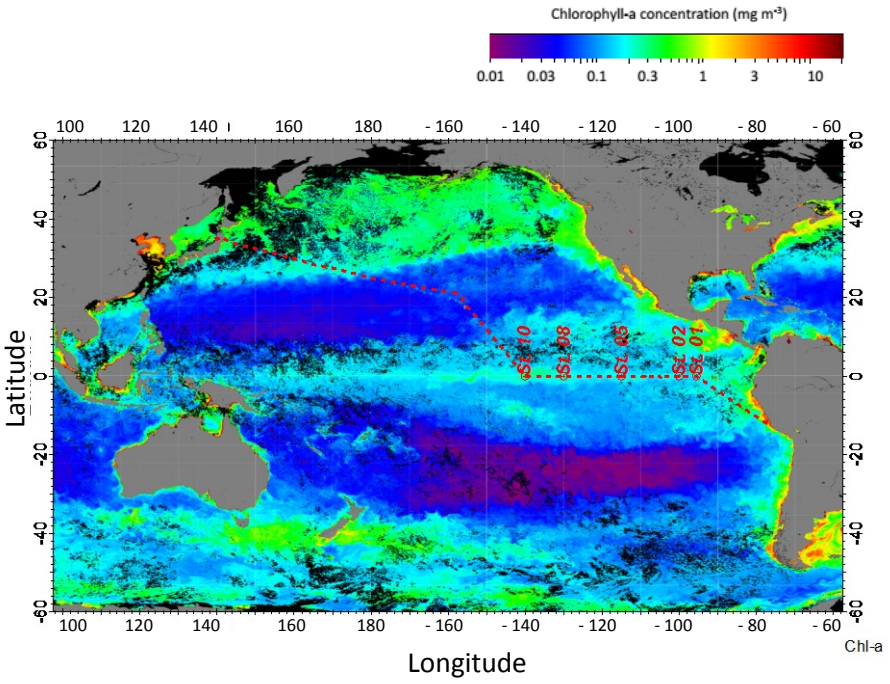

Fig. 4. 2.1. Cruise track and sampling station in EEP-2012 cruise displayed with the composite satellite image of monthly surface -Chl-a (mg m^{-3}) in February 2012; http://oceancolor.gsfc.nasa.gov

4.2.1. Phosphorus composition and its distribution in surface water

In EEP-2012, concentrations of dissolved phosphorus were contributed to approximately 98% of the total phosphorus (**Fig. 4.2.2)**. The concentrations of soluble reactive phosphorus (SRP) in SML, SUR and SSW were relatively similar in values and ranged between 0.35 ± 0.06 (SSW, St. 02) to 1.14 ± 0.03 µM (SML and SSW, St. 05). Percent of dissolved organic phosphorus (%DOP) obtained from the differences of total dissolved phosphorus (TDP) and SRP was in the range of 36% - 59%.

The enrichment factor (EF) determined by the chemical concentration ratio between SML and SSW for SRP and DOP were demonstrated neither clear SML depletion nor repletion (EF = 0.9 – 1.6). Therefore, there is no significant SML enrichment in the dissolved phosphorus in EEP-2012 cruise. Previous study reported also the enrichment of nutrients ranging at about 1.5 [Liss and Duce,

1997]. Exception was for the measurement in slick samples that found particularly high phosphate enrichment factor (EF= 3 - 4) and this was not the case in this study [Södergren, 1993].

In contrast, the enrichment of total particulate phosphorus (TPP) was markedly higher especially, at St. 01, where the enrichment of TPP raised up to the factor of 72 (SML_{TPP}= 590 – 1,300 nM; **Table 4.2.2)**. Except for St. 01, the TPP concentration ranged between 9.3 $\pm$ 1.5 nM (SSW; St.05) to 41.6 $\pm$ 2.0 (SML, St.05) and contributed to only 2% of total phosphorus (**Table 4.2.2**; **Fig. 4.2.2)**. These ranges of TPP concentration were quite similar to the reported values in the open ocean (less than 20 nM in the euphotic zone surface water and less than 5 nM for below depths; Lomas et al., 2010, Yoshimura, et al., 2007).

At St. 01, the remarkably high TPP concentration had contributed to the changes of phosphorus composition in the SML (**Fig. 4.2.3**). This change was observed in both SML-D and SML-GP therefore there was not an artifact from the SML samples at St. 01 (0˚N, 95.5˚W).

Table 4.2.2. Sampling locations, thickness, and meteorological condition in EEP-2012 cruise and concentration of dissolved phosphorus (µM), particulate phosphorus (nM), and particulate phase-elements (in µM for Al, Si, S, Ca and nM for Fe)

Station	Method	Thickness	Chl-a.	Dissolved phosphorus		Particulate phosphorus						
		(µm)	µg/l	SRP (µM)	%DOP	TPP (nM)	%POP	pSi (µM)	pS (µM)	pCa (µM)	pAl (nM)	pFe (nM)
St.01	SML-GP	45.7	-	0.84 ± 0.14 (1.0)	n.a.	587.80 ± 129.9 (32.7)	58.59					
	SML-D	38.1	-	0.85 ± 0.30 (1.0)	n.a.	1286.20 ± 43.5 (71.5)	57.42	2.94 ± 0.05 (6.1)	1.83 ± 0.03 (6.3)	0.54 ± 0.05 (3.9)	137.5 ± 40 (2.9)	81.0 ± 13.0 (11.3)
	SUR*	0.3	0.17	0.70 ± 0.03	n.a.	15.40 ± 2.70	48.82	0.20 ± 0.04	0.14 ± 0.02	0.06 ± 0.01	19.3 ± 10	22.3 ± 4.3
	SSW*	1.5	-	0.88 ± 0.09	n.a.	18.00 ± 11.90	64.44	0.48 ± 0.06	0.29 ± 0.01	0.14 ± 0.01	47.2 ± 10	7.2 ± 2.2
St.02	SML-GP	45.6	-	0.45 ± 0.02 (1.3)	58.72	9.60 ± 2.5 (2.6)	29.41					
	SML-D	35.8	-	0.57 ± 0.16 (1.6)	47.71	12.90 ± 10.1 (3.5)	27.45	1.08 ± 0.05 (5.6)	0.14 ± 0.02 (1.2)	0.14 ± 0.01 (2.3)	105.8 ± 20 (5.7.)	25.0 ± 2.2 (5.2)
	SUR*	0.3	0.15	0.54 ± 0.12	50.46	13.50 ± 2.70	60.45	0.23 ± 0.07	0.12 ± 0.01	0.17 ± 0.07	23.1 ± 10	2.3 ± 2.2
	SSW*	1.5	-	0.35 ± 0.06	59.77	3.70 ± 3.30	25.55	0.19 ± 0.02	0.12 ± 0.01	0.06 ± 0.01	18.6 ± 30	4.8 ± 2.2
St.05	SML-GP	32.2	-	0.97 ± 0.05 (0.9)	45.51	25.80 ± 14.7 (2.8)	69.03					
	SML-D	33.4	-	1.14 ± 0.03 (1.0)	44.93	41.60 ± 2.0 (4.5)	74.85	3.19 ± 0.03 (2.3)	0.42 ± 0.01 (6.0)	0.16 ± 0.01 (1.8)	107.2 ± 30 (1.0)	42.2 ± 6.9 (2.8)
	SUR*	0.3	0.20	0.93 ± 0.12	36.73	23.60 ± 2.70	42.71	0.70 ± 0.14	0.10 ± 0.03	0.05 ± 0.01	27.7 ± 10	L.D.
	SSW*	1.5	-	1.14 ± 0.03	46.23	9.30 ± 1.50	31.90	1.37 ± 0.11	0.07 ± 0.01	0.09 ± 0.01	106.8 ± 40	15.2 ± 5.8
St.08	SML-GP	48.3	-	0.95 ± 0.04 (0.9)	49.74	15.60 ± 13.5 (1.6)	57.71					
	SML-D	39.6	-	1.10 ± 0.08 (1.1)	53.19	10.90 ± 6.6 (1.1)	58.89	0.63 ± 0.02 (3.4)	0.32 ± 0.02 (8.0)	0.13 ± 0.01 (2.8)	43.8 ± 20 (1.6)	45.4 ± 10.7 (5.0)
	SUR*	0.3	0.20	1.10 ± 0.08	55.82	13.50 ± 2.00	70.22	0.29 ± 0.04	0.08 ± 0.02	0.04 ± 0.01	14.7 ± 10	4.8 ± 4.3
	SSW*	1.5	-	1.03 ± 0.15	48.76	9.50 ± 3.20	71.25	0.19 ± 0.02	0.04 ± 0.01	0.05 ± 0.01	26.9 ± 30	9.0 ± 6.9
St.10	SML-GP	55.6	-	0.57 ± 0.02 (1.1)	56.82	25.70 ± 15.8 (1.7)	74.44					
	SML-D	41.4	-	0.66 ± 0.03 (1.3)	42.61	30.20 ± 24.3 (2.0)	61.80	2.56 ± 0.24 (1.0)	0.39 ± 0.04 (3.5)	0.24 ± 0.02 (4.0)	111.5 ± 30 (1.9)	38.1 ± 15.7 (n.a.)
	SUR*	0.3	0.37	0.50 ± 0.03	52.83	17.30 ± 2.00	65.27	0.53 ± 0.18	0.13 ± 0.01	0.04 ± 0.01	59.4 ± 40	L.D.
	SSW*	1.5	-	0.52 ± 0.06	46.94	14.80 ± 2.00	78.86	2.58 ± 0.16	0.11 ± 0.01	0.06 ± 0.01	70.4 ± 10	L.D.

WS= Wind speed 30min. Avergae; Method; SML- GP = Glass plate, D = Drum; * depth in meter ; n.a. = data not available; L.D = less than limit of detection;
[number in blanket] indicated Enrichment Factor between SML and SSW

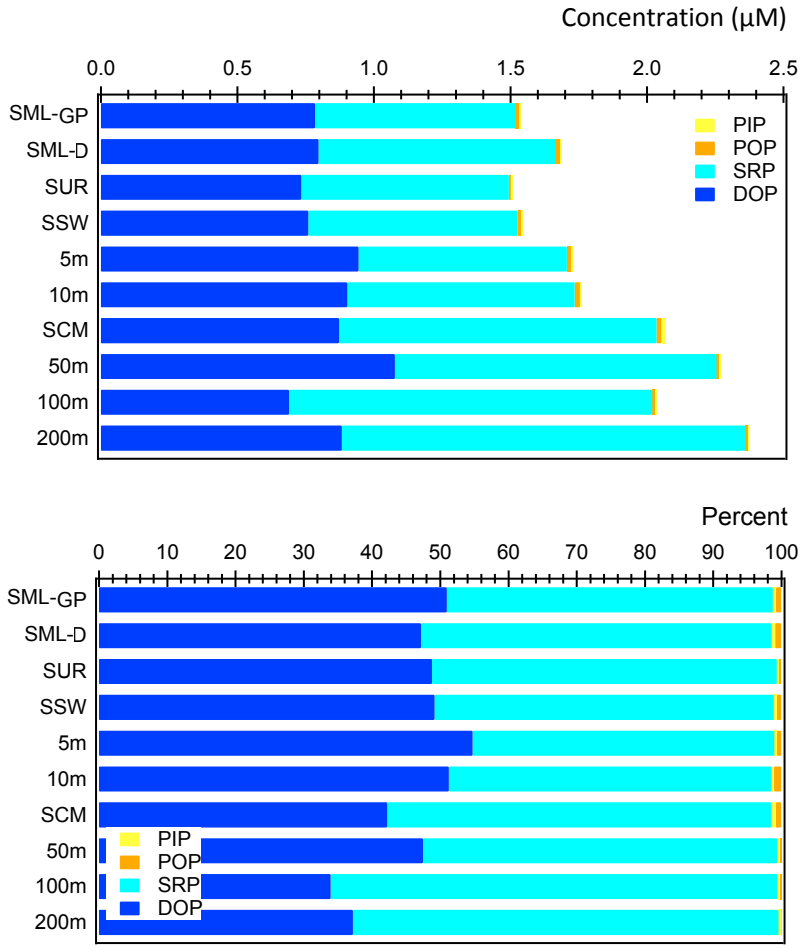

Fig. 4.2.2. Vertical profile of phosphorus composition as SRP (soluble reactive phosphorus), DOP (dissolved organic phosphorus), PIP (particulate inorganic phosphorus) and POP (particulate organic phosphorus), data presented the average concentration of samples from St.02, St.05, St.08 and St.10. Data from St.01 was excluded due to its exceptionally high particulate content

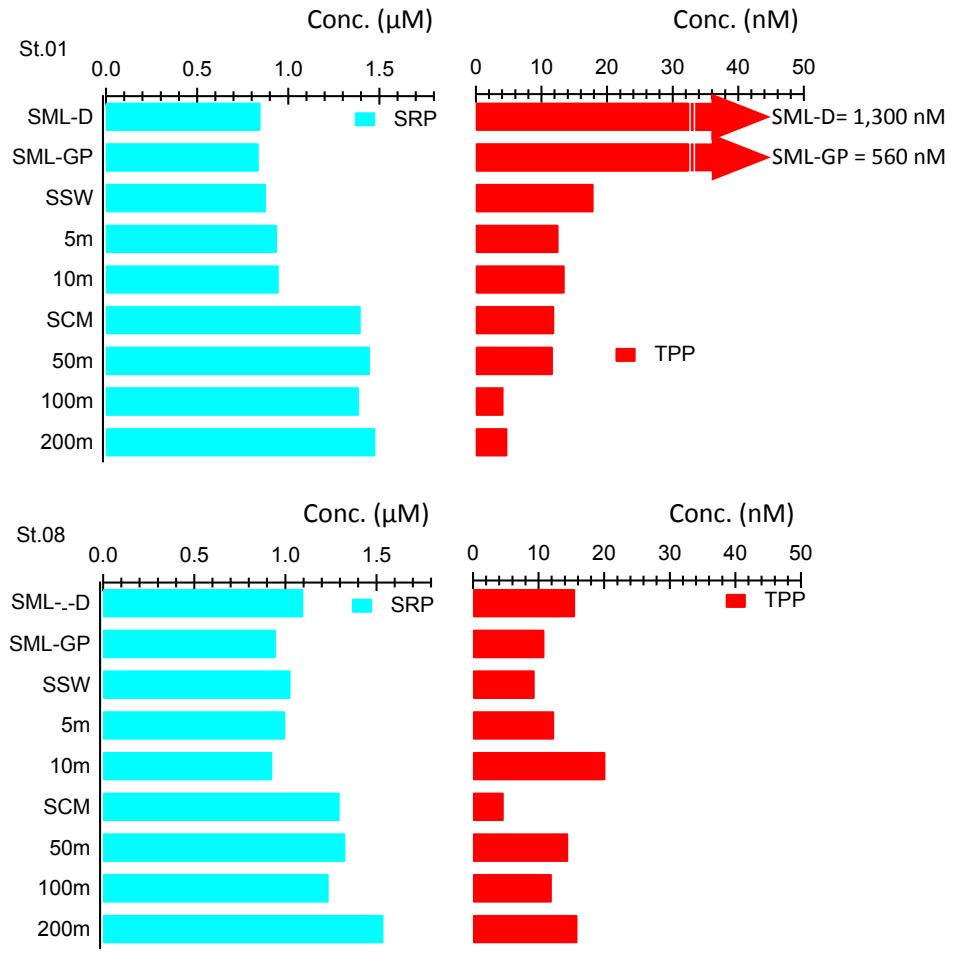

Fig. 4.2.3. Fraction of phosphorus composition; soluble reactive phosphorus (SRP) and total particulate phosphorus (TPP) comparing among the first 200 m of seawater collecting at St.01 and St.08 (as the representative station of the EEP-2012)

4.2.2. Enhancement of particulate phosphorus and iron

Beside particulate phosphorus, particulate elements showed also high enrichments. Apparently, particulate elements that showed the highest concentrations in the SML sample at St.01 were including aluminum (pAl), sulfur (pSi), calcium (pCa) and iron (pFe). (**Fig. 4.2.4** and **Table 4.2.2**)**.** Noteworthy, high enrichment of pFe is very interesting as it is one of the lacking nutrients and a factor limiting the primary productivity in this region [Kaupp et al., 2011]. In general, sufficient pFe addition to the surface water could potentially induce the biological production as well as increase the suspended particulate matter.

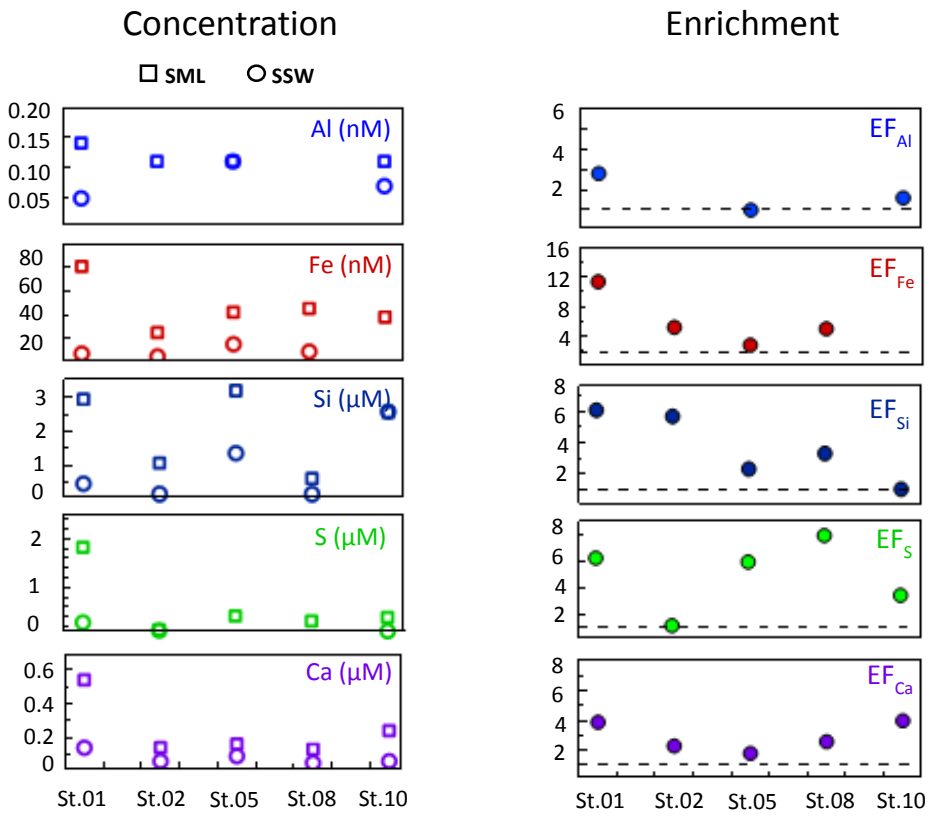

Fig. 4.2.4. Concentration (left panel) of the particulate elements; pCa, pSi and pS in µM and pFe and pAl in nM in SML (open-square) and SSW (open-circle) and corresponding enrichment factor (right panel) for samples measured in EEP-2012

4.3. Comparison of suspended particulate matter in the SML and SSW at St. 01

Suspended particulate matter from SML and SSW samples collected at St.01 was examined intensively to determine for species and morphology and elemental content by a single particle analytical technique using a Field Emission Scanning Electron Microscope with light element energy dispersive spectroscopy (SEM/EDX, S-4800II, Hitachi Co., Japan). An operational accelerating voltage and a beam current were 15kV and 10μA, respectively.

4.3.1. Particle number and volume size distribution

Diameters (D) of particles defined as an area equivalent diameter in the particles a range of 0.4 - 100 μm were size-separated and binned by its differences in the area equivalent diameters, morphology, with the cut-off sizes at diameter of 2, 5, 10, 20, 30, 40, and 50 μm and counted per known area of the SEM images. The average particle number concentration was estimated by dividing the number particles by the total volume of filtered seawater and were 3,240 and 3,110 particles L^{-1} for SML and SSW, respectively (**Fig. 4.3.1.a, Table 4.3.1**).

Although particle numbers were similar, particle size distributions were clearly different (**Fig. 4.3.1.a**). While 79% of SSW particles existed in the smallest size fraction (D = 0.4 - 2 μm), SML particles were found in larger size, particularly in size fractions of 20 - 30, 5 - 10, and 2 - 5 μm, and accounted for 30%, 24% and 19% of the total number of particles. The overall volume concentration was 9,130 ppbv (or x 10^3 μm^3 mL^{-1}) for SML particles or 4-fold larger than that of particle volume of SSW particles (1,840 ppbv), due to the abundance of the larger particles in the SML (D > 20 μm, **Fig. 4.3.1.b**).

By the differences in morphology and sizes, particles were categorized into 38 types and then grouped into 5 simplified particle groups namely diatom (16 types), dinoflagellate (2 types), silicoflagellate (1 type), other microorganism (10 types) and other particle (9 types, including the inorganic particles). Micrographs of particle in different classes were showed in **Fig. 4.3.2**.

In SSW sample, the most abundant particles (D < 2 µm) were mixtures of other-particles and other-microorganisms particle, where in SML sample were composed with diatom particles and other-microorganism particles (**Fig. 4.3.1.a**, **Fig. 4.3.1.c**). The diatom particles significantly dominated in the 2-10 and 20-40 µm size-fraction of SML. Total number of diatom particles (in all size - fraction) in SML were higher than SSW. The number of diatom particles were 1,900 and 290 particles mL^{-1} in SML and SSW, respectively. The other-microorganism particles also presented in higher number in the SML, especially in the particle fractions of 6-10 and 30-40 µm. Noted that diatom and microorganism particle with regular shape and complete form not fragment were counted on known area of SEM micrographs. In addition, there was an unidentified microorganism particles presented in larger number in the 30-40 size fraction of SML and were observed profoundly under the microscopic views during the SEM observation (**Fig. 4.3.1.b, Fig. 4.3.2.e**).

Table 4.3.1. Number concentration of particle in SML and SSW (particle L^{-1}) classified by its species. Particle number was presented by particle class for diatom, dinoflagellate, silicoflagellate, other organisms and other particles in 8 sized fractions

Particle	No.Type	Avg. No. Particle		SML particles (number mL^{-1})					SSW-particles (number mL^{-1})				
		SML	SSW	Diatom	Dino-Flag	Silico-Flag	Other-Org	Other-par	Diatom	Dino-Flag	Silico-Flag	Other-Org	Other-par
0.4-2 µm	4	144	2466	2	0	0	110	32	6	0	0	1324	1136
2-5 µm	5	603	44	558	0	0	45	0	44	0	0	0	0
5-10 µm	4	780	201	571	0	0	97	112	32	0	0	19	150
10-20 µm	8	246	42	85	0	0	0	161	15	0	0	0	27
20-30 µm	5	1015	188	357	1	1	1	655	41	1	1	1	144
30-40 µm	4	283	69	260	0	0	20	3	67	1	0	0	1
40-50 µm	4	63	58	59	0	0	2	2	56	0	0	0	2
>50 µm	4	105	42	49	0	0	1	55	30	0	0	0	12
total	38	3,239	3,110	1,941	1	1	276	1,020	291	2	1	1,344	1,472

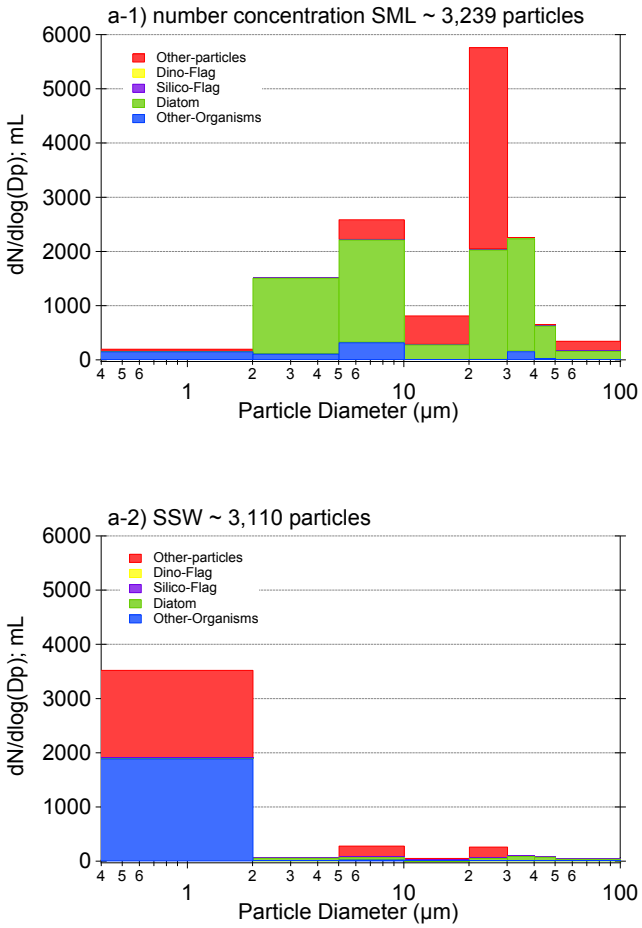

Fig. 4.3.1.a. Particle number distribution by size and particle classes from SML and SSW at St. 01 in EEP-2012. Particle classification was based on the single-particle size and the elemental characterization by SEM/EDX. Particle size is defined as an area equivalent diameter and volume distributions were estimated using observed particle-number size distributions.

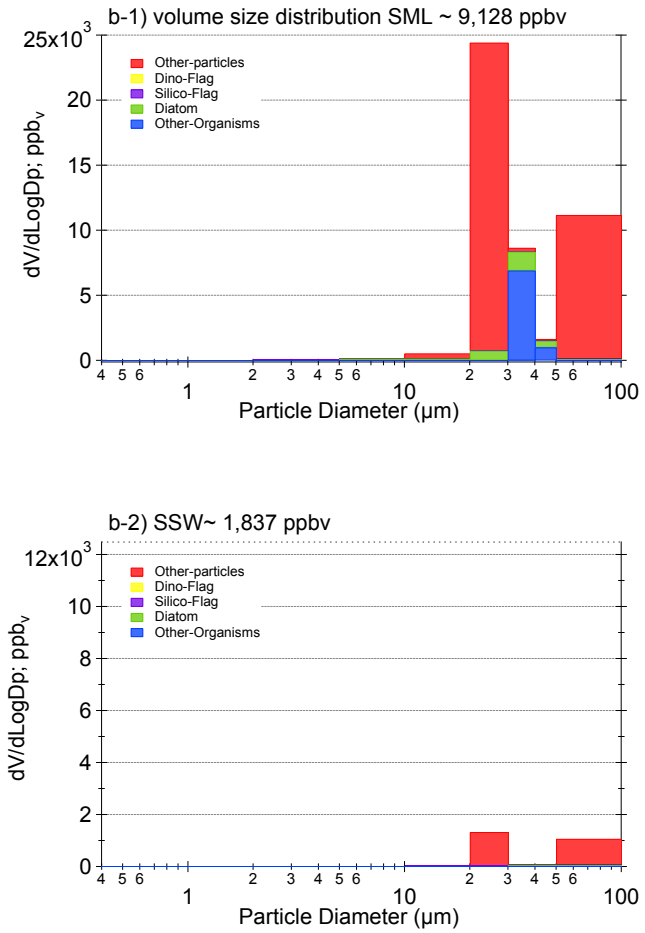

Fig. 4.3.1.b. Particle distributions by volume from SML and SSW at St. 01 in EEP-2012. Particle classification was based on the single-particle size and the elemental characterization by SEM/EDX. Particle size was defined as an area equivalent diameter and volume distributions were estimated using observed particle-number size distributions.

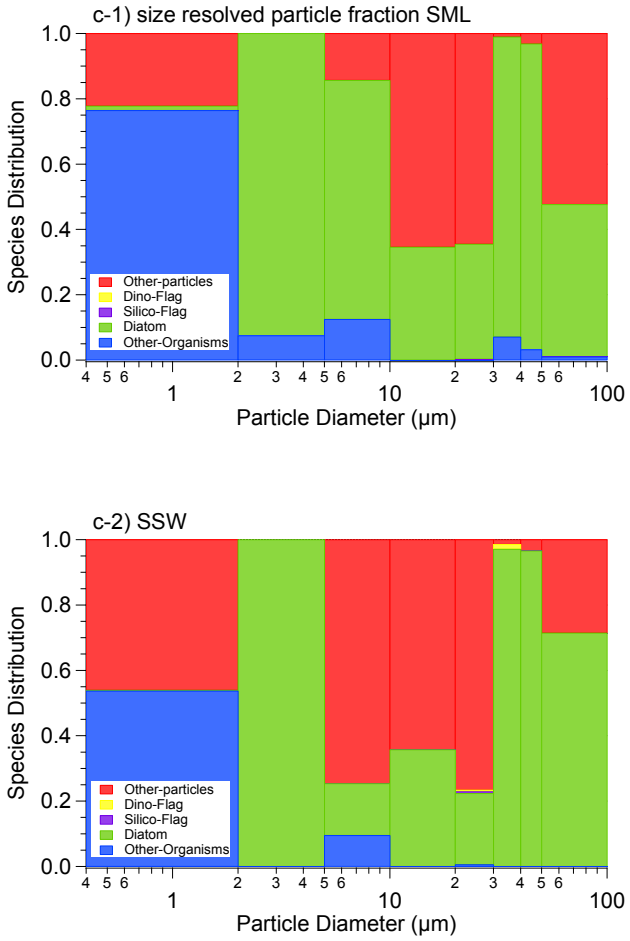

Fig. 4.3.1.c. The size-resolved relative particle classes from SML and SSW at St. 01 in EEP-2012. Particle classification was based on the single-particle size and the elemental characterization by SEM/EDX. Particle size is defined as an area equivalent diameter and volume distributions were estimated using observed particle-number size distributions.

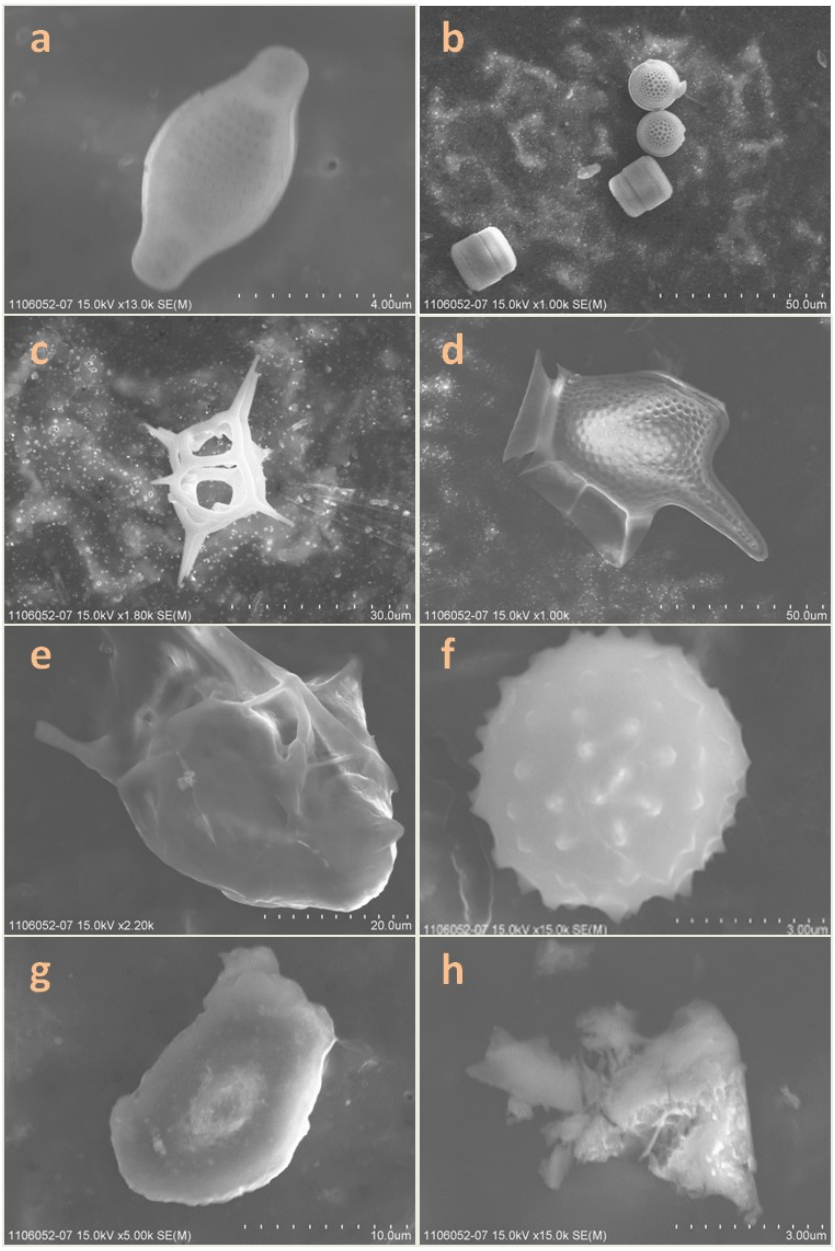

Fig.4.3.2. Micrographs showed the particles classified as (a-b) diatom, (c) silicoflagellate, (d) dinoflagellate, and (e-f) other microorganisms, (g) other particles, organic-like and (h) other particles, inorganic-like (Fe-containing particles).

4.3.2. Particulate elemental composition

The elemental composition for single particle was analyzed by a SEM/EDX with acquisition time of 60 sec per particle. From previous work, it has suggested that high organic contents often caused weak and poor elemental signals study [Bigg et al., 2004; Xhoffer et al., 1992]. The detectable elements with producing elemental signals greater than 3-fold a signal-to-noise ratio (S/N) > 3 was concluded in the calculation for the relative elemental composition analysis. The intensities of the X-ray, however, is depending on the surface shape, the respective element concentration, and the shooting point. Therefore 3-5 shooting was conducted for each single particle.

The sum of the analyzed elements (O, Na, Mg, Al, Si, P, S, Cl, K, Ca, Fe, Cu, Zn and Ti) was rescaled to obtain a constant sum of 100% [Schleicher et al., 2012]. In total, there were 66 and 45 SML and SSW particles in this analysis.

Seventy seven % of the total number of SML particles was P-detected particles, while only 11% of the SSW particles were P-contained (**Table 4.3.2**). The average %P content in the SML particles, expressed as a relative weight percentage of the sum of the analyzed elements, was also much higher (4.1%) than in the SSW particles (1.8%) for the individual particle species and for the overall average of the same particle types.

Previous study also reported similar findings with a frequent detection of the bio-related elements like phosphorus and sulfur in organic suspended particulate matter. When compared with those of other trace elements, this was suggested to cause by the adsorption or aggregation of organic particles [Iwamoto, 2008].

Table 4.3.2. Average relative percentages of elemental composition of the classified particle types by SEM/EDX single-particle analysis for particles in the SML and SSW (St. 01, EEP-2012). The sum of the raw EDX signal intensities of all elements in the table was treated as 100% for each analyzed particle (n=3-5) and averaged with the total numbers of analyzed particles in the same group. If the elemental signal did not exceed S/N = 3, the element was treated as "not detected".

Particle Group	No. Particles		Relative percentages of elemental composition												
	Total	P_{detect}	Na	Mg	Al	Si	P	S	Cl	K	Ca	Fe	Cu	Zn	Ti
SSW particles	45	5					[1.8]								
Diatoms	18	3	20.2	4.9	-	46.8	0.1	3.7	21.9	-	0.4	-	-	-	-
Other Microorganisms	8	2	29.5	11.3	-	6.9	4.2	6.5	42.7	0.2	1.1	-	1.2	-	-
Other Particles	19	0													
Organic-like	10	0	40.0	3.3	-	-	-	1.0	45.3	0.4	0.1	-	-	-	-
Inorganic-like	9	0	25.3	3.2	9.7	43.3	-	0.6	11.3	4.2	1.6	0.7	-	-	-
Type I-Fe-particle (0.4-2µm)	(10)		25.9	1.4	5.7	53.7	-	-	3.9	6.0	2.2	1.2	-	-	-
SML particles	66	51					[4.1]								
Diatoms	15	10	11.2	1.4	-	70.2	2.8	1.4	10.3	-	0.1	-	-	-	-
Other Microorganisms	24	20	24.2	3.9	0.1	16.7	5.8	10.4	36.6	0.2	1.7	-	1.5	-	-
Other Particles	27	21													
Organic-like	6	5	25.3	4.6	-	-	3.9	7.9	41.6	-	-	-	-	-	-
Inorganic-like	21	16	12.7	2.8	0.3	9.8	3.6	2.5	20.7	-	0.3	17.5	0.1	-	0.4
Type I-Fe-particle (0.4-2µm)	(2)		10.0	3.5	0.7	4.0	5.4	0.5	22.5	-	0.7	18.0	-	-	1.3
Type II-Fe-particle(6-10µm)	(5)		1.8	0.1	0.1	0.4	0.2	0.4	7.9	-	-	34.5	0.4	-	-

note: number in [brackets] represents the %Pavg

4.3.3. Comparative calculation of particulate phosphorus enrichment factor by single particle analysis

This section was aimed to compare the results of the single-particle analysis with bulk chemical analysis. Single particle SEM/EDX data were used to estimate an amount of phosphorus contained in the particles by the following conversion:

$TPP_{SEM/EDX}$ = total particle mass concentration x $\%P_{avg}$ / 100 x $fraction_{p\text{-}detected}$

Where $\%P_{avg}$ is the average %P in a particle samples (**Table 4.3.2**, number in brackets)

$fraction_{P\text{-}detected}$ is the fraction of P-detected particle (SML=0.77; SSW = 0.1)

By applying volume-mass particle density conversion for total suspended particulate matter (2.2 mg mL^{-1}; Pak, 1973) to volume concentration mentioned in previous section, the total SML and SSW mass concentrations were calculated as 24 and 6 µg L^{-1}, and the $TPP_{SEM/EDX}$ values were estimated for 0.75 and 0.01 µg L^{-1}, respectively.

With the calculation mentioned, the resultant of EF_{TPP} in EDX/XRF analysis for St. 01 was 75. This number was well agreed and presented at the same magnitude with the observed EF_{TPP} by colorimetric measurement (EF_{SML-D} = 72 and EF_{SML-GP}= 33), confirming that the observed large enrichment of particulate phosphorus in the SML was not an artifact but a natural occurrence. It should be noted again that such a large enrichment of TPP was not observed in the SML samples collected at the other four stations in EEP-2012 cruise.

The average %P in SML particles was presented with similar percentages even among the different particle groups and can be explained by the surface adsorption of phosphorus-particles [Iwamoto, 2008; Liss and Duce, 1997]. Typically, particulate phosphorus composed of living and dead plankton, precipitates of phosphorus mineral, phosphorus-adsorbed particulates and amorphous phosphorus phase [Yoshimura et al., 2007]. The particulate phosphorus can undergo continuously transformation and turn into dissolved inorganic and organic phosphorus through plankton and microorganism assimilation and excretion [Paytan and McLaughlin, 2007].

Through this observation, the increase of particulate phosphorus can be identified as the results of the increase of phosphorus adsorbed- particles such as the surface adsorptive area of diatom and other-microorganisms. Even though, the accumulation of plankton in the SML has been suggested to cause via the advection [Joux et al., 2006], however, the findings of high pFe in the SML has suggested also the possible occurrence of pFe induced the biogeochemical activities, biological production and degradation in the SML.

4.4. Potential cause of particle enrichment in the SML at St. 01

In Eastern Equatorial Pacific region, there are two main iron sources supplied to the surface water, i.e., upwelled of subsurface equatorial undercurrent water with colloidal Fe and aeolian particulate iron deposition [Mackey et al, 2002]. The upwelled water annually supplied the most iron by approximately 2 orders of magnitude higher than that of aeolian sources [Kaupp et al., 2011].

From the vertical profile, the highest concentration of particulate phosphorus and particulate iron were shown in the SML together with pSi, pCa, and pAl (**Fig. 4.4.1 and Fig. 4.4.2**). This occurrence observed only in the SML interior but not the bulk seawater suggested that this enhancement of particulate phosphorus and particulate elements were occurred via the atmospheric pathway. The 7-day backwards trajectory of the air mass history prior the sampling period (**Fig. 4.4.3**) showed that at St.01, air parcel was transported from the South Pacific. Therefore, there was no special dust event occurring. Concerning the thickness of SML, the long range transportation and natural deposition of atmospheric particle was considered as the possible source. Atmospheric deposited particles containing lacking nutrients such as iron could trigger the biological responses with in the SML interior.

.

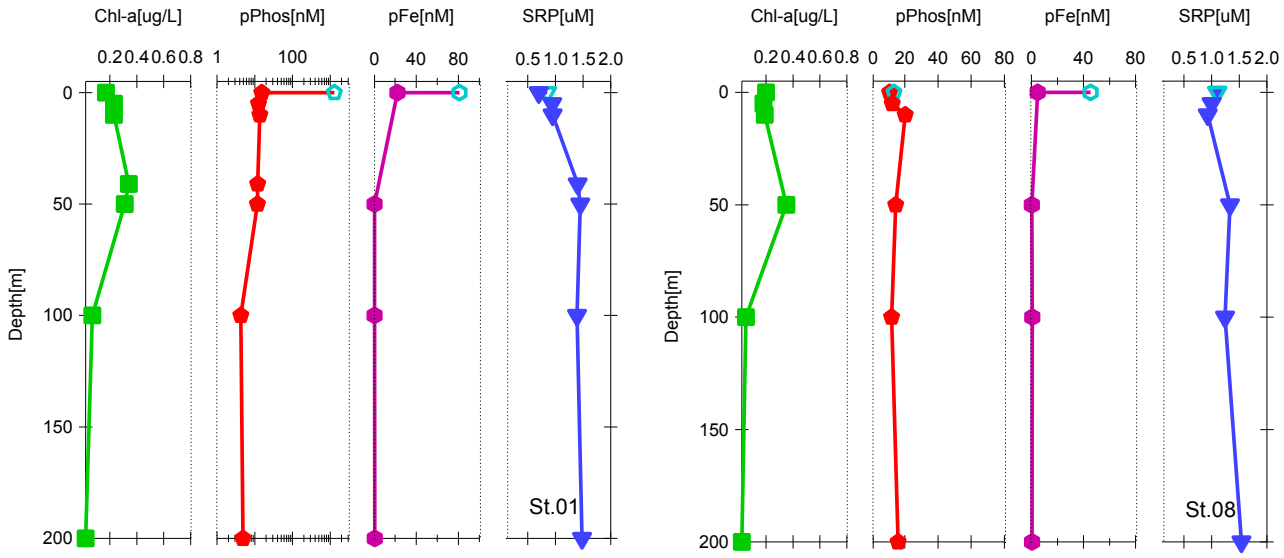

Fig. 4.4.1. Vertical profiles of chlorophyll-a (Chl-a), total articulate phosphorus (TPP), particulate Fe (pFe), and soluble reactive phosphorus (SRP) observed at St. 01 (0˚N, 95.5˚W) and the St. 08 (0˚N, 130˚W). The open markers (light blue) represent the measurements in the SML. A large enrichment of TPP and pFe were observed at St. 01, and the profiles suggested that there might be atmospheric deposition to the surface ocean during the collection

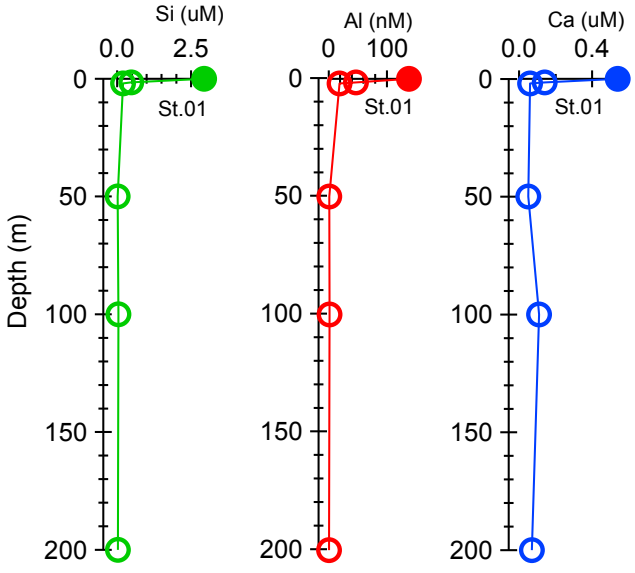

Fig. 4.4.2. Vertical profiles of particulate element; pSi, pAl and pCa at St. 01 (0˚N, 95.5˚W). Particulate element pAl, pSi and pCa exhibited the highest concentration in the SML. The open markers represent measurements in bulk seawater and close marker was the SML

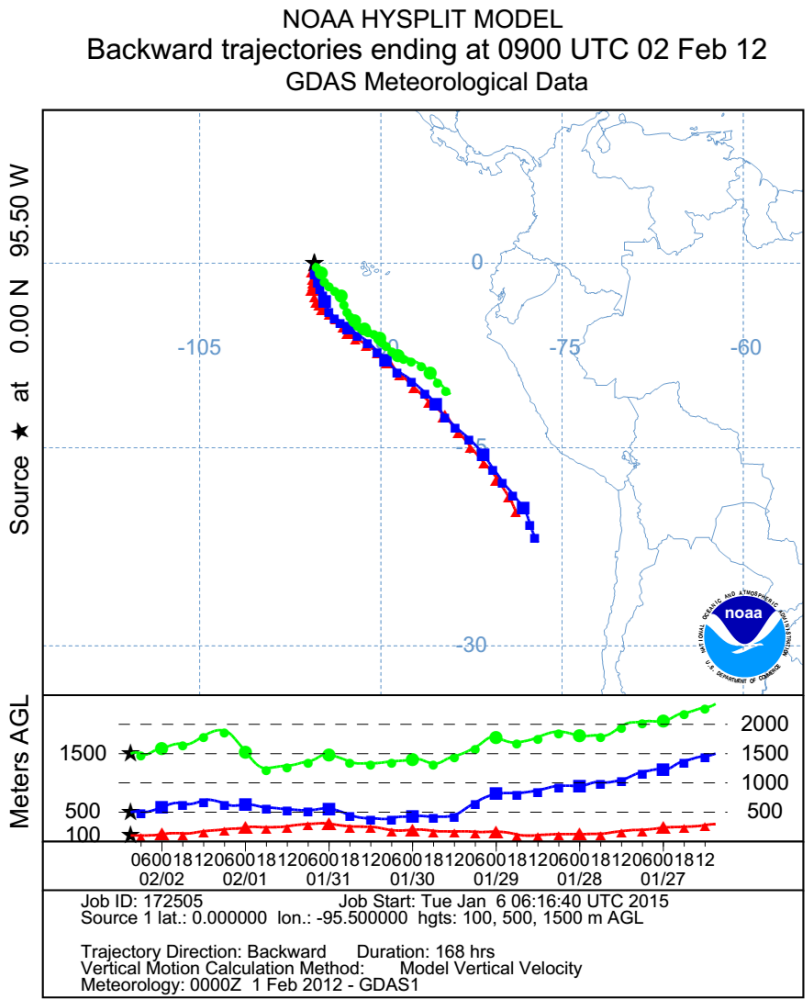

4.4.3. Seven day-backward trajectory at St. 01 in EEP-2012 cruise on the same sampling day; February 2, 2012. [Draxler and Rolph, 2014; *HYSPLIT (HYbrid Single-Particle Lagrangian Integrated Trajectory) Model access via NOAA ARL READY Website (http://www.arl.noaa.gov/HYSPLIT.php)]*

4.5. Biogeochemical implication for the SML

The atmosphere is well acknowledged as the significant pathway to transport continent materials to ocean, including particulate iron [Duce et al., 1991], however, the residence time of particulate iron (pFe) in an oceanic mixed layer was reported to less than 10 days [Croot et al., 2004; Jickells, 1999]. Even more, the resident time of pFe in the SML was reported to less than 2 seconds [Liss and Duce, 1997]. If this the case, it was not possible to observe any biological activities

occurred internally in the SML. However, the recent study about diffusion-limited retention of porous particles showed an evident that at the interface (pycnocline) layer, porosity was controlled the retention time (3 mins-3.3 day) and enhanced the accumulation of particles at the interface [Kindler et al., 2010]. If this applied also to the density interface layer of the SML, it cloud lengthen the retention time of particles in the SML, allowing the biological activities such as carbon and phosphorus transformation and remineralization to occur in the SML.

Boyd et al. (2010) suggested that solubility of pFe can be neglected, in the SML. Instead, passive dissolution and biogenic transformation are at most active process. The biogeochemical responding to atmospheric deposition in the SML was suggested to occur in which the particulate iron was undergone size partitioning and transforming to biogenic particulate iron by ranges of Fe-intake mechanisms such as iron solubilization by bacterial siderophores [Yoshida et al., 2002; Brantley et al., 2004], meso-zooplankton grazing and ingestion of colloidal Fe [Stukel et al., 2011] and particle aggregation [Frew et al., 2006; Twining et al., 2004]. Consequently, SML was endorsed and enhanced with microbial activities and its products hence enrichment of particulate matter.

Because this observation was conducted in the HNLC region where iron fertilization has successfully increased biological responses. The meso-scale iron fertilization has increase of primary production by doubling biomass production and drawing down the nitrogen in surface water [Martin et al., 1994; Coale et al., 1996]. The recorded species that response to iron fertilization were pennate diatom [Martin et al., 1999; Pennington, et al., 2006]. The biological responses to the iron fertilization was also confirmed by an on-board EEP-2012 experiment. At St.01 in bottle study, there was 12 folds increased in chlorophyll-a concentration after 4 day Fe-incubation [Takeda, 2012; personal communication].

Therefore such aeolian deposition; the passible cause of this circumstance, may supply lacking micronutrients in this context (pFe in the SML). The aeolian Fe deposition likely stimulated

additional biological productivity within the SML and resulted in the formation of more biomass in the SML under HNLC condition. Microscopic observations also clearly demonstrated the differences in particle composition in the SML sample at St.01 compared with SSW and the representative station of EEP-2012 sample; St.08 (**Fig. 4.4.3**). However, due to the thinness of SML (a small reservoir of materials), such biogeochemical responses seem to be not only anomalous but also rapid, indicating its variable nature in time and space.

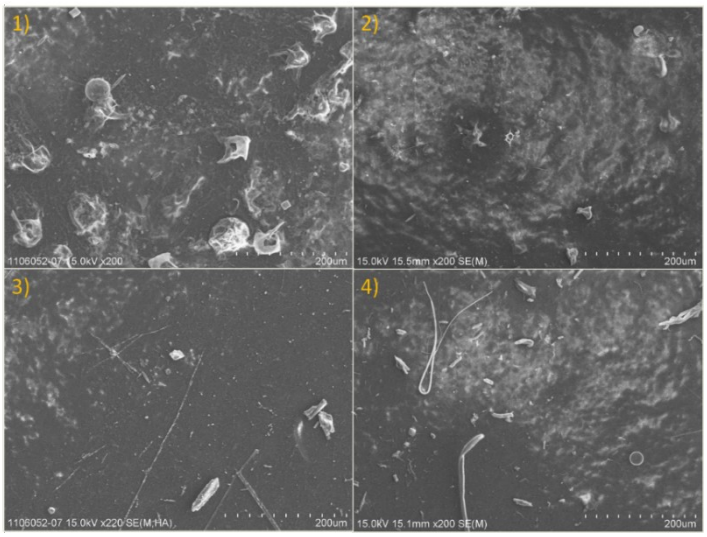

Fig. 4.4.3. Micrographs showed the SML (1-2) and SSW (3-4) particles at St. 01 (left panels) and St. 08 (right panels), demonstrating the different particle type in the SML. At St. 01, the other organism particles was dominated in the SML sample.

Summary

The remarkable increase of total particulate phosphorus (TPP) concentration (0.59-1.29 µM) to the same level of soluble reactive phosphorus (SRP = 0.84 µM) in the SML, and the highest enrichment factor of TPP (EF_{TPP}=72) was observed at the Eastern Equatorial Pacific Ocean (St. 01, 0.0°N, 95.5°W; EEP-2012). This finding was concurred with the higher number of biogenic particles, especially diatoms, in which the number of diatom particles was 1,900 particles mL^{-1} in SML or 7

times greater than that in the SSW. Further investigation of the individual particles by a scanning electron microscopy with energy dispersive X-ray spectroscopy (SEM/EDX) demonstrated that most analyzed particles in the SML (77% of total number) contained higher phosphorus content ($\%P_{avg}$=4.1). While only diatom and other-microorganisms particle types of the SSW particles contained phosphorus ($\%P_{avg}$=1.8) and were occupied for 11% of total analyzed particles. Therefore, there was an increase of particle surface active area for the adsorption of phosphorus as a result of the increase in number of larger particles including bio-particles (diatom and other microorganism) in the SML.

The concentration of particulate Fe was also highest in the SML (81 nM; EF_{pFe} = 11). The vertical profiles of TPP and pFe showed also the peaks in the SML along with other particulate element namely pSi, pAl and pCa, indicating the enhancement was occurred in the SML interior. The most probable explanation of this occurrence was that it was the resultant of the external atmospheric deposition of scarce micronutrients to the SML.

Although SML is quite a small material reservoir, its biogeochemical dynamics and properties are unique. The observed *biogeochemical enrichment* emphasizes its rapid response to external perturbation and its significant role in microbe-mediated materials synthesis and transformation of chemical compositions and their cycling, further indicating that a slight amount of additional iron input enabled the dramatic increase in SML biological production. This is possibly occasional but a unique finding of the *biogeochemical enrichment* in the SML addresses its significance in biogeochemical and physicochemical processes in which SML is involved. Further investigation on the behaviors and mechanisms of materials transformation and its retention time in SML will be valuable.

5. Bubble bursting experiment on the SML seawater

5.1. Introduction

Ocean is one of the significant sources for atmospheric aerosols. The major constituent of ocean-derived particles; sea spray aerosols is produced primarily by mechanical interaction of wind stress at the sea surface [O'Down and de Leeuw, 2007] and forms inorganic sea salt particles with some coagulation of various organic components that are available at the surface water.

Sea spray producing via the bubble bursting process are film and jet drops [Blanchard, 1989, **Fig. 5.1.1**] and are distributed from sub micrometer to a few micrometer [O'Down and de Luuew, 2007]. At wind speed greater than the whitecap formation (onset wind speed is 4 m s^{-1}), directs tearing of wave crests and results to the formation of bigger particles.

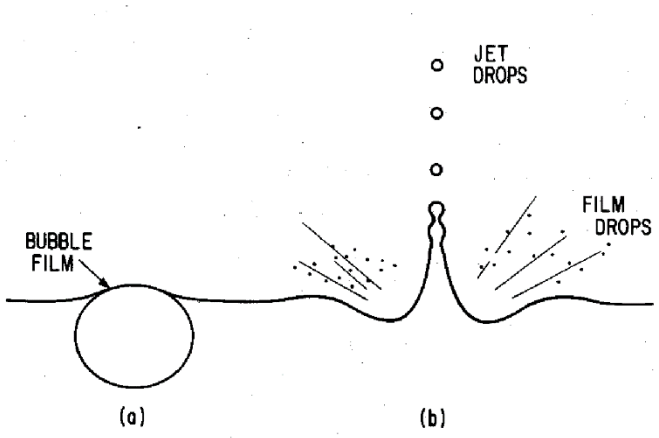

Fig. 5.1.1. The diagram for the ejection of drop from the sea to the air (a) the bubble rests at the surface and (b) the production of jet and film drops from a bursting air bubble [Blanchard, 1989].

Primarily, marine aerosols consist of sea salts and organic materials, bacteria and virus. The annual production flux of sea spray is estimated at 10 g m^{-2} yr^{-1} and corresponding to the total global production rate of 3.5×10^{12} kg yr^{-1} [de Leeuw et al., 2011]. This amount has suggested to

account for as much as 90% of cloud condensation nuclei (CCN) in non-perturbation marine regions [Russell et al., 2010].

Aerosols is known to affect the radiative balance in the atmosphere, directly by light adsorbing or scattering solar radiation or indirectly by modify the cloud properties as the CCN [IPCC, 2007]. Sea salts are good at light scattering and highly hygroscopic. It is served effectively as the cloud seeding. The organic fraction in marine aerosols is found to suppress the hygroscopic growth and is reduced CCN activity [Fuentes et al, 2011]. Unlike the stable sea salts, organic materials tend to adverse chemical structural changes under the exposure of tultraviolet light and atmospheric acidification process [Bigg and Leck, 2008].

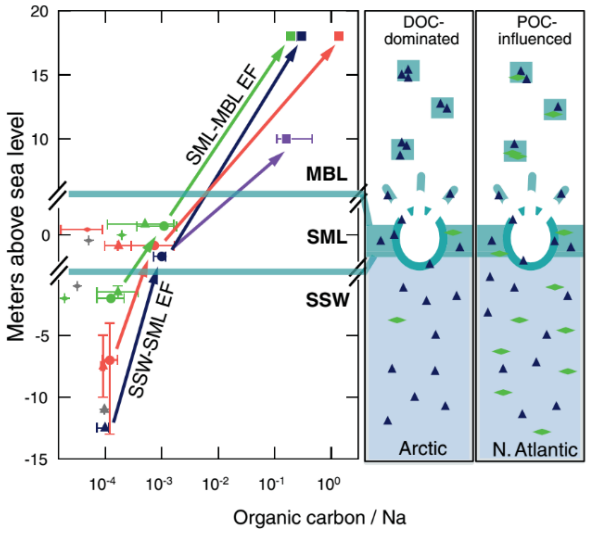

Fig. 5.1.2. Organic carbon to sudium ratio of sea-surface microlayer (SML), subsurface water (SSW) and marine boundary layer (MBL). The arrows indicated the estimated MBL-SML-SSW enrichment factors (EF) based on the measurements for TOC/Na. The right panel illustrated the differences of organic phase contribution to the particle formation via bubble bursting in the Arctic and North Atlantic regions. [Russell et al., 2010]

Since SML positioning at the interface, it poses the vital influences not only on the aerosol chemical composition but also the effectiveness of bubble bursting process. The stability of surface film is suggested to weaken the bubble structure and hasten the bursting. Hence, the ejected film droplets may contain only the surface active materials without seawater [Bigg and Leck, 2008]. The ratios of marine organic mass to sodium has also observed in the submicron particle at the factor of 10^2 to 10^3 [Russell et al., 2010, **Fig. 5.1.2**].

This chapter aimed to better understanding the mechanism of bubble bursting process , its sea to air fractionation for phosphorus, and the influences of chemical and organic substances in SML towards the atmospheric phosphorus formation especially organic phosphorus.

5.2. Material and method for on board bubble bursting experiment

5.2.1. Bubble bursting system and condition

There were 3 types of seawater utilizing as bubbling solution in the experiment namely sea-surface microlayer (SML), subsurface seawater (SSW) and surface seawater (SUR). These seawater samples were obtained during EEP-2012 cruise. SML water was collected using drum sampler, SSW was collected during SML sampling by sinking the bottle with weight at depth of 1.5 m. SUR was collected on board by bucket sampling. Prior the experiment, samples were kept in dark and cool room (20°C).

A simplified bubble experiment system was fabricated in a 10-L polycarbonate carboy Nalgene™ with a closure modification to connect with aeration system including 1) sweep air - at flow rate of 15 L min^{-1}, 2) bubbling air - at flow rate of 400 mL min^{-1}, and 3) a filter holder set to collect fresh aerosols. Bubble was generated by passing clean air to the 12 mm diameter fritted (40-60 μM pore size) cylinder borosilicate tube. Dispersed air pass through the glass fritted at depth of

20 cm created the bubble cloud and later bursted at surface (see the diagram of the bubble bursting in **Fig. 5.2.1**).

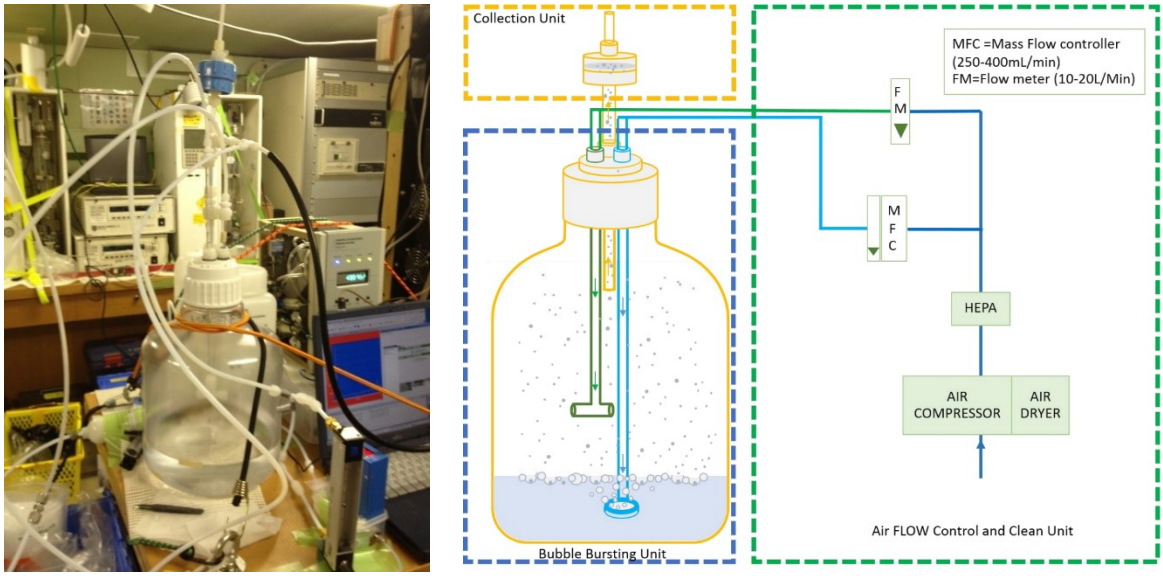

Fig. 5.2.1. Diagram and photo of the bubble bursting experimental unit on the EEP-2012.

Condition of the experiment was listed in **Table 5.2.1**. This selected condition had been modified from the study of Keene et al. (2007) and was tested in laboratory prior shipboard experiment. At any experiments, glass fritted was flush with MQ-water several times and dried prior the next experiment and carboy container was pre-cleaned and rinsed twice with the sample water. The fresh aerosols was collected on to pre-combusted quartz filters (47mm diameter) and

kept frozen (-20°C) for phosphorus analysis. For water soluble ionic species, aerosol filters were extracted with 20 mL of MQ-water and analyzed by ion chromatography (IC; Dionex-320, Thermo Scientific Dionex).

Table 5.2.1. Operating conditions of the bubble bursting experiment

Bubble Bursting experiment	
Sample Water Volume	3.5 L
Head space depth	20 cm
Bubbling rate	400 mL min^{-1}
Sweep air rate	15 L min^{-1}
Total air volume	0.135 m^{-3}
Total bubbling time	90 min
Hight of aerosol collection	1 m

5.2.2. Definition of enrichment and standardized chemical fractionation notation

The standardized chemical fractionation nomenclatures for sea to air chemical interaction describing as the followings, [Duce and Hoffman, 1976]

$$\text{Fractionation: } F_{Na}(X) = \frac{(X/Na)_{aerosol}}{(X/Na)_{seawater}} \qquad 5.1)$$

Where $(X/Na)_{aerosol}$ and $(X/Na)_{seawater}$ are the mass ratio of substance X to sodium in the bubble generated-aerosols and in the seawater samples (SML, SSW and SUR). The $F_{Na}(X)$ equals to 1, indicating neither positive nor negative enrichment.

5.3. Sea to air fractionation of atmospheric particles generated by bubble bursting

5.3.1. Sea to air fractionation of phosphorus

Sea to air fractionation (F_{Na}) displayed in term of total phosphorus (Total.P), inorganic phosphorus (Inorg.P) and organic phosphorus (Org.P) in **Table 5.3.1**. By all forms, F_{Na} value was greater than 1 indicating the positive enrichment of phosphorus in generated aerosols and were valued at the factor of 10^2-10^3. Inorganic phosphorus was fractionated more effectively than the organic phosphorus by 0.5 – 7 times. This F_{Na} as high as a factor of 10^3 has been reported in Duce

and Hoffman (1976) study and has suggested to occur in associated with the film droplets production. The high fractionation of inorganic phosphorus can be explained by its high potential as the counter ions (small size with large charge) of the opposite surface active component charge of the SML [MacIntyre, 1970].

Aerosols generated from the bubble bursting experiment using SML, SSW and SUR seawater as bubbling solution contained varyingly sodium and organic phosphorus concentration. The average concentration of sodium in aerosols from SML, SSW and SUR experiments were 2.90, 2.79 and 5.09 µmol Na m^{-3} while the average concentration of total phosphorus in ejected aerosols remained quite consistent at 7.05, 7.82 and 6.69 nmol P m^{-3}, respectively. Even though, seawater concentration ratio between organic phosphorus to sodium and organic to inorganic phosphorus were similar among different kinds, the bubbles generated aerosols from SML experiment contained higher organic phosphorus concentration (**Table 5.3.2)**. When comparing the ejected aerosols that contained similar sodium mass, it was clear that aerosols from SML experiment contained higher organic phosphorus than the SSW and SUR generated aerosols (**Fig. 5.3.1**). Degree fractionation of organic phosphorus was conversely related to its concentration in seawater samples, the increase of organic phosphorus to sodium ratio in seawater tended to have lowered fractionation factor. This was found particularly in SML experiment (**Fig. 5.3.2**).

Ratio of phosphorus to sodium in the depth of view (from atmosphere to the interface; SML and in seawater; SSW and SUR) expressed clearly the enrichment of phosphorus in the bubble generated aerosols (**Fig. 5.3.3**). When comparing this ratio with organic carbon to sodium (**Fig. 5.1.2**; Russell et al., 2010), there was 2 orders of magnitudes lower (OC/Na = 10^{-1} - 10^{0}, OP/Na = 10^{-3} - 10^{-2}). The fractionation of organic phosphorus reported here was displayed at the similar factor with the organic carbon fractionation study (F_{Na} Org.P = 100 – 900 in this study, F_{Na} Org.C = 100 -300, Keene et al., 2007; Russell et al., 2010). However, previous study reports low

enrichment of organic carbon in the SML (EF~ 1-1.1, van Pinxteren et al., 2012; EF~1-3, Liss and Duce, 1997) and determined that the contribution of organic carbon in SML is probably accounted to a minor fractions of the injected carbon [Fuentes et al, 2011].

In this study, the uses of SML and SUR bubble solution had drawn to the different conclusion, despite the fact that enrichment factor of organic phosphorus was valued at a similar factor with organic carbon ($EF_{Org.P}$= 1 – 1.3). F_{Na} Org.P from SML and SSW experiment showed vary different fractionation factor for organic phosphorus. The SUR experiment represented the natural seawater condition (a mixture of SML and SSW seawater); on the other hand, had demonstrated closer fractionation factor of organic phosphorus to the SML experiment. In addition, F_{Na} Org.P in the SSW experiment was less than one - third of the fractionation values presented in the SML (**Table 5.3.1**).

The single particle mass spectra of bubble generated aerosols from SML and SSW seawater (St. 08, EEP-2012) also identified that beside sea salts particles containing organic content, the organic particles were generated in greater number in the SML experiment in comparative to the SSW experiment [Furutani, 2012; personal communication]. Those particles were found to distributed greatly in the small size-fraction (<1 µm) whereby in the SSW this fraction has been taken place by the formation of carbon particles embedded with K. It was clearly indicated that organic contents in SML had influenced towards the fractionation of organic particles especially in the submicron particles.

Table 5.3.1. Concentrations of phosphorus (Inorg.P and Org.P) and sodium in experiment seawater and aerosols collected from bubble bursting experiment (BBX). Phosphorus concentration in seawater demonstrated in total dissolved phosphorus (TDP), soluble dissolved phosphorus (SRP) total particulate phosphorus (TPP) and particulate inorganic phosphorus (PIP). The inorganic phosphorus (Inorg.P) in seawater obtained from the sum of SRP and PIP, and organic phosphorus (Org.P) obtained from the sum of TDP and TPP minus the Inorg.P. The aerosols concentration and sea to air fractionation (F_{Na}) of phosphorus displayed by forms in the Total.P, Inorg.P and Org.P. SML, SSW, SUR referred to the uses of such seawater in the experiment.

	Water samples							Filtered Aerosol samples				Fractionation (F_{Na})		
	Sodium	Inorg.P	Org.P	TDP(μm)	SRP(μm)	TPP(nM)	PIP(nM)	Sodium	Total.P	Inorg.P	Org.P	Phosphorus		
	(M)	(μM)	(μM)	(μM)	(μM)	(nM)	(nM)	(μmol m^{-3})	(nmol m^{-3})	(nmol m^{-3})	(nmol m^{-3})	Total.P	Inorg.P	Org.P
BBX-SML														
St.05	0.72	1.15	0.96	2.07 ± 0.1	1.14 ± 0.0	41.6 ± 0.0	10.5 ± 5.7	3.58	6.01 ± 0.0	2.25 ± 0.0	3.76	571	393	784
St.08	0.45	1.10	1.26	2.35 ± 0.5	1.10 ± 0.1	10.9 ± 6.6	4.5 ± 0.5	2.90	6.95 ± 3.1	3.78 ± 1.0	3.17	462	537	396
St.10	0.56	0.67	0.51	1.15 ± 0.1	0.66 ± 0.0	30.2 ± 24.3	11.5 ± 2.9	2.21	8.18 ± 2.2	6.34 ± 4.9	1.84	1759	2397	917
average	0.58	0.98	0.91					2.90	7.05 ± 0.8	4.12 ± 1.5	2.92	931	1109	699
BBX-SSW														
St.05	0.74	1.15	0.98	2.12 ± 0.2	1.14 ± 0.0	9.3 ± 1.5	6.3 ± 5.7	2.93	13.52 ± 0.0	13.52 ± 0.0	-	1594	2961	-
St.08	0.61	1.03	0.99	2.01 ± 0.3	1.03 ± 0.2	9.5 ± 3.2	2.7 ± 1.6	3.41	4.90 ± 0.4	4.21 ± 1.0	0.70	431	723	125
St.10	0.57	0.52	0.47	0.98 ± 0.2	0.52 ± 0.1	14.8 ± 0.0	3.1 ± 2.8	2.03	5.04 ± 0.4	4.50 ± 0.4	0.53	1420	2414	317
average	0.64	0.90	0.81					2.79	7.82 ± 3.8	7.41 ± 4.1	0.41	1148	2033	147
BBX-SUR														
St.02	0.58	0.55	0.56	1.09 ± 0.2	0.54 ± 0.1	13.5 ± 2.7	5.3 ± 3.6	5.52	5.04 ± 1.5	3.41 ± 2.3	1.63	609	833	389
St.03	0.53	0.88	0.76	1.63 ± 0.1	0.88 ± 0.1	17.3 ± 0.0	4.3 ± 2.7	5.85	5.04 ± 0.7	4.03 ± 0.7	1.01	316	471	137
St.04	0.71	0.91	0.81	1.67 ± 0.3	0.90 ± 0.2	54.3 ± 2.7	9.8 ± 2.7	3.46	4.75 ± 0.0	3.78 ± 3.4	0.97	452	681	196
St.05	0.63	0.94	0.55	1.47 ± 0.1	0.93 ± 0.1	23.6 ± 2.7	13.5 ± 2.7	3.29	6.01 ± 0.0	6.01 ± 0.0	-	899	1423	-
St.06	0.44	0.65	0.85	1.48 ± 0.1	0.64 ± 0.2	13.5 ± 0.0	7.9 ± 2.7	6.19	5.04 ± 1.5	2.90 ± 1.8	2.13	330	438	247
St.07	0.63	0.90	0.51	1.41 ± 0.1	0.90 ± 0.2	5.8 ± 5.6	3.4 ± 2.7	4.06	4.53 ± 0.7	4.15 ± 0.7	0.39	448	642	105
St.08	0.65	1.10	1.40	2.49 ± 0.5	1.10 ± 0.1	13.5 ± 0.0	4.0 ± 2.5	6.86	13.36 ± 5.9	9.20 ± 5.9	4.16	507	791	282
St.10	0.52	0.51	0.57	1.06 ± 0.2	0.50 ± 0.0	17.3 ± 0.0	6.0 ± 4.0	5.52	9.78 ± 5.1	4.76 ± 2.3	5.03	849	879	822
average	0.59	0.81	0.75					5.09	6.69 ± 2.4	4.78 ± 1.4	2.19	551	770	311

Table 5.3.2. Concentrations of phosphorus as inorganic phosphorus (Inorg.) and organic phosphorus (Org.P) and sodium in the experimental seawater and aerosols generated from the bubble bursting experiment displayed with the ratio concentration between Org.P to Total.P, Inorg.P and sodium. SML, SSW, SUR referred to the uses of such seawater.in bubble bursting experiment (BBX)

	Water samples			Concentration Ratio				Filtered Aerosol samples			Concentration Ratio			
	Sodium (M)	Inorg.P (μM)	Org.P (μM)	Org.P/Total.P	Inorg.P:Total.P	Org.P:Inorg.P	Org.P:Na	Sodium (μmol m^{-3})	Inorg.P (nmol m^{-3})	Org.P (nmol m^{-3})	Org.P:Total.P	Inorg.P:Total.P	Org.P:Inorg.P	Org.P:Na
BBX-SML														
St.05	0.72	1.15	0.96	0.46	0.54	0.84	1.3E-06	3.58	2.25	3.76	0.63	0.38	1.67	1.0E-03
St.08	0.45	1.10	1.26	0.53	0.47	1.14	2.8E-06	2.90	3.78	3.17	0.46	0.54	0.84	1.1E-03
St.10	0.56	0.67	0.51	0.43	0.57	0.76	9.1E-07	2.21	6.34	1.84	0.22	0.78	0.29	8.3E-04
average	0.58	0.98	0.91	0.47	0.53	0.91	1.7E-06	2.90	4.12	2.92	0.44	0.56	0.93	9.9E-04
BBX-SSW														
St.05	0.74	1.15	0.98	0.46	0.54	0.86	1.3E-06	2.93	13.52	-	-	1.00	-	-
St.08	0.61	1.03	0.99	0.49	0.51	0.96	1.6E-06	3.41	4.21	0.70	0.14	0.86	0.17	2.0E-04
St.10	0.57	0.52	0.47	0.47	0.53	0.90	8.3E-07	2.03	4.50	0.53	0.11	0.89	0.12	2.6E-04
average	0.64	0.90	0.81	0.47	0.53	0.90	1.3E-06	2.79	7.41	0.41	0.12	0.92	0.14	2.3E-04
BBX-SUR														
St.02	0.58	0.55	0.56	0.51	0.49	1.02	9.7E-07	5.52	3.41	1.63	0.32	0.68	0.48	3.0E-04
St.03	0.53	0.88	0.76	0.46	0.54	0.86	1.4E-06	5.85	4.03	1.01	0.20	0.80	0.25	1.7E-04
St.04	0.71	0.91	0.81	0.47	0.53	0.90	1.1E-06	3.46	3.78	0.97	0.20	0.80	0.26	2.8E-04
St.05	0.63	0.94	0.55	0.37	0.63	0.58	8.7E-07	3.29	6.01	-	-	1.00	-	-
St.06	0.44	0.65	0.85	0.57	0.43	1.31	1.9E-06	6.19	2.90	2.13	0.42	0.58	0.73	3.4E-04
St.07	0.63	0.90	0.51	0.36	0.64	0.57	8.1E-07	4.06	4.15	0.39	0.08	0.92	0.09	9.5E-05
St.08	0.65	1.10	1.40	0.56	0.44	1.27	2.1E-06	6.86	9.20	4.16	0.31	0.69	0.45	6.1E-04
St.10	0.52	0.51	0.57	0.53	0.47	1.13	1.1E-06	5.52	4.76	5.03	0.51	0.49	1.06	9.1E-04
average	0.59	0.81	0.75	0.48	0.52	0.95	1.3E-06	5.09	4.78	2.19	0.29	0.74	0.47	3.9E-04

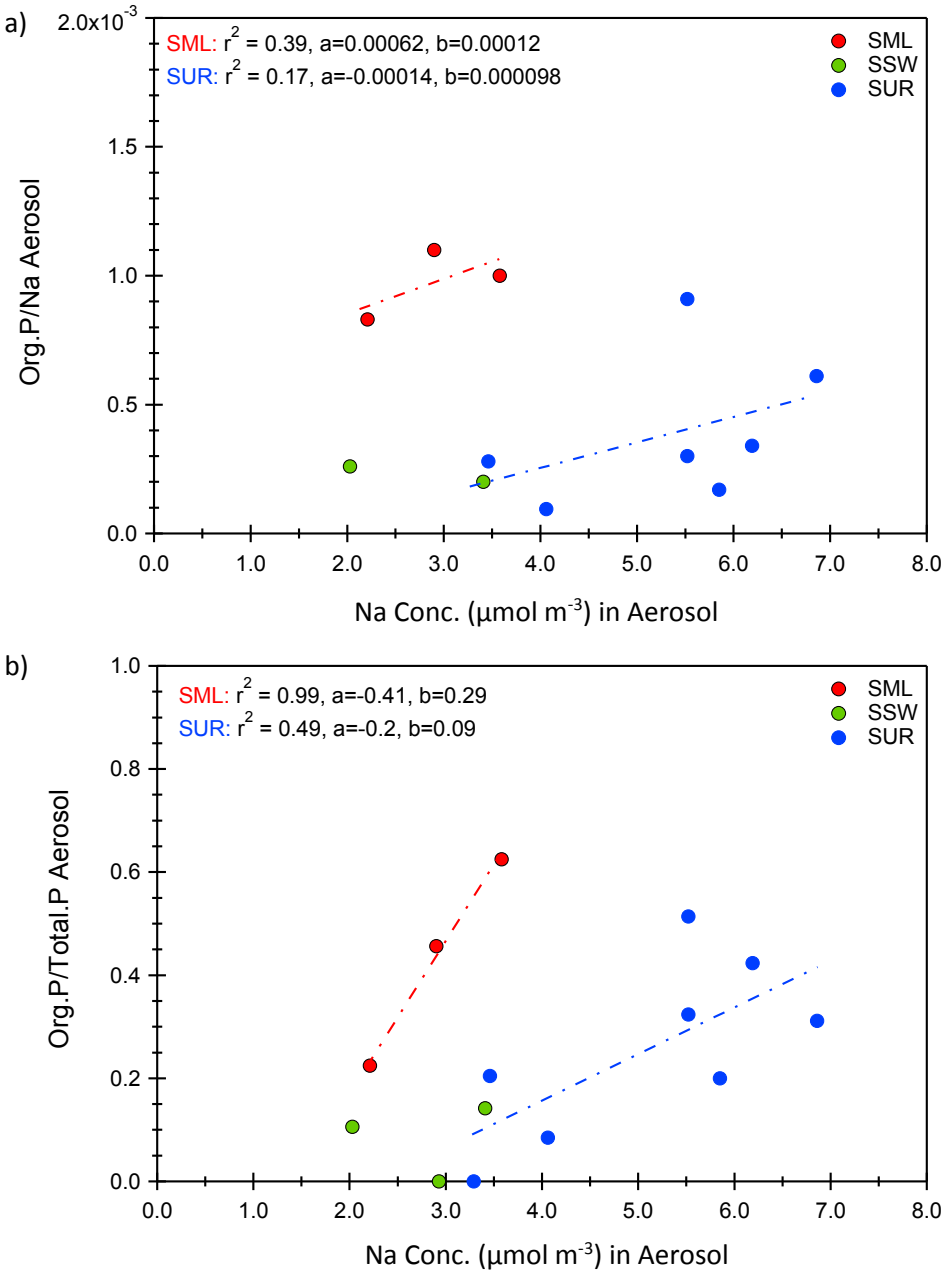

Fig. 5.3.1. Concentration of sodium (µmol m^{-3}) in aerosols generated from bubblebursting experiment; SML, SSW and SUR as a funtion a) concentration ratio of organic phosphorus (Org.P) and sodium and b) concentration ratio of Org.P and total phosphorus (Total.P) in generated aerosols. Aerosols generated from the SML experiment contained less sodium concentration but high Org.P content in comparative to SSW and SUR experiment.

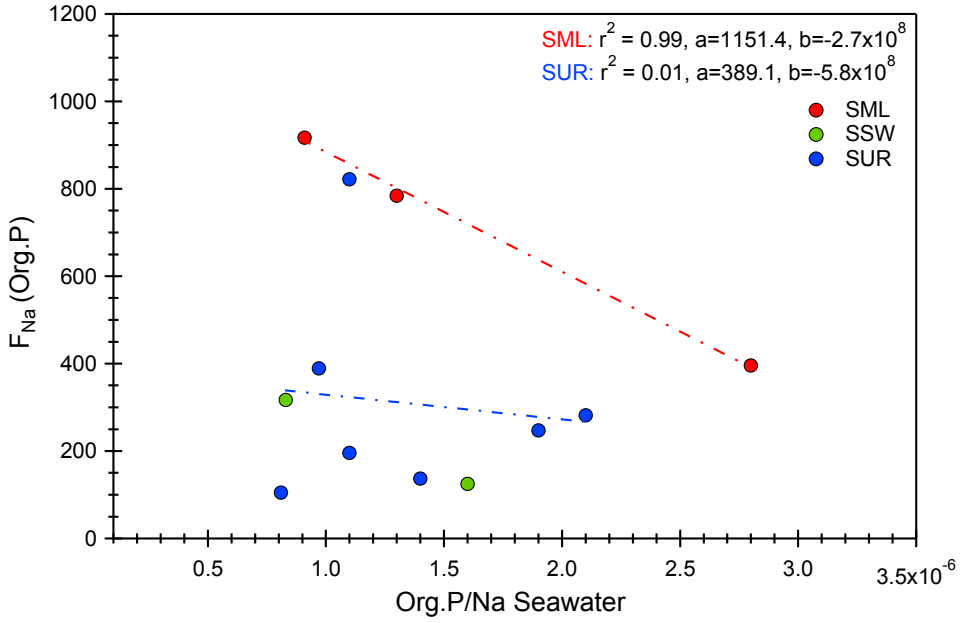

Fig. 5.3.2. Sea to air fractionation (F_{Na}) of organic phosphorus (Org.P) as a function of concentration ratio of Org.P to sodium in aerosols generated from the bubble bursting experiment. SML, SSW and SUR refer to the bubble solution in the experiment. The increase of organic phosphorus in relative to sodium concentration in seawater decreased F_{Na} of Org.P.

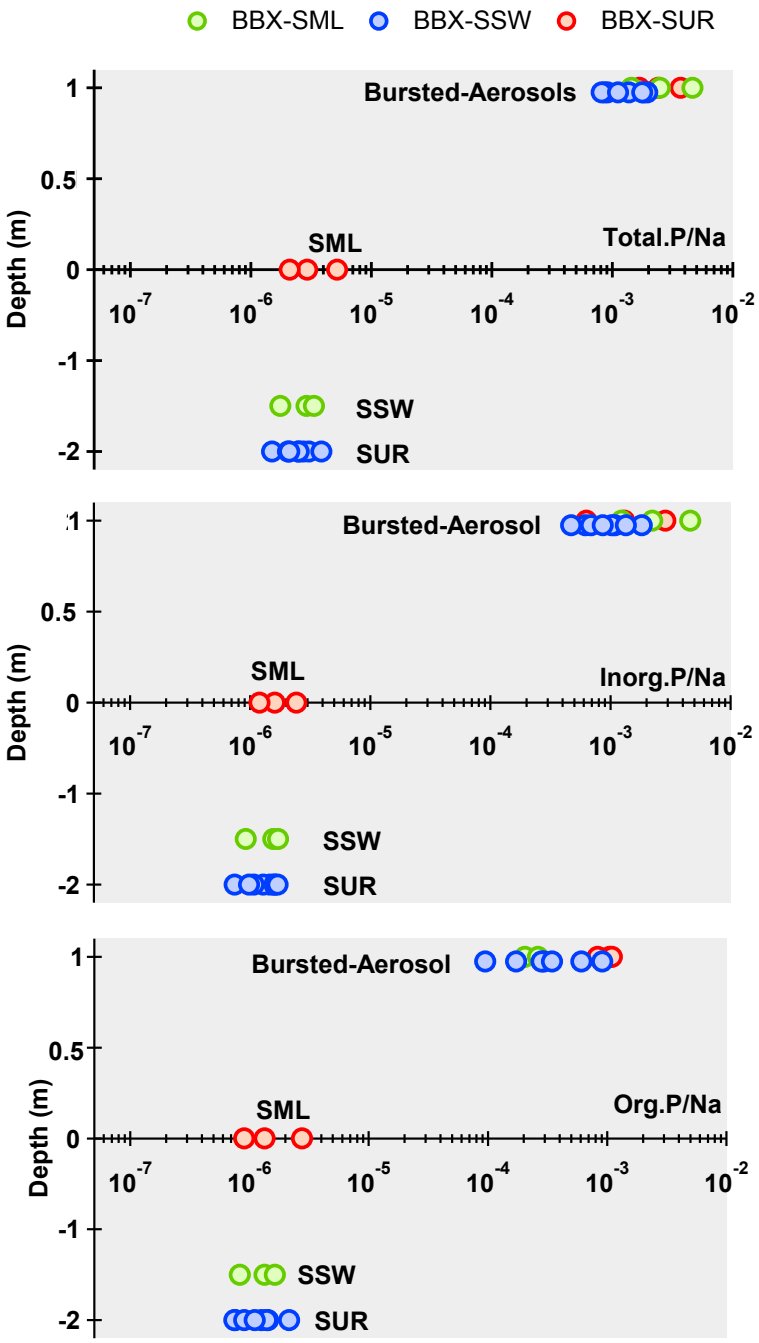

Fig. 5.3.3. Depth of view schematic diagram of phosphorus to sodium ratio. From top to bottom panels displayed the number ratio of total phosphorus (Total.P), inorganic phoshorus (Inorg.P) and organic phosphorus (Org.P), respectively. BBX referred to bubble bursting experiment and SML, SSW, SUR referred to the uses of such water for bubble bursting. When number ratio in the bursted aerosols greater than in seawater, it demonstrated enrichement of that ionic species in aerosols.

5.3.2. Sea to air fractionation of ionic species

Beside the positive sea to air fractionation in phosphorus species, there was the positive enrichment (F_{Na} >1) reported in some water soluble ionic species (**Fig. 5.3.4)**. Concentration of major ionic species in seawater and particles ejected from the bubble experiment including sodium, alkali and alkali earth metals (Ca, Mg and K), halogen (Cl, Br and F), nitrate and sulfate were presented in **Table 5.3.3.** Sea to air fractionation of ionic species were reported in **Table 5.3.4**.

For alkali and alkali earth metals, F_{Na} obtained at 1 or lower indicated negative enrichment towards aerosols production especially in SML experiment. In SML, none of these chemical species presented in the positive enrichment (F_{Na}>1). In SSW, the enrichment was slightly greater than 1 for K^+ and Ca^{2+}. In SUR experiment, F_{Na} Mg^{2+} and F_{Na} K^+ were obtained as a factor of 1 – 3.5. Concentration of K^+, Mg^{2+} in ejected aerosol particles were greather in SUR experiment, while in SML and SSW experiment, aerosol concentration were presented at similar number (**Table 5.3.3, Fig. 5.3.4.a**).

For halogen, chlorine was presented as the major mass component in sea salts and often displayed the enrichment in sea to air fractionation. In this study, the F_{Na} Cl was slightly enriched at a factor of 1 - 2. For bromine, F_{Na} was expressed at a factor of 1-1.5. SUR experiment reported the slightly higher F_{Na} Br^+ than SML and SSW experment. For fluoride, the enrichment was not exhibited in any bubble bursting experiments (**Fig. 3.3.4.b)**.

F_{Na} of nitrate and sulfate, were obtained at a factor of 0 to 2 in most experiments. The observation of high F_{Na} up to 100 was found in aerosols containing relatively low sodium concentration (**Fig. 3.3.4.c)**. The formation of nitrate aerosols from ocean was formed associated with the formation of sea salts absorbed nitric acid. The conversion of sulfur gas and organic sulfides

to particulate sulfate was the suggested mechanism for atmospheric particulate sulfate formaiton [Hoffman and Duce, 1976].

Ionic species fractionated due to its potential as the counter ions (prefer over Na^+or Cl^- in sea salt aerosol formation) of the opposite surface active component charge of the bursting surface or binding with unchanged organic or the colloidal components in the bubble solution [MacIntyre, 1970]. Upon bursting, under rich organic or colloidal components like SML seawater, there was the coagulation of sea salts with organic substances in seawater, suppressing the fractionation of such ionic species as seen in the SML experiment.

Table 5.3.3 Concentrations of ionic species in seawater and ejected aerosols from bubble bursting experiment (BBX). SML, SSW, SUR referred to the uses of such seawater in the experiment.

	Water samples									Filtered Aerosol samples							
	mol L^{-1}		mmol L^{-1}							µmol m^{-3}		nmol m^{-3}					
	Na^+	Cl^-	Br^-	F^-	NO_3^-	SO_4^{2-}	Ca^{2+}	Mg^{2+}	K^+	Na^+	Cl^-	Br^-	F^-	NO_3^-	SO_4^{2-}	Ca^{2+}	Mg^{2+}	K^+
BBX-SML																		
St.05	0.7	1.6	1.6	206.8	2.9	47.7	13.5	84.3	14.3	3.6	7.9	7.4	340.0	12.6	0.3	48.9	381.5	76.2
St.08	0.5	0.9	1.0	62.7	1.7	43.9	7.4	46.1	8.0	2.9	9.2	4.4	232.4	13.8	0.3	45.7	263.6	58.0
St.10	0.6	1.1	0.9	115.8	8.8	49.4	12.2	66.6	11.7	2.2	5.1	5.0	131.0	19.5	0.2	28.9	238.0	60.3
BBX-SSW																		
St.05	0.7	1.6	1.5	270.1	1.3	46.3	15.8	89.3	13.9	2.9	6.6	5.0	268.3	0.3	0.2	53.0	339.2	61.8
St.08	0.6	1.2	1.5	56.6	1.3	42.9	12.0	69.5	12.8	3.4	7.7	7.1	110.5	12.5	0.3	55.0	427.5	86.8
St.10	0.6	1.2	1.9	91.6	10.1	41.5	10.8	63.4	11.2	2.0	4.6	3.7	528.8	9.2	0.2	38.9	225.0	36.1
BBX-SUR																		
St.02	0.6	1.2	0.8	80.8	0.6	37.0	10.5	67.3	10.4	5.5	15.1	28.5	542.0	9.9	1.1	44.8	1625.9	262.7
St.03	0.5	1.1	0.8	104.6	1.8	34.0	10.0	54.7	9.8	5.8	13.1	12.4	348.6	7.9	0.4	48.9	656.6	125.5
St.04	0.7	1.5	1.6	145.7	0.7	42.7	12.2	81.3	12.5	3.5	7.6	7.0	413.1	4.2	0.3	49.0	374.4	65.8
St.05	0.6	1.4	3.1	193.5	1.8	38.4	10.8	69.2	10.2	3.3	10.7	19.2	653.5	176.5	4.6	50.4	1048.8	186.1
St.06	0.4	0.9	1.0	137.1	1.1	25.0	7.9	43.3	8.0	6.2	13.7	9.9	440.6	7.9	0.5	85.9	589.6	123.2
St.07	0.6	1.3	1.3	174.3	1.7	44.2	11.5	66.0	11.5	4.1	14.6	7.4	584.9	1251.8	27.2	37.1	437.6	82.3
St.08	0.7	1.3	2.0	85.9	1.8	47.2	12.1	71.7	12.9	6.9	14.5	11.8	151.3	16.0	0.5	108.4	589.6	121.0
St.10	0.5	1.1	0.9	110.7	1.1	37.1	9.3	58.0	9.5	5.5	12.0	8.9	253.0	18.0	0.3	66.7	496.9	100.8

Table 5.3.4 Concentration of sodium in seawater, generated aerosols and sea to air fractionation (F_{Na}) of ionic species in bubble bursting experiment. Enrichment of ionic species between aerosols and seawater determined when F_{Na} is greater than 1.

	Water	Aerosol	Fractionation (F_{Na})							
	mol Na L^{-1}	µmol Na m^{-3}	Cl^-	Br^-	F^-	NO_3^-	SO_4^{2-}	Ca^{2+}	Mg^{2+}	K^+
BBX-SML										
St.05	0.7	3.6	1.0	1.0	0.3	0.9	1.2	0.7	0.9	1.1
St.08	0.5	2.9	1.6	0.7	0.6	1.3	0.9	1.0	0.9	1.1
St.10	0.6	2.2	1.1	1.5	0.3	0.6	0.8	0.6	0.9	1.3
BBX-SSW										
St.05	0.7	2.9	1.0	0.9	0.2	0.1	1.3	0.8	1.0	1.1
St.08	0.6	3.4	1.1	0.9	0.3	1.7	1.2	0.8	1.1	1.2
St.10	0.6	2.0	1.1	0.5	1.6	0.3	1.0	1.0	1.0	0.9
BBX-SUR										
St.02	0.6	5.5	1.3	3.7	0.7	1.9	3.1	0.4	2.5	2.6
St.03	0.5	5.8	1.1	1.4	0.3	0.4	1.1	0.4	1.1	1.2
St.04	0.7	3.5	1.1	0.9	0.6	1.2	1.5	0.8	0.9	1.1
St.05	0.6	3.3	1.5	1.2	0.6	18.4	23.0	0.9	2.9	3.5
St.06	0.4	6.2	1.1	0.7	0.2	0.5	1.3	0.8	1.0	1.1
St.07	0.6	4.1	1.8	0.9	0.5	117.8	95.8	0.5	1.0	1.1
St.08	0.7	6.9	1.0	0.6	0.2	0.8	1.1	0.8	0.8	0.9
St.10	0.5	5.5	1.1	0.9	0.2	1.5	0.9	0.7	0.8	1.0

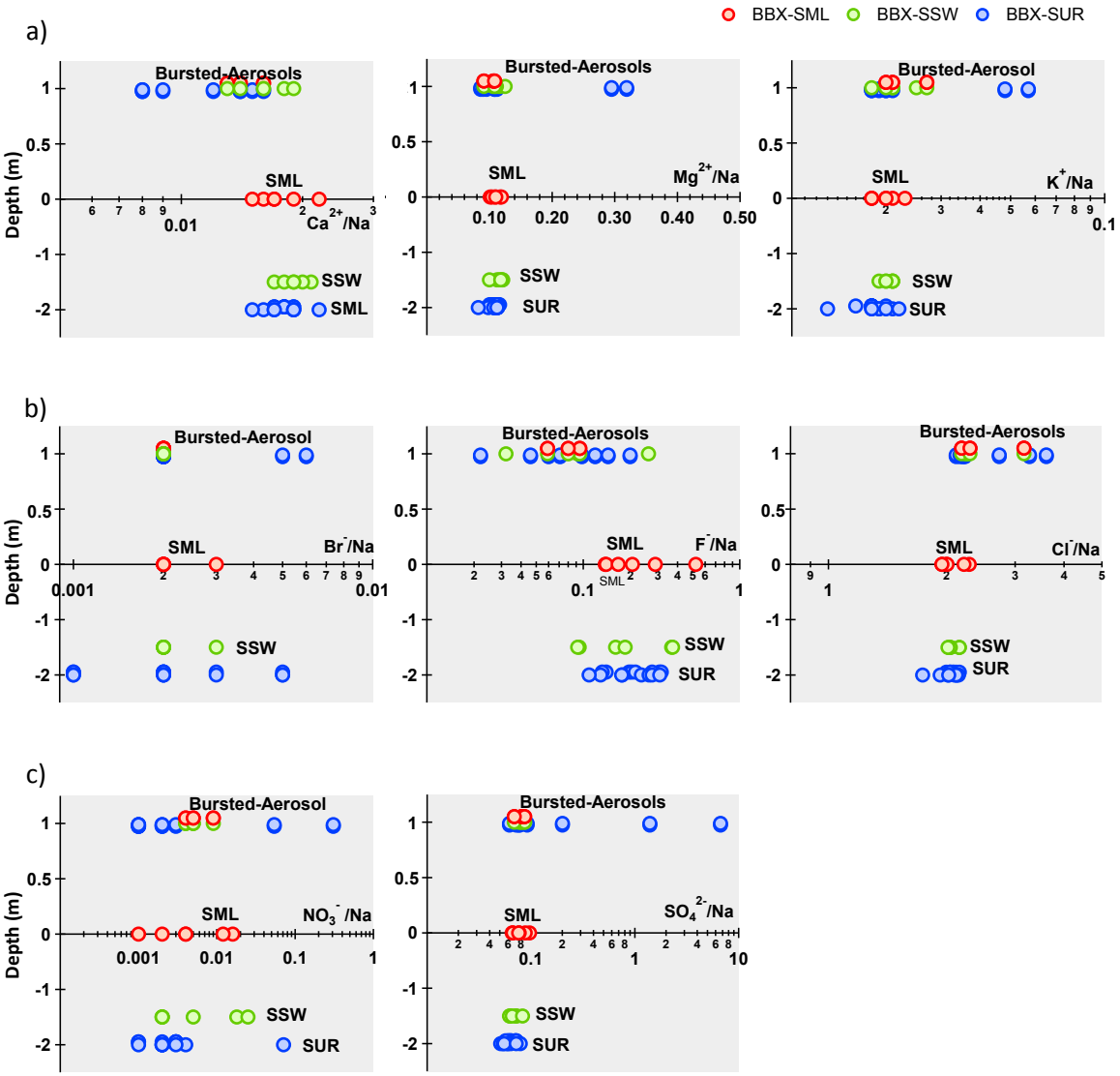

Fig. 5.3.4. Depth of view schematic diagram of ionic species to sodium ratios for a) alkaline and alkaline earth metals b) halogen and c) nitrate and sulfate, in the seawater (SML, SSW and SUR) and bubble bursted aerosols. When number ratio in the bursted aerosols greater than in seawater, it demonstrated enrichement of that ionic species in aerosols.

5.4. Concentration ratio of atmospheric phosphorus to sodium in ejected aerosols

Average concentration of phosphorus and sodium in aerosols generated from the bubble experiment were compared with marine aerosol from previous field measurement in North Pacific Ocean (**Table 5.4.1**). Concentration of generated aerosols from the bubble experiment were about 3 magnitudes greater than the real measurement but the ratio concentration of total phosphorus to sodium in marine aerosols and in bubble generated particles was agree well (**Table 5.4.2**). This similarity of phosphorus to sodium ratio indicated that seawater as source had contributed considerably amount of oceanic particles into the atmosphere during the bubble bursting process.

Table 5.4.1. Distribution of phosphorus and sodium in aerosols and surface water in Northern Pacific Ocean and in the bubble bursting experiment.

Aerosols	Concentration (nmol m^{-3})				Reference
	Na	Total.P	Inorg.P	Org.P	
Tropical/Subtropical Northern Pacific	56.55	0.08			[1]
Central North Pacific	64.38	0.08			[1], ASW
Northern North Pacific	112.66	0.09			[1], ASW
Western North Pacific	63.07	0.24			[1], ASW
Buble bursting experiment (90 min.) EEP-2012					This study
SML-water (90min)	2898	7.05	4.12	2.92	
SSW-water	2789	7.82	7.41	0.41	
SUR-water	5093	6.69	4.78	2.19	
Surface seawater	Na (mM)	Concentration (μM)			
		Total.P	Inorg.P	Org.P	
Subtropical Northern Pacific Ocean	477.6	0.32	0.01	0.31	[2],[4]
Equatorial Pacific Ocean	485.3	0.67	0.44	0.23	[3],[4]
Average Surface Water (ASW)*	481.5	0.50			average number
Eastern Equatorial Pacific Ocean	475.5	1.51	0.79	0.72	This study
Buble bursting experiment (90 min.) EEP-2012					
SML-water	578.5	1.88	0.98	0.91	
SSW-water	636.1	1.71	0.90	0.81	
SUR-water	586.7	1.56	0.81	0.75	

[1] [Furutani et al., 2010], [2] [Yoshimura et al., 2007], [3] [Suzumura et al., 2004], and [4] [Lin et al., 2012]

Table 5.4.2. Ratio concentration of phosphorus to sodium of atmospheric particles from previous field measurement and the bubble generated particles from bubble bursting experiment.

Aerosols*	Concentration (nmol m^{-3})				Ratio Concentration in Aerosol ($x10^{-3}$)		
	Na	Total.P	Inorg.P	Org.P	Total.P/Na	Inorg.P/Na	Org.P/Na
Tropical/Subtropical Northern Pacific	56.55	0.08			1.37		
Central North Pacific	64.38	0.08			1.25		
Northern North Pacific	112.66	0.09			0.80		
Western North Pacific	63.07	0.24			3.74		
Buble bursting experiment (90 min.) EEP-2012							
SML-water (90min)	2898	7.05	4.12	2.92	2.43	1.42	1.01
SSW-water	2789	7.82	7.41	0.41	2.80	2.66	0.15
SUR-water	5093	6.69	4.78	2.19	1.31	0.94	0.43

*[Furutani et al., 2010]

The study of source apportionment analysis has indicated that the contribution of seawater towards the atmospheric phosphorus was accounted to less than 1% [Furutani et al., 2010]. However, as displayed in previous section, fractionation of phosphorus was considerably high. Furthermore, the influence of SML chemical properties in suppressing the bigger particles formation and producing more organic aerosols were clearly observed. Therefore, using the ratio of phosphorus to sodium in seawater as the apportionment fraction was suggested to underestimate the formation of atmospheric phosphorus especially the organic phosphorus. Data of the organic phosphorus in marine aerosols, the sophisticated bubble bursting experiment representing the sea surface dynamic condition, the setting velocity of such generated particles were suggested for further investigation on the real effects and to determine the contribution fraction of seawater towards the formation of atmospheric phosphorus.

Even though, phosphorus generated from bubble bursting process was not considered as the new phosphorus supply to ocean; in other words, the recycled phosphorus. The re-suspension of the generated phosphorus particles on to the ocean surface (or in land) after long distance transportation was able to supply phosphorus back to the ocean cycle and recycle in marine biological activities, maintaining marine productivity in certain ocean district.

Summary

The atmospheric particles derived from the ocean can be significanlty contributed to the atmospheric chemical composition. The bubble bursting experiments offered the study of ocean-derived substances without such background concentration. In bubble bursting experiment, phosphurus is vastly enriched in aerosols both inorganic and organic content. Enrichment of organic phosphorus was occurred in general and can be observed in all SML, SSW and SUR bubble bursting experiments. However, the highest fractionation of organic phosphorus was observed in the SML experiment.

The fractionation of phosphorus by all forms was displayed at a factor of 10^2 - 10^3. F_{Na} greater than 1 indicating the enrichment of ejected aerosols with the phosphorus derived from the seawater. The production of aerosols from the SML and SSW experiment contained less sodium content than those in the SUR experiment. However, the average total phosphorus concentration in generated aerosols was expressed at the same level (~7 nmol m^{-3}). Therefore, comparing with sodium content, aerosols produced from SML experiment contained promisingly higher organic phosphorus than those from generated from SSW and SUR experiments. For the observation of ionic species fractionation, the positive enrichment was obeserved in alkali and alkali earth metals (K and Mg) , sulfate and nitrate only in SUR experiment. Halogen species were shown the negative to non enrichment in most samples. In addition, single chemical mass spectra of bubble generated particles demonstrated that SML generated particles were enriched with organic carbon particles. It was produced in greater number in comparative to the SSW generated particles especially for submicron organic particles (D_a < 1 µm).

The similar fractionation factor of organic phosphorus in the SML and SUR (a mixture of SML and SSW seawater) experiments indicated that the fractionation of organic phosphorus was specifically influenced by organic rich content in the SML. The similarity of the ratio concentration

of total phosphorus to sodium between marine aerosols and the bubble bursting generated particles indicated that aerosols production from bubble bursting process had considerably contributed to certain amount of atmospheric phosphorus and can re-suspended after sometimes into ocean surface maintaining marine productivity in remote ocean.

6. Conclusions

Sea-surface microlayer (SML) is a thin boundary layer between atmosphere and ocean. An interface layer of the complex mixture of hydrated gelatinous carbonate, protein, and lipids [Wurl and Holmes; 2008] with approximately 50 μm depth layer lying on top of underlying subsurface seawater (SSW). It is distinguishable apart from the underneath by its differences in biological and physiochemical properties. Covers up to 70% of the earth surface, SML expresses its importance in air – sea exchange of heat, gases, liquid, and solids [Cunliffe et al., 2013; Liss and Duce, 1997]. As the micro scale environment, SML is serving as modulating media for materials synthesis, transformation and cycling in biogeochemical process [Wheeler, 1975].

This field study reported the results from seawater and atmospheric particulate sampling from 3 cruises on the SWNP-2010 in Subtropical Western North Pacific during spring, the CRI-2010 in the Coastal Sea around Ryukyu Islands and the EEP-2012 during winter time in Eastern Equatorial Pacific region. Phosphorus was selected for the study of the interaction of substances between atmosphere and ocean. The uniform distribution of phosphorus concentration over the marine air in the remote North Pacific Ocean (0.07-0.09 nmol m^{-3}, Furutani et al., 2010) has suggested to the additional source contribution of the atmospheric phosphorus and seawater has been considered. In particular, the interface layer; SML is expected to involve in this contribution in supplying phosphorus as well as a media for the atmospheric particulate phosphorus formation.

The composition of phosphorus in SML exhibited differently from SSW as a result of the interfacial physical and biogeochemical process. In surface water including SML samples, concentration of phosphorus in dissolved form was accounted for 0.1-0.4 μM in low productivity seawater collecting during the SWNP-2010 cruise and CRI-2010 cruise. In a High Nitrate, Low Chlorophyll-a (HNLC) condition in EEP-2012 cruise, dissolved phosphorus concentration was ranged

from 0.9 – 2 μM. For the particulate phosphorus, concentration was ranged from 14-50 nM in SWNP-2010 and CRI-2010, and 3-40 nM in EEP-2012.

Total dissolved phosphorus (TDP) was a major phosphorus pool in the SML and accounted for 90-98% of total. Within TDP fraction, dissolved organic phosphorus (DOP) was generally more dominant in SML than soluble reactive phosphorus (SRP). For particulate phosphorus pool, except for the SNWP-2010, particulate organic phosphorus (POP) was a dominant species. The low background concentration of particulate phosphorus explained by the higher enrichment factor in the SML.

Under the low productivity seawater in the SWNP-2010, enrichment factor (EF) or the concentration ratio between SML and SSW was more pronounced particular for SRP. The biological consumption of SRP depleted its concentration in bulk seawater. In coastal water of CRI-2010, the more biological complex of coastal water fasten the turnover rate of particulate phosphorus in seawater and exhibited much higher DOP and particulate phosphorus enrichment (EF_{SRP}=0.1-1, EF_{DOP} = 1-2.7, EF_{TPP} ~ 5).

In EEP-2012, dissolved phosphorus showed non enrichment signals due to the lack of trace nutrient, lowering biological production. Enrichment of particulate phosphorus was considerably high due to its low background. The exceptional increased in the enrichment factor of total particulate phosphorus to 72, (in St. 01; EEP-2012) while the cruise average EF_{TPP} was 2.5 indicated to the different enrichment process. The particulate iron (pFe) was found concurringly increasing in SML with EF_{pFe} equaled to 11 (81 nM). The single particle analysis by a scanning electron microscopy with energy dispersive X-ray spectroscopy (SEM/EDX) showed the greater number of biogenic particles especially diatom and microorganism particles in the SML. Percentage of phosphorus content in single particles measured by SEM/EDX analysis was generally higher in the SML particles than those in SSW and the enrichment factor estimated by the SEM/EDX analysis was

75. The increase of surface active area for phosphorus adsorption added up to the greater in number of larger biogenic particles presented in the SML was the explanation for this pronounced enrichment. As evidence related to, the possible cause of such high particulate phosphorus was linked to the external drive. It was likely that the spike of the lacking nutrient (i.e., pFe) in the surface ocean induced the increase of the number particles, hence the particulate phosphorus.

Not only receiving substances from the atmosphere, ocean including SML also supplies marine aerosols via bubble-bursting at surface seawater and ejected film and jet droplets into the atmosphere. SML as an interface involving with bubble bursting process by supplying substances and providing space for the interaction. Bubble bursting experiment conducted on board EEP-2012 utilizing SML, SSW and SUR (surface seawater collected by the bucket sampling) as the bubble soultion. The use of SML seawater benefited for the study of the influences of the organic substnace in SML towards the oceanic aerosol formation.

Sea to air fractionation (F_{Na}) of phosphorus is a factor of concertration ratio between phosphorus to soduim in generated particles and seawater. By all phosphorus forms, F_{Na} presented by a factor of 10^2 - 10^3. This indicated the positive enrichment in the ejected aerosol ($F_{Na} > 1$) in relative to seawater. Aerosols from SML and SSW experiment contained less sodium content but presented with the same amount of total phosphorus (~7 nmol m^{-3}). When comparing with sodium ratio, the ejected aerosols from the SML contained promisingly higher organic phosphorus than those from the SSW. Furthermore, similar fractionation factor of organic phosphorus in the SML and SUR (a mixture of SML and SSW seawater) experiments was observed and identified that organic content in SML was specifically influenced to sea to air fractionation by organic atmospheric phosphorus. In addition, the chemical mass spectra of single particle generated from SML seawater showed the abundance with sea salts particles coagulating with organic content in the ejected

aerosols. Moreover, organic particles were greater in number in submicron particle in comparative to the SSM results.

The ratio concentration of total phosphorus to sodium in marine aerosols from previous study were compared with the results from the experiment. Ratio number was displayed with the similar number and was implied that aerosols generated from bubble bursting process had considerably contributed to certain amount of atmospheric phosphorus.

The study of phosphorus biogeochemistry at atmosphere and ocean interface: sea-surface microlayer demonstrated the significant enrichment of particulate phosphorus in the SML. The extended study for veticle profile gave a better picture of the enrichment process. Beside the accumuation of substances via upward transportation and bubble scavening, the internal microbiological activity and its by-products also increase and aggregated within the layer. The enhancement of microbioactivity within the SML by the external pertubation had lead to the changes of chemical composition (phosphorus) in SML, ditiguishable from the underlying seawater. This shown that the thin SML layer was capable for retaining particles to certain time through its excess settling velocity and its organic content that lowered surface tension. The study of bubble bursting experiment had addressed also the significance the ejected aerosols contained organic phosphorus to the atmosphere. The significant of SML properties in suppressing the lager particles formation and producing more organic aerosols in the atmosphere has its important implication in marine biogeochemical cycle of phosphorus. The resuspened of generated phosphorus particles on to surface ocean after the long length tranaportation can supply phosphorus back to the ocean cycle, furthur maintaining the marine productivity.

7. Acknowledgement

I would like to extend my sincerest thanks and appreciation to those help for this accomplishment. First, I would like to express my deepest gratitude to my advisor, Professor Mitsuo Uematsu, at the Atmosphere and Ocean Research Institute (AORI), the University of Tokyo for his invaluable suggestion, technical guidance, educational comments, moral supports and kindness concerns throughout my study and for my daily life in Japan. He also provided me with the invaluable opportunities for participation in the research cruises and travel domestic and oversea for conferences and summer school.

I am sincerely grateful to Dr. Hiroshi Furutani for his generosity, his invaluable opinions and discussions and his suggestions for everything from research question, cruises preparation, moving or even translation. My grateful thanks are also extended to Dr. Yasushi Narita for his professional guidance for observations on the shipboard and valuable support in laboratory and Japanese documents and ITs.

Special gratitude also express to my thesis committee members and advisors Professor Atsushi Tsuda, Professor Shigenobu Takeda, Professor Hajime Obata and Professor Koji Hamasaki and Professor Uematsu sensei for his valuable times and comments and the great guidance and professional suggestiond for my dissertation.

I am grateful to the captains and crews of R/V Hakuho Maru and R/V Tansei Maru for their enthusiastic assistance in sea-surface microlayer samplings during the SNWP-2010, CRI-2010 and EEP-2012 cruises. I would also like to express my great appreciation to the principal investigators for the following cruises; Professor Atsushi Tsuda (for SNWP-2010 cruise), Professor Mitsuo Uematsu (for CRI-2010 cruise and EEP-2012 cruise). Without his kind concerns and help for conducting the study on board, this study would not be completed.

Special thanks to Dr. Fumiyoshi Kondo for his professional assistances during shipboard observation on SWMP-2010 and Dr. Jung Jin Young for his help in laboratory work and Japanese documents throughout his time in AORI. Great thanks also extended to Ms Yoshiko Murashima, Mr. Hiroyasu Nakayama, Mr. Daisuke Morimoto, Mr. Ryou Kawata, and Ms. Mary Mar P. Noblezada, for their help for observations, laboratory works and discussions.

This work was partly supported by the Sasakawa Scientific Research Grant from the Japan Science Society. I have been financially supported by the University of Tokyo Fellowship and research assistant of AORI, Department of Aquatic Bioscience, and the University of Tokyo.

Finally, I would like to express my deepest gratitude to my family for their love, encouragement and moral support and comfort throughout my entire life.

8. Reference

Adjou, M., P. Tréguer, C. Dumousseaud, R. Corvaisier, M. a. Brzezinski, and D. M. Nelson (2011), Particulate silica and Si recycling in the surface waters of the Eastern Equatorial Pacific, *Deep Sea Res. Part II Top. Stud. Oceanogr.*, *58*(3-4), 449–461, doi:10.1016/j.dsr2.2010.08.002.

Aller, J. Y., M. R. Kuznetsova, C. J. Jahns, and P. F. Kemp (2005), The sea-surface microlayer as a source of viral and bacterial enrichment in marine aerosols, *J. Aerosol Sci.*, *36*(5-6), 801–812, doi:10.1016/j.jaerosci.2004.10.012.

APHA, AWWA-WEF (1998). *Standard method for the examination of water and wastewater* 4500-P.

Baastrup-Spohr, L., and P. A. Staehr (2009), Surface microlayers on temperate lowland lakes, *Hydrobiologia*, *625*(1), 43–59, doi:10.1007/s10750-008-9695-3.

Baker, A. R., T. D. Jickells, M. Witt, and K. L. Linge (2006), Trends in the solubility of iron, aluminium, manganese and phosphorus in aerosol collected over the Atlantic Ocean, *Mar. Chem.*, *98*(1), 43–58, doi:10.1016/j.marchem.2005.06.004.

Benitez-Nelson, C. R. (2000), The biogeochemical cycling of phosphorus in marine systems, *Earth-Science Rev.*, *51*(1-4), 109–135, doi:10.1016/S0012-8252(00)00018-0.

Bigg, E. K., C. Leck, and L. Tranvik (2004), Particulates of the surface microlayer of open water in the central Arctic Ocean in summer, *Mar. Chem.*, *91*(1-4), 131–141, doi:10.1016/j.marchem.2004.06.005.

Bigg, E. K., and C. Leck (2008), The composition of fragments of bubbles bursting at the ocean surface, *J. Geophys. Res.*, *113*(D11), 1–7, doi:10.1029/2007JD009078.

Björkman, K. M., and D. M. Karl (1994), Bioavailability of inorganic and organic phosphorus compounds to natural assemblages of microorganisms in Hawaiian coastal waters, *Mar. Ecol. Process Ser.*, *111*(3), 265–273, doi:10.3354/meps111265.

Blanchard, D. C. (1989), The Ejection of Drops from the Sea and Their Enrichment with Bacteria and Other Materials: A Review, *Estuaries*, *12*(3), 127, doi:10.2307/1351816.

Boyd, P. W., Mackie, D. S., and Hunter, K. A. (2010), Aerosol iron deposition to the surface ocean—Modes of iron supply and biological responses, *Mar. Chem., 120* (1), 128-143, doi: 10.1016/j.marchem.2009.01.008.

Brantley, S. L., L. J. Liermann, R. L. Guynn, A. Anbar, G. a. Icopini, and J. Barling (2004), Fe isotopic fractionation during mineral dissolution with and without bacteria, *Geochim. Cosmochim. Acta*, *68*(15), 3189–3204, doi:10.1016/j.gca.2004.01.023.

Brzezinski, M. A. et al. (2011), Co-limitation of diatoms by iron and silicic acid in the equatorial Pacific, *Deep Sea Res. Part II Top. Stud. Oceanogr.*, *58*(3-4), 493–511, doi:10.1016/j.dsr2.2010.08.005.

Calvo, E., C. Pelejero, L. D. Pena, I. Cacho, and G. a Logan (2011), Eastern equatorial pacific productivity and related-CO2 changes since the last glacial period., *Proc. Natl. Acad. Sci. U. S. A.*, *108*(14), 5537–5541, doi:10.1073/pnas.1009761108.

Carlson, D. J. (1982), A field evaluation of plate and screen microlayer sampling techniques, *Mar. Chem.*, *11*(3), 189–208, doi:10.1016/0304-4203(82)90015-9.

Carlson, D. J. (1983), Dissolved organic materials in surface microlayers: Temporal and spatial variability and relation to sea state, *Limnol. Oceanogr, 28(3)*, 415-431.

Carlson, D. J., J. L. Cantey, and J. J. Cullen (1988), Description of and results from a new surface microlayer sampling device, *Deep Sea Res. Part A. Oceanogr. Res. Pap.*, *35*(7), 1205–1213, doi:10.1016/0198-0149(88)90011-8.

Cauwet, G. (1978), Organic-chemistry of sea-water particulates concepts and developments*, Oceanol. Acta, 1*(1), 99–105.

Chen, H. Y., C. C. Hung, T. H. Fang, and G. C. Gong (2008), Dry deposition and particle-size distribution of phosphorus in the marine atmosphere over the northeastern coast of Taiwan, *Cont. Shelf Res.*, *28*(6), 756–766, doi:10.1016/j.csr.2007.12.008.

Chen, H.-Y., T.-H. Fang, M. R. Preston, and S. Lin (2006), Characterization of phosphorus in the aerosol of a coastal atmosphere: Using a sequential extraction method, *Atmos. Environ.*, *40*(2), 279–289, doi:10.1016/j.atmosenv.2005.09.051.

Chen, L., R. Arimoto, and R. A. Duce (1985), The sources and forms of phosphorus in marine aerosol particles and rain from Northern New Zealand, *Atmos. Environ.*, *19*(5), 779–787, doi:10.1016/0004-6981(85)90066-6.

Coale, K.H., K. H., Johnson, S. E. Fitzwater, R. M. Gordon, S. Tanner, F. P. Chavez, L. Ferioli, C. Sakamoto, P. Rogers, F. Millero, P. Steinberg, P. Nightingale, D. Cooper, W. P. Cochlan, M. R. Landry, J. Constantinou, G. Rollwagen, A. Trasvina, R. Kudela (1996), A massive phytoplankton bloom induced by an ecosystem-scale iron fertilization experiment in the equatorial Pacific Ocean, *Nature, 383 (6600)*, 495-501, doi: 10.1038/383495a0.

Croot, P. L., K. Andersson, M. Öztürk, and D. R. Turner (2004), The distribution and speciation of iron along 6°E in the Southern Ocean. *Deep-Sea Res. Part II Oceanogr. Res. Pap. 51*, 2857-2879, doi: 10.1016/j.dsr2.2003.10.012.

Cunliffe, M., and J. C. Murrell (2009). The sea-surface microlayer is a gelatinous biofilm*, ISME J., 3(9*), 1001–3, doi:10.1038/ismej.2009.69.

Cunliffe, M., A. Engel, S. Frka, B. Gašparovic´, C. Guitart, C. Murrell, M. Salter, C. Stolle, R. Upstill-Goddard, and O. Wurl (2013), Sea-surface microlayers : A unified physicochemical and biological perspective of the air – ocean interface, *Prog. Oceanogr.*, *109*, 104–116, doi:10.1016/j.pocean.2012.08.004.

Cunliffe, M and Wurl, O (2014). *Guide to best practices to study the ocean's surface*. Occasional Publications of the Marine Biological Association of the United Kingdom, Plymouth, UK. 11 8 pp.

Cunliffe, M., R. C. Upstill-Goddard, and J. C. Murrell (2011), Microbiology of aquatic surface microlayers., *FEMS Microbiol. Rev.*, *35*(2), 233–46, doi:10.1111/j.1574-6976.2010.00246.x.

Danos, S. C., J. S. Maki, and C. C. Remsen (1983), Stratification of microorganisms and nutrients in the surface microlayer of small freshwater ponds, *Hydrobiologia, 98* (3), 193-202, doi: 10.1007/BF00021021.

de Leeuw, G., E. L. Andreas, M. D. Anguelova, C. W. Fairall, E. R. Lewis, C. O'Dowd, M. Schulz, and S. E. Schwartz (2011), Production flux of sea spray aerosol, *Rev. Geophys.*, *49*(2), RG2001, doi:10.1029/2010RG000349.

Del Vento, S., and J. Dachs (2007), Influence of the surface microlayer on atmospheric deposition of aerosols and polycyclic aromatic hydrocarbons*, Atmos. Environ., 41*(23), 4920–4930, doi:10.1016/j.atmosenv.2007.01.062.

Draxler, R.R. and Rolph, G.D. HYSPLIT (HYbrid Single-Particle Lagrangian Integrated Trajectory) Model access via NOAA ARL READY Website (http://www.arl.noaa.gov/HYSPLIT.php). NOAA Air Resources Laboratory, College Park, MD.

Donaldson, D. J. and C. George (2012), Sea-Surface Chemistry and Its Impact on the Marine Boundary Layer, *Environ. Sci. and Tech. 46 (*19), 10385-10389; doi: 10.1021/es301651m.

Duce, R. A, and E. J. Hoffman (1976), Chemical Fractionation at the Air/Sea Interface, *Annu. Rev. Earth Planet. Sci.*, *4*(1), 187–228, doi:10.1146/annurev.ea.04.050176.001155.

Duce, R. A. et al. (1991), The atmospheric input of trace species to the world ocean, *Global Biogeochem. Cycles, 5*(3), 193, doi:10.1029/91GB01778.

Falkowska, L. (1999), Sea-surface microlayer: A field evaluation of teflon plate, glass plate and screen sampling techniques. Part 1. Thickness of microlayer samples and relation to wind speed, *Oceanologia*, *41*(2), 211–221.

Fowler, S. W., and G. A. Knauer (1986), Role of large particles in the transport of elements and organic compounds through the oceanic water column, *Prog. Oceanogr.*, *16*(3), 147–194, doi:10.1016/0079-6611(86)90032-7.

Franklin, M. P., I. R. McDonald, D. G. Bourne, N. J. P. Owens, R. C. Upstill-Goddard, and J. C. Murrell (2005), Bacterial diversity in the bacterioneuston (sea-surface microlayer): the bacterioneuston through the looking glass., *Environ. Microbiol., 7*(5), 723–36, doi:10.1111/j.1462-2920.2004.00736.x.

Frew, N. M. et al. (2004), Air-sea gas transfer: Its dependence on wind stress, small-scale roughness, and surface films, *J. Geophys. Res.*, *109*(C8), C08S17, doi:10.1029/2003JC002131.

Frew, R. D., D. a. Hutchins, S. Nodder, S. Sañudo-Wilhelmy, a. Tovar-Sanchez, K. Leblanc, C. E. Hare, and P. W. Boyd (2006), Particulate iron dynamics during FeCycle in subantarctic waters southeast of New Zealand, *Global Biogeochem. Cycles*, *20*(1), GB1S93, doi:10.1029/2005GB002558.

Frka, S., Z. Kozarac, and B. Ćosović (2009), Characterization and seasonal variations of surface active substances in the natural sea-surface micro-layers of the coastal Middle Adriatic stations, *Estuar. Coast. Shelf Sci.*, *85*(4), 555–564, doi:10.1016/j.ecss.2009.09.023.

Frka, S., S. Pogorzelski, Z. Kozarac, and B. Ćosović (2012), Physicochemical signatures of natural sea films from Middle Adriatic stations., *J. Phys. Chem. A, 116*(25), 6552–9, doi:10.1021/jp212430a.

Fuentes, E., H. Coe, D. Green, and G. McFiggans (2011), On the impacts of phytoplankton-derived organic matter on the properties of the primary marine aerosol – Part 2: Composition, hygroscopicity and cloud condensation activity, *Atmos. Chem. Phys.*, *11*(6), 2585–2602, doi:10.5194/acp-11-2585-2011.

Furutani, H., A. Meguro, H. Iguchi, and M. Uematsu (2010), Geographical distribution and sources of phosphorus in atmospheric aerosol over the North Pacific Ocean, *Geophys. Res. Lett.*, *37*(3), L03805, doi:10.1029/2009GL041367.

Furutani, H. (2012), personal communication, Mass spectra of particle ejected from bubble experiment using an aerosols time-of-flight mass spectrometry (ATOFMS) at St.08 in EEP-2012 cruise.

Garrett, W. (1965), Collection of slick-forming materials from the sea-surface, *Limnol. Oceanogr.*, *10*, 602–605.

Gladyshev, M. I. (2002), *Biophysics of the surface microlayer of aquatic systems*, 148 pp., IWA Publishing, London.

Goering, J. J., and D. Wallen (1967), The vertical distribution of phosphate and nitrite in the upper one-half meter of the southeast Pacific Ocean, *Deep Sea Res. Oceanogr. Abstr.*, *14*(1), 29–33, doi:10.1016/0011-7471(67)90026-5.

Gordon, R. M., K. H. Coale, and K. S. Johnson (1997), Iron distributions in the equatorial Pacific: Implications for new production, *Limnol. Oceanogr.*, *42*(3), 419–431, doi:10.4319/lo.1997.42.3.0419.

Graham, W. F., and R. A. Duce (1979), Atmospheric pathways of the phosphorus cycle, *Geochim. Cosmochim. Acta*, *43*(8), 1195–1208, doi:10.1016/0016-7037(79)90112-1.

Graham, W. F., and R. a. Duce (1982), The atmospheric transport of phosphorus to the western North Atlantic, *Atmos. Environ.*, *16*(5), 1089–1097, doi:10.1016/0004-6981(82)90198-6.

Graham, W. F., S. R. Piotrowicz, and R. A. Duce (1979), The sea as a source of atmospheric phosphorus, *Mar. Chem.*, *7*(4), 325–342, doi:10.1016/0304-4203(79)90019-7.

Grammatika, M., and W. B. Zimmerman (2001), Microhydrodynamics of flotation processes in the sea-surface layer, *Dyn. Atmos. Ocean., 34*(2-4), 327–348, doi:10.1016/S0377-0265(01)00073-2.

Grasshoff, K., M. Ehrhardt, and K. Kremling (1999). *Methods of seawater analysis*. 600 pp. Wiley-VCH.

Hardy, J. T. (1982), The sea-surface microlayer: Biology, chemistry and anthropogenic enrichment, *Prog. Oceanogr.*, *11*(4), 307–328, doi:10.1016/0079-6611(82)90001-5.

Hardy, J. T., and C. W. Apts (1989), Photosynthetic carbon reduction: high rates in the sea-surface microlayer, *Mar. Biol.*, *101*(3), 411–417, doi:10.1007/BF00428138.

Hardy, J. T., C. W. Apts, E. A. Crecelius, and N. S. Bloom (1985), Sea-surface microlayer metals enrichments in an urban and rural bay, *Estuar. Coast. Shelf Sci.*, *20*(3), 299–312, doi:10.1016/0272-7714(85)90044-7.

Harvey, G. (1966), Microlayer collection from the sea surface: a new method and initial results, *Limnol. Oceanogr.*, *11*(4), 608–613.

Harvey, G. W. and L. A. Burzell (1972), A simple microlayer method for small samples*, Limnol. Oceanogr*., *17(1),* 156–157, doi: 10.4319/lo.1972.17.1.0156.

Hillbricht-ilkowska, A., and I. Kostrzewska-szlakowska (2004), Surface microlayer in lakes of different trophic status: nutrients concentration and accumulation, *POLISH J. Ecol.*, *52*(4), 461–478.

Hoffman, E. J., and R. A. Duce (1976), Factors influencing the organic carbon content of marine aerosols: A laboratory study, *J. Geophys. Res. Ocean Atmos.*, *81*(21), 3667–3670, doi:10.1029/JC081i021p03667.

Hultin, K. A. H., E. D. Nilsson, R. Krejci, E. M. Mrtensson, M. Ehn, Å. Hagström, and G. de Leeuw (2010), In situ laboratory sea spray production during the Marine Aerosol Production 2006 cruise on the northeastern Atlantic Ocean, *J. Geophys. Res. Atmos.*, *115*(6), 1–19, doi:10.1029/2009JD012522.

Hultin, K. A. H., R. Krejci, J. Pinhassi, L. Gomez-Consarnau, E. M. Mårtensson, Å. Hagström, and E. D. Nilsson (2011), Aerosol and bacterial emissions from Baltic Seawater, *Atmos. Res.*, *99*(1), 1–14, doi:10.1016/j.atmosres.2010.08.018.

Hunter, K. A. (1980), Processes affecting particulate trace metals in the sea-surface microlayer, *Mar. Chem., 9* (1), 49-70, doi: 10.1016/0304-4203(80)90006-7.

IPCC (2007), Climate Change 2007: The Physical Science Basis. Contribution of Working Group I to the Fourth Assessment Report of the Intergovernmental Panel on Climate Change. , Cambridge University Press, Cambridge, United Kingdom and New York, NY, USA

Iwamoto, Y. (2008), *Biogeochemical processes of suspended particles in the North Pacific*, Ph.D. dissertation, 123 pp. Univ.of Tokyo.

Iwamoto, Y., and M. Uematsu (2014), Spatial variation of biogenic and crustal elements in suspended particulate matter from surface waters of the North Pacific and its marginal seas, *Prog. Oceanogr.*, *126*, 211–223, doi:10.1016/j.pocean.2014.04.019.

Iwamoto, Y., Y. Narita, A. Tsuda, and M. Uematsu (2009), Single particle analysis of oceanic suspended matter during the SEEDS II iron fertilization experiment, *Mar. Chem.*, *113(3-4),* 212–218, doi:10.1016/j.marchem.2009.02.002.

Jickells, T. D. (1999), The inputs of dust derived elements to the Sargasso Sea; a synthesis, *Mar. Chem., 68*, 5-14, doi: 10.1016/S0304-4203(99)00061-4.

Joux, F., H. Agogué, I. Obernosterer, C. Dupuy, T. Reinthaler, G. Herndl, and P. Lebaron (2006), Microbial community structure in the sea-surface microlayer at two contrasting coastal sites in the northwestern Mediterranean Sea, *Aquat. Microb. Ecol.*, *42*, 91–104, doi:10.3354/ame042091.

Karl, .D. M., and G. Tien (1992), MAGIC: a sensitive and precise method for measuring dissolved phosphorus in aquatic environments, *Lim. Oceanogr*., 37(1), 105-116, doi: 10.4319/lo.1992.37.1.0105.

Karl, D. M., and G. Tien (1997), Temporal variability in dissolved phosphorus concentrations in the subtropical North Pacific Ocean, *Mar. Chem.*, *56*(1-2), 77–96, doi:10.1016/S0304-4203(96)00081-3.

Kaupp, L. J., C. I. Measures, K. E. Selph, and F. T. Mackenzie (2011), The distribution of dissolved Fe and Al in the upper waters of the Eastern Equatorial Pacific, *Deep Sea Res. Part II Top. Stud. Oceanogr.*, *58*(3-4), 296–310, doi:10.1016/j.dsr2.2010.08.009.

Keene, W. C. et al. (2007), Chemical and physical characteristics of nascent aerosols produced by bursting bubbles at a model air-sea interface, *J. Geophys. Res. Atmos.*, *112*(21), 1–16, doi:10.1029/2007JD008464.

Kindler, K., A. Khalili, and R. Stocker (2010), Diffusion-limited retention of porous particles at density interfaces., *Proc. Natl. Acad. Sci. U. S. A.*, *107*(51), 22163–8, doi:10.1073/pnas.1012319108.

Lal, D., and A. Lerman (1973), Dissolution and behavior of particulate biogenic matter in the ocean: Some theoretical considerations, *J. Geophys. Res.*, *78*(30), 7100, doi:10.1029/JC078i030p07100.

Lechtenfeld, O. J., B. P. Koch, B. Gašparović, S. Frka, M. Witt, and G. Kattner (2013), The influence of salinity on the molecular and optical properties of surface microlayers in a karstic estuary, *Mar. Chem.*, *150*, 25–38, doi:10.1016/j.marchem.2013.01.006.

Lewis, E. R., and Schwartz, S. E. (2004), Sea Salt Aerosol Production: Mechanisms, Methods, tpp 413. AGU. Washington, D.C.

Lin, P., L. Guo, M. Chen, J. Tong, and F. Lin (2012), The distribution and chemical speciation of dissolved and particulate phosphorus in the Bering Sea and the Chukchi–Beaufort Seas, *Deep Sea Res. Part II Top. Stud. Oceanogr.*, *81-84*, 79–94, doi:10.1016/j.dsr2.2012.07.005.

Liss, P. S., and R. A. Duce (1997), *The sea surface and global change*. 519 pp, Cambridge Univ. Press, New York.

Liu, K., and R. M. Dickhut (1998), Effects of wind speed and particulate matter source on surface microlayer characteristics and enrichment of organic matter in southern Chesapeake Bay, *J. Geophys. Res.*, *103*(D9), 10571, doi:10.1029/97JD03736.

Liu, S., Y. Zhao, J. Ren, J. Zhang, S. Sun, J. Jin, and G. Zhang (2010), Assessment of the conventional molybdenum-blue and magnesium-induced coprecipitation procedures in phosphorus measurement in various aquatic environments, *Acta Oceanol. Sin.*, *29*(1), 42–51, doi:10.1007/s13131-010-0006-2.

Lomas, M. W., A. L. Burke, D. A. Lomas, D. W. Bell, C. Shen, S. T. Dyhrman, and J. W. Ammerman (2010) , Sargasso Sea phosphorus biogeochemistry: an important role for dissolved organic phosphorus (DOP), *Biogeosciences*, 2, 695-710, doi: 10.5194/bg-7-695-2010.

Mackey, D. J., J. E. O'Sullivan, and R. J. Watson (2002), Iron in the western Pacific: A riverine or hydrothermal source for iron in the Equatorial Undercurrent?, *Deep. Res. Part I Oceanogr. Res. Pap.*, *49*(5), 877–893, doi:10.1016/S0967-0637(01)00075-9.

Mahowald, N. et al. (2008), Global distribution of atmospheric phosphorus sources, concentrations and deposition rates, and anthropogenic impacts, *Global Biogeochem. Cycles*, *22*(4), 1–19, doi:10.1029/2008GB003240.

Macintyre, F. (1970), Geochemical fractionation during mass transfer from sea to air by breaking bubbles, *Tellus A*, *02139*(1959), doi:10.3402/tellusa.v22i4.10238.

Martin, J. H. et al. (1994), Testing the iron hypothesis in ecosystems of the equatorial Pacific Ocean. *Nature, 371*,123-129, doi:10.1038/371123a0.

McCave, I. N. (1984), Size spectra and aggregation of suspended particles in the deep ocean, *Deep Sea Res. Part A. Oceanogr. Res. Pap.*, *31*(4), 329–352, doi:10.1016/0198-0149(84)90088-8.

Murphy, J. and J. P. Riley (1962), A modified single solution method for the determination of phosphate in natural waters, *Anal. Chim. Acta, 27*, 31-36, doi: 10.1016/S0003-2670(00)88444-5.

Nordmeyer, T., and K. A. Prather (1994), Real-Time Measurement Capabilities Using Aerosol Time-of-Flight Mass Spectrometry, *Anal. Chem.*, *66*(20), 3540–3542.

Norris, S. J., I. M. Brooks, G. de Leeuw, a. Sirevaag, C. Leck, B. J. Brooks, C. E. Birch, and M. Tjernström (2011), Measurements of bubble size spectra within leads in the Arctic summer pack ice, *Ocean Sci.*, *7*(1), 129–139, doi:10.5194/os-7-129-2011.

Obernosterer, I., P. Catala, R. Lami, J. Caparros, J. Ras, a Bricaud, C. Dupuy, F. Van Wambeke, and P. Lebaron (2008), Biochemical characteristics and bacterial community structure of the sea surface microlayer in the South Pacific Ocean, *Biogeosciences Discuss.*, *4*(4), 693–705, doi:10.5194/bgd-4-2809-2007.

O'Dowd, C. D., and G. de Leeuw (2007), Marine aerosol production: a review of the current knowledge, *Philos. Trans. A. Math. Phys. Eng. Sci.*, *365*(May), 1753–1774, doi:10.1098/rsta.2007.2043.

O'Dowd, C. D., M. C. Facchini, F. Cavalli, D. Ceburnis, M. Mircea, S. Decesari, S. Fuzzi, Y. J. Yoon, and J.-P. Putaud (2004), Biogenically driven organic contribution to marine aerosol, *Nature, 431*,676–680, doi:10.1038/nature02959.

Okin, G. S. et al. (2011), Impacts of atmospheric nutrient deposition on marine productivity: Roles of nitrogen, phosphorus, and iron, *Global Biogeochem. Cycles*, *25*(2), GB2022, doi:10.1029/2010GB003858.

Pak, H. (1973), Distribution of Suspended Particles in the Equatorial Pacific Ocean, Suspended Solids in Water, *Marine Science, 4*, edited by Gibbs, R. J., pp. 261-270, Platinum press, New York.

Paytan, A., and K. McLaughlin (2007), The Oceanic Phosphorus Cycle, *Chem. Rev., 107* (2), 563-576; doi: 10.1021/cr0503613.

Pennington, J. T., K.L. Mahoney, V.S. Kuwahara, D.D Kolber, R. Calienes, and F. P. Chavez (2006), Primary production in the eastern tropical Pacific: A review. *Prog. Oceanogr., 69*(2), 285-317, doi: 10.1016/j.pocean.2006.03.012.

Reinthaler, T., E. Sintes, and G. J. Herndl (2008), Dissolved organic matter and bacterial production and respiration in the sea-surface microlayer of the open Atlantic and the western Mediterranean Sea, *Limnol. Oceanogr.*, *53*(1), 122–136, doi:10.4319/lo.2008.53.1.0122.

Russell, L. M., L. N. Hawkins, A. A. Frossard, P. K. Quinn, and T. S. Bates (2010), Carbohydrate-like Russell, L. M., L. N. Hawkins, A. A. Frossard, P. K. Quinn, and T. S. Bates (2010), Carbohydrate-like composition of submicron atmospheric particles and their production from ocean bubble bursting, *Proc. Natl. Acad. Sci. U. S. A.*, *107*(15), 6652–7, doi:10.1073/pnas.0908905107.

Ruttenberg, K.C. (2003), The Global Phosphorus Cycle, in *Treatise on Geochemistry, 8*, edited by H. D. Holland and K. K. Turekian, pp 585 – 643, Pergamon, doi: 10.1016/B0-08-043751-6/08153-6.

Sañudo-Wilhelmy, S. A., A. Tovar-Sanchez, F. X. Fu, D. G. Capone, E. J. Carpenter, and D. A. Hutchins (2004), The impact of surface-adsorbed phosphorus on phytoplankton Redfield stoichiometry, *Nature, 432*, 897–901, doi:10.1038/nature03125.

Slauenwhite, D. E., and B. D. Johnson (1996), Effect of organic matter on bubble surface tension, J. Geophys. Res., 101(C2), 3769, doi:10.1029/95JC02633.

Södergren, A. (1993), Role of aquatic surface microlayer in the dynamics of nutrients and organic compounds in lakes, with implications for their ecotones, *Hydrobiologia, 251*(1-3), 217–225, doi:10.1007/BF00007181.

Solorzano L. and J.H. Sharp (1980). Determination of total dissolved phosphorus and particulate phosphorus in natural water. *Liminol.Oceanogr* 24 (4), 754-758.

Soloviev, A. and R. Lukas, (2006). *The Near-Surface Layer of the Ocean: Structure, Dynamics and Applications* (Vol. 31). Springer.

Strickland, J. D. H. and T. R. Parsons (1972), *A Practical handbook of seawater analysis,* 293 pp., Fisheries Research Board of Canada, Bulletin 167, Ottawa.

Stolle, C., M. Labrenz, C. Meeske, and K. Jürgens (2011), Bacterioneuston Community Structure in the Southern Baltic Sea and Its Dependence on Meteorological Conditions, *Appl. Environ. Microbiol., 77* (11), 3726-3733, doi: 10.1128/AEM.00042-11.

Stukel, M. R., M. R. Landry, and K. E. Selph (2011), Nanoplankton mixotrophy in the eastern equatorial Pacific, *Deep Sea Res. Part II Top. Stud. Oceanogr.*, *58*(3-4), 378–386, doi:10.1016/j.dsr2.2010.08.016.

Suzumura, M., and E. D. Ingall (2004), Distribution and dynamics of various forms of phosphorus in seawater: Insights from field observations in the Pacific Ocean and a laboratory experiment, *Deep. Res. Part I Oceanogr. Res. Pap.*, *51*, 1113–1130, doi:10.1016/j.dsr.2004.05.001.

Takeda, S. (2012), personal communication; On-board Fe-fertilization during EEP-2012 cruise.

Taylor, S. R. (1964), Abundance of chemical elements in the continental crust: a new table, *Geochim. Cosmochim. Acta*, *28*, 1273–1285, doi:10.1016/0016-7037(64)90129-2.

Tsai, W., and K. K. Lui (2003), An assessment of the effect of sea surface surfactant on global atmosphere-ocean CO_2 flux, *J. Geophys. Res.*, *108*, 1–16, doi:10.1029/2000JC000740.

Twining, B. S., S. B. Baines, J. B. Bozard, S. Vogt, E. A. Walker, and D. M. Nelson (2011), Metal quotas of plankton in the equatorial Pacific Ocean, Deep-Sea Res. II, 58 (3), 325-341, doi: 10.1016/j.dsr2.2010.08.018.

van Pinxteren, M., C. Müller, Y. Iinuma, C. Stolle, and H. Herrmann (2012), Chemical characterization of dissolved organic compounds from coastal sea surface microlayers (Baltic Sea, Germany), *Environ Sci Technol., 46(19)*,10455-6, doi: 10.1021/es204492b.

Wakeham, S. G., and E. A. Canuel (1988), Organic geochemistry of particulate matter in the eastern tropical North Pacific Ocean: Implications for particle dynamics, *J. Mar. Res.*, *46*(1), 183–213, doi:10.1357/002224088785113748.

Wang, R., Y. Balkanski, O. Boucher, P. Ciais, J. Peñuelas, and S. Tao (2014), Significant contribution of combustion-related emissions to the atmospheric phosphorus budget, *Nat. Geosci., 8*, 4–10, doi:10.1038/ngeo2324.

Wang, S. H., N. C. Hsu, S. C. Tsay, N.-H. Lin, A. M. Sayer, S. J. Huang, and W. K. M. Lau (2012), Can Asian dust trigger phytoplankton blooms in the oligotrophic northern South China Sea?, *Geophys. Res. Lett., 39*(5), L05811, doi:10.1029/2011GL050415.

Wheeler, J. R. (1975), Formation and collapse of surface films, *Limnol. Oceanogr., 20* (3), 338-342, doi: 10.4319/lo.1975.20.3.0338.

Worsfold, *et al* (2005). Sampling, sample treatment and quality assurance issues for the determination of phosphorus species in natural waters and soils. *Talanta* 66, 273-293.

Wurl, O., and J. P. Obbard, (2004), A Review of Pollutants in the Sea-Surface Microlayer (SML): A Unique Habitat for Marine Organisms. *Mar. Pollut. Bull., 48* (11-12), 1016-1030 doi: 10.1016/j.marpolbul.2004.03.016.

Wurl, O., and M. Holmes (2008), The gelatinous nature of the sea-surface microlayer, *Mar. Chem., 110* (1–2), 89-97, doi: 10.1016/j.marchem.2008.02.009.

Wurl, O., E. Wurl, L. Miller, K. Johnson, and S. Vagle (2011), Formation and global distribution of sea-surface microlayers, *Biogeosciences*, *8*(4), 121–135, doi:10.5194/bg-8-121-2011.

Wurl, O., S. Karuppiah, and J. P. Obbard (2006), The role of the sea-surface microlayer in the air-sea gas exchange of organochlorine compounds, *Sci. Total Environ.*, *369*(1-3), 333–43, doi:10.1016/j.scitotenv.2006.05.007.

Xhoffer, C., L. Wouters, and R. Van Grieken (1992), Characterization of individual particles in the North Sea-surface microlayer and underlying seawater: comparison with atmospheric particles, *Environ. Sci. Technol.*, *26*(11), 2151–2162, doi:10.1021/es00035a013.

Yoshida, T., K. Hayashi, and H. Ohmoto (2002), Dissolution of iron hydroxides by marine bacterial siderophore, *Chem. Geol., 184* (1-2), 1-9, doi: 10.1016/S0009-2541(01)00297-2.

Yoshimura, T., J. Nishioka, H. Saito, S. Takeda, A. Tsuda and M. L. Wells (2007), Distributions of particulate and dissolved organic and inorganic phosphorus in North Pacific surface waters, *Mar. Chem., 103*, 112 – 121, doi: 10.1016/j.marchem.2006.06.011.

Zhang, Z., L. Liu, C. Liu, and W. Cai (2003). Studies on the sea-surface microlayer: II. The layer of sudden change of physical and chemical properties*, J. of Colloid and Interface Science, 264 (1),* 148-159, doi: 10.1016/S0021-9797(03)00390-4.

Zhang, Z., C. Liu, and L. Liu (2006), Physicochemical Studies of the Sea-Surface Microlayer, *Front. Chem. China*, *1*(1), 1–14, doi:10.1007/s11458-005-0003-8.